universität wien

DISSERTATION

Lead-free solder alloys: Thermodynamic properties and surface tension

Investigations on the Ag-Au-Sn, Au-Sb-Sn, Au-Sb and the Ag-Bi-Sn system

Verfasser

Magister Michael Hindler

angestrebter akademischer Grad

Doktor der Naturwissenschaften (Dr. rer.nat.)

Wien, am 11. Januar 2011

Studienkennzahl lt. Studienblatt:	A 091 419
Dissertationsgebiet lt. Studienblatt:	Chemie
Betreuer:	Ao. Univ. -Prof. i. R. Dr. Adolf Mikula

Acknowledgement

The present investigations were carried out in the Institute of Inorganic Chemistry/Materials Chemistry of the University of Vienna during the period from June 2007 to December 2010.

First of all I want to thank my supervisor Prof. Adolf Mikula who gave me the opportunity to graduate to Dr. rer nat. in his group, for his trust and the possibility to do independent research.

Special thanks to my fiancée Beatrix Preimesberger. There would be too many things to count them.

I would like to thank the head of our institute Prof. Herbert Ipser for all the support he gave me.

I would also like to thank Prof. Peter Terzieff for having deep discussions, both about research and life.

I would like to thank Dr. Sabine Knott, who always took time for discussions and never got bored of questions.

Many thanks to our glassblower Mrs. Beatrice Turski who always helped to keep things working.

I would like to thank all my colleagues at the Institute of Inorganic Chemistry/Materials Chemistry for the pleasant atmosphere, support and many interesting discussions.

Special thanks to MSc. Zhongnan Guo who supported me in the last year of my thesis and became a very good friend of mine.

I would also like to thank my family and specially my mother who always cared during her whole life in spite of massive health problems.

Thanks to all my friends, who may not be named here.

Financial support from the Austrian Science Foundation (FWF) under Grant Nos. P19461-N19 and P20488-N19 is gratefully acknowledged.

Table of contents:

Chapter 1: Introduction

1.1 Lead free solders

It is well known that the toxic effect of lead affects environment and human life. Various body processes are concerned and the toxic effect to many organs and tissues including the heart, bones, intestines, kidneys, and reproductive and nervous systems is a serious problem. Lead interferes with the development of the nervous system and is therefore particularly toxic to children. Consequences are permanent learning and behavior disorders. Symptoms caused by lead are abdominal pain, headache, anemia, irritability, and in severe cases seizures, coma, and death. Ways of lead into the body are possible by inhalation, ingestion or absorption through the skin. Routes of exposure to lead include contaminated air, water, soil, food, and consumer products. The toxicity is determined by the amount of lead in the blood and tissues, as well as the time of exposure.[2003 Pearson]

Lead poisoning may be acute from intense exposure of short duration or chronic from repeated low-level exposure over a prolonged period. The latter is much more common.[2007 Trevor]

Diagnosis and treatment of lead exposure are based on the blood lead level, measured in micrograms of lead per deciliter of blood (µg/dl). The US Centers for Disease Control and Prevention and the World Health Organization state that a blood lead level of 10 µg/dl or above is a cause for concern. However, lead may impair development and have harmful health effects even at lower levels, and there is no known safe exposure level. [2005 Barbosa, 2008 Rossi] Authorities such as the American

Academy of Pediatrics define lead poisoning as blood lead levels higher than 10 µg/dl. [2009 Ragan]

The concern about the use of lead in the electronics industry stems from occupational exposure, lead waste derived from the manufacturing process, and the disposal of electronic assemblies. Although the consumption of lead by the electronic industry appears to be minimal by absolute numbers, the potential for lead exposure is probably ubiquitous and poses a real threat to the human population and its well-being. Potential sources for occupational exposure in electronics are some of the soldering processes due to inhalation of lead vapors or lead bearing dust generated by dross during the wave soldering operation. The problems arising from the disposal of lead containing waste will probably be of even greater importance in the future. It will be the waste from the industrial processes themselves or the rapidly increasing amounts of electronic assemblies containing lead solders (personal computers, radio, TV, mobile phones, household appliances …) that go out of operation. The subsequent disposed lead in landfills can eventually be leached out and can contaminate underground water sources and subsequently find its way into the human ecosystem in an ingestible form. The path of lead from the lead containing electronics to the human body is shown in Fig. 1.1 [2006 Li].

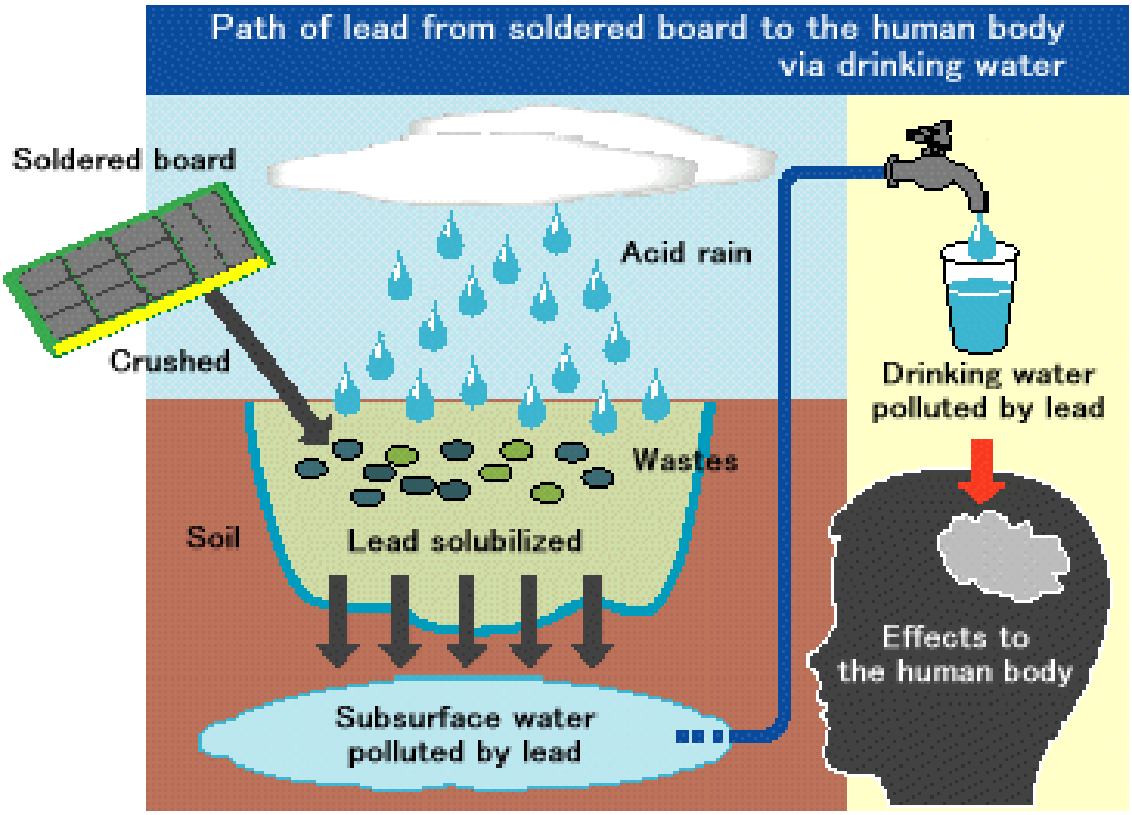

Fig. 1.1: Path of lead from the lead containing electronics to the human body [2006 Li].

The Directive on the restriction of the use of certain hazardous substances in electrical and electronic equipment 2002/95/EC; commonly referred to as the Restriction of Hazardous Substances Directive or RoHS, was adopted in February 2003 by the European Union. [2003 EU] The RoHS directive took effect on July 1, 2006, and is required to be enforced and become law in each member state. This directive restricts the use of six hazardous materials, namely lead, mercury, cadmium, hexavalent chromium, polybrominated biphenyls and polybromated diphenyl ether. The metals are restricted in the manufacture of various types of electronic and electrical equipment. It is closely linked with the Waste Electrical and Electronic Equipment Directive (WEEE) 2002/96/EC which sets collection, recycling and recovery targets for electrical goods and is part of a legislative initiative to solve the problem of huge amounts of toxic electronic waste.

Each European Union member state will adopt its own enforcement and implementation policies using the directive as a guide.

RoHS is often referred to as the lead-free directive, but it restricts the use of the previously named six substances:

1. Lead (Pb)
2. Mercury (Hg)
3. Cadmium (Cd)
4. Hexavalent chromium (Cr^{6+})
5. Polybrominated biphenyls (PBB)
6. Polybrominated diphenyl ether (PBDE)

PBB and PBDE are flame retardants used in several plastics.

The maximum permitted concentrations are 0.1% or 1000 ppm (except for cadmium, which is limited to 0.01% or 100 ppm) by weight of homogeneous material. This means that the limits do not apply to the weight of the finished product, or even to a component, but to any single part that could (theoretically) be separated mechanically. Examples are the sheath on a cable or the tinning on a component lead.

Everything that can be identified as a homogeneous material must meet the limit. So if it turns out that the case of a radio was made of plastic with 2 ppm (0.2%) PBB used as a flame retardant, then the entire radio would fail the requirements of the directive.

In an effort to close RoHS loopholes, in May 2006 the European Commission was asked to review two currently excluded product categories (monitoring and control equipment, and medical devices) for

future inclusion in the products that must fall into RoHS compliance. In addition the commission entertains requests for deadline extensions or for exclusions by substance categories, substance location or weight.

The directive applies to equipment as defined by a section of the WEEE directive. The following numeric categories apply:

1. Large and small household appliances.
2. IT equipment.
3. Telecommunications equipment (although infrastructure equipment is exempt in some countries)
4. Consumer equipment.
5. Lightning equipment including light bulbs.
6. Electronic and electrical tools.
7. Toys, leisure, and sports equipment.
8. Medical devices (currently exempt)
9. Monitoring and control instruments (currently exempt)
10. Automatic dispensers.

It does not apply to fixed industrial plants and tools. Compliance is the responsibility of the company that puts the product on the market, as defined in the Directive; components and sub-assemblies are not responsible for product compliance. Of course, given the fact that the regulation is applied at the homogeneous material level, data on substance concentrations needs to be transferred through the supply chain to the final producer. The Association Connecting Electronics Industries IPC (former Institute for Interconnecting and Packaging Electronic Circuits) has recently developed and published an IPC standard to facilitate this data exchange, namely IPC-1752. [2010 IPC]

RoHS applies to these products in the EU whether made within the EU or imported. Certain exemptions apply, and these are updated on occasion by the EU.

1.2 Aim of this work

The primary driving forces behind the development of lead-free solders are performance demands and environmental as well as health concerns. It is substantiated that the common thermal fatigue failure for solder interconnections is linked with the Pb-rich phase. Because of limited solubility and precipitation, Sn solute atoms cannot effectively strengthen this Pb-rich phase. Under temperature cycling conditions, this Pb-rich phase tends to coarsen and, eventually, lead to a solder joint crack. It is expected that the absence of a Pb phase of a properly designed, lead-free, tin-based solder may impart improved mechanical behavior, resulting in strengthened solders. The aim of this work is to determine thermodynamic properties and surface tension of materials that could be used as replacements for Pb solders for high-temperature applications as it is a part of the COST action MP0602: Advanced Solder Materials for High Temperature Application (HISOLD). This action is basically focusing on the named aims of this work.

So the study of lead free systems is essential for daily life with growing electronic waste as lead is harmful to environment and health. In order to develop these new materials, information on the phase diagrams, the phase equilibria and the melting behavior are necessary. Some of the other properties like the melting temperature, the solidification path and the surface properties also need to be determined. In Pb-Sn solders the effect of fatigue is affiliated to the lead rich phase [2000 Hwang] which

tends to embrittle with thermomechanical variation in stress which leads to cracking. It is expected that replacements for lead will induce better mechanical behavior and stability.

Chapter 2: Experimental techniques

2.1 Electromotive force method (emf)

Thermodynamic properties of metallic systems (partial and integral values) are determined in dependence from temperature, pressure and concentration. The emf method is one of the most accurate methods to obtain thermodynamic properties of alloys. A cell whose cell reaction consists of a concentration difference between two electrodes is called a concentration cell. This cell can be used to measure the activity of one component in an alloy. Two different methods are available to measure the emf. The emf method with a liquid electrolyte for temperatures up to 1073 K and the emf method with a solid electrolyte for temperatures higher than 873 K. In this work the liquid emf was used. Reviews about the emf method were given by Mikula [1997 Chang] and Ipser [2010 Ipser].

2.1.1 Conditions for accurate emf measurements

There are several conditions that must be fulfilled to achieve accurate emf measurements:

1. The charge of the electropositive ion Me^{n+} has to be known exactly.
2. Me^{n+} should be the only charge transfer trough the electrolyte and the only reaction on the surface of the electrodes.
3. The electronic conduction through the electrolyte should be purely ionic.
4. No reaction of the electrode and the electrolyte with the apparatus should occur.
5. Concentration changes of the electrodes and the electrolyte during the measurement must be taken into account.

6. During the emf measurement no electricity should pass through the cell, which can be achieved by using a voltmeter with an input impedance of more than 10^{10} Ohm.
7. At higher temperatures, for KCl-LiCl at approximately 1123 K, the electrolyte could get some electronic conductivity. This will be the upper temperature limit for emf measurements with KCl-LiCl electrolyte.

2.1.2 Principle of the emf method

An emf method with a liquid electrolyte was used to determine the activity of metals in liquid alloys. The electrolyte consists of the eutectic mixture of KCl (purity 99.5%) and LiCl (purity 99%) with addition of a small amount of the metal halide corresponding to the metal which activity should be determined. All used salts were products of Merck KGaA, Germany. Cleaning of the electrolyte is described Chapter 2.1.3.

For the emf measurements, the following cell arrangement was used:

$$W, Me_{(l)}(Pure)/Me^{Z+}, electrolyte/Me\ in\ the\ Alloy_{(l)}, W$$

with the electrode Me as pure metal and the other electrodes as an alloy containing Me.

Under reversible conditions the Gibbs free energy change for the reaction is given by

$$\Delta\overline{G}_{Me} = -z \cdot F \cdot E = RT \cdot \ln a_{Me} \qquad (2.1)$$

where *z* is the number of exchanged electrons, *F* the Faraday constant (96485 C/mol), *E* the electromotive force in volt, *R* the universal gas constant (8.3145 J K^{-1} mol^{-1}), *T* the temperature in K and a_{Me} the

thermodynamic activity of the pure metal in the ternary alloy. As reference electrode, pure metal was used.

The emf versus temperature were least square fitted and the emf was expressed by the equation

$$E(mV) = a(\mathrm{mV}) + b(\mathrm{mV \cdot K^{-1}}) \cdot T(\mathrm{K}) \tag{2.2}$$

where a is the ordinate intercept and b the slope.

From the temperature dependence of *E* the partial molar enthalpy $\Delta\overline{H}_{Me}$ and the partial molar entropy $\Delta\overline{S}_{Me}$ were derived using the following equations:

$$\Delta\overline{H}_{Me} = z \cdot F \left[E - T\left(\frac{\partial E}{\partial T}\right)\right]_{x,p} = -z \cdot a \cdot F \tag{2.3}$$

$$\Delta\overline{S}_{Me} = z \cdot F \left(\frac{\partial E}{\partial T}\right)_{x,p} = z \cdot b \cdot F \tag{2.4}$$

2.1.3 Calculation of thermodynamic properties

As the thermodynamic properties of real solutions differ from ideal ones, the mixing thermodynamic properties of real solutions are described as the sum of an ideal contribution and an excess contribution. Applying to partial molar properties leads to:

$$\Delta\overline{G_i^{xs}} = RT \cdot \ln \gamma_i \tag{2.5}$$

$$\Delta\overline{S_i^{xs}} = -R \cdot \ln \gamma_i - \left(\frac{\partial \ln \gamma_i}{\partial T}\right)_P \tag{2.6}$$

where γ_i is the activity coefficient of the component *i*.

In the multi-component solution, the molar quantity ΔZ is the sum of the individual partial molar quantities multiplied by the mole fraction:

$$\Delta Z = \sum_i x_i \Delta \overline{Z_i} \tag{2.7}$$

As the partial molar properties of only one component in a concentration cell are measured by an emf method, the integral properties cannot be obtained directly by eq.2.7. The Gibbs-Duhem equation is used to solve that problem:

$$\sum_i x_i d\Delta\overline{Z_i} = 0 \tag{2.8}$$

Partially differentiation of the equation with respect to x_i while keeping x_j:x_k:… constant and combining the result with the Gibbs-Duhem equation leads to:

$$\left[\frac{\partial}{\partial x_i}\left(\frac{\Delta}{1-x_i}\right)\right]_{x_j:x_{k\ldots}} = \frac{\Delta\overline{Z_i}}{(1-x_i)^2} \tag{2.9}$$

In a ternary system, where the partial molar properties of component 3 are measured by the emf method, integration of equation (2.9) from x_1=0 to x_3 at constant molar ration of x_1 and x_2 gives [1951 Elliott]:

$$\Delta Z = (1-x_3)[\Delta Z_{x_3=0} + \int_0^{x_3} \frac{\Delta\overline{Z}_3}{(1-x_3)^2} dx_3]_{x_1/x_2} \tag{2.10}$$

The integral enthalpy of mixing and the integral excess Gibbs free energy were determined by adopting the Gibbs-Duhem equation given by Darken [1950 Darken] and Elliot and Chipman [1951 Elliott] as:

$$\Delta H = (1-X_{Me})[\Delta H_{Me=0} + \int_0^{X_{Me}} \frac{\Delta\overline{H}_{Me}}{(1-X_{Me})^2} dX_{Me}]_{X_1/X_2} \tag{2.11}$$

$$\Delta G^{xs} = (1-X_{Me})[\Delta G^{xs}_{Me=0} + \int_0^{X_{Me}} \frac{\Delta\overline{G^{xs}_{Me}}}{(1-X_{Me})^2} dX_{Me}]_{X_1/X_2} \tag{2.12}$$

$\Delta G_{Me=0}^{xs}$ and $\Delta H_{Me=0}$ are representing the limiting excess Gibbs energy and enthalpy values of the binary system from which the investigations started. X_{Me} is the substance amount fraction of tin in the alloy.

For the integration of the partial excess Gibbs free energy an additional function is used derived by:

$$\Delta\overline{G_{Me}^{xs}} = RT \cdot ln\gamma_{Me} \tag{2.13}$$

with γ_{Me} as the activity coefficient.

So the integrand becomes the alpha function:

$$\alpha = \left(\frac{ln\gamma_{Me}}{(1-x_{Me})^2}\right) \tag{2.14}$$

Inserting into equation 2.12 gives:

$$\Delta G^{xs} = (1 - X_{Me})[\Delta G_{Me=0}^{xs} + RT \int_0^{X_{Me}} \alpha \, dX_{Me}]_{X_1/X_2} \tag{2.15}$$

2.1.4 Preparation of the electrolyte

The choice of the electrolyte is depending on the temperature range chosen for the experiment. Frequently liquid electrolytes are used for emf measurements. In most cases the electrolyte consists of alkali chlorides, containing a small amount of a salt of the most electropositive metal chloride. For the measurements in this work the eutectic mixture of LiCl and KCl was used.

There are some advantages concerning liquid electrolytes:

1.) The thermodynamic equilibrium is reached much faster than in solid electrolytes so that no diffusion processes have to be taken into account.
2.) The electrolyte covers the electrodes and hinders evaporation of metals or alloys with high vapor pressure e.g. antimony.

3.) The molten salts can be used at relatively low temperatures because the melting point of the eutectic mixture of LiCl and KCl is 627 K [1966 Lumsden]
4.) No microcracks and porosity can occur in the liquid electrolyte.

But there are also some disadvantages which have to be taken into account:

1.) The electrolyte can just be used for one measurement and has to be prepared very carefully, because any impurification could cause side reactions which falsify the results.
2.) At approximately 1123 K the electrolyte can get some electronic conductivity.
3.) Possible reactions of the electrode materials with the electrolyte must be taken into account.
4.) The electrolyte is highly hygroscopic and cannot be stored under air.

The steps for cleaning the electrolyte are following: The eutectic mixture of LiCl and KCl are weight and put into a furnace at 383 K for drying overnight. In those alkali-halide mixtures the major impurities are water and hydroxides. The following method is preferred to dry and clean the halides:

A stream of dry gas (e.g. nitrogen or argon) is passed through the powdered salt. After this the temperature is slowly raised until the salt mixture is molten. Through the melt hydrogen chloride or in our case chlorine gas is passed through followed by a stream of argon. The advantage of chlorine gas over hydrogen chloride is a lower residual water and hydroxide content.

The following reactions can occur:

$$OH^- + Cl_2 \rightarrow Cl^- + HCl + \frac{1}{2}O_2$$

$$O^{2-} + Cl_2 \rightarrow \frac{1}{2}O_2 + 2Cl^-$$

$$H_2 + Cl_2 \rightarrow 2HCl$$

For our measurements we prepared the LiCl-KCl electrolyte with the equipment shown in Fig.2.1.

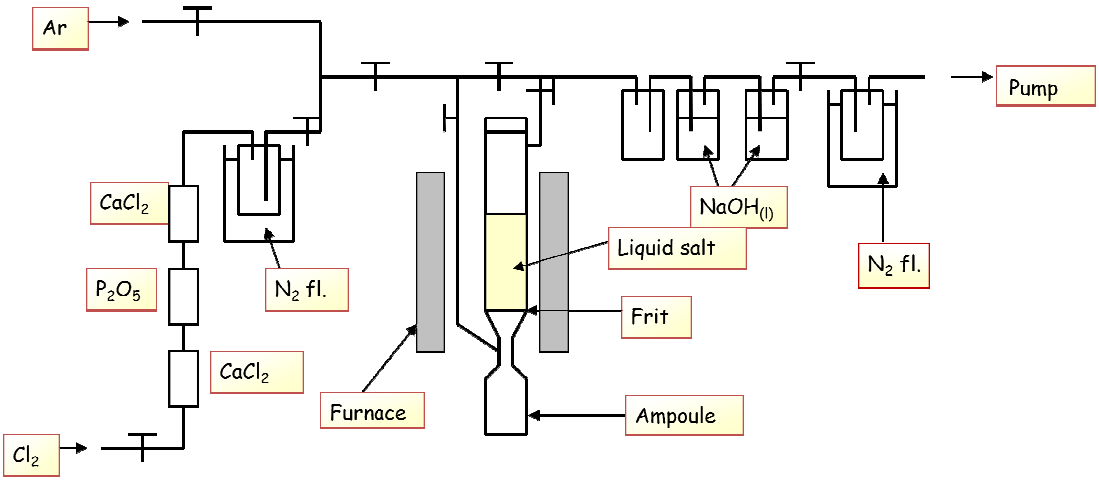

Fig. 2.1: Equipment for cleaning the electrolyte.

First argon is passed through the fine powdered salt mixture which is above the frit. After a few minutes the furnace is turned on and the salt is slowly heated until it is molten. The liquid salt is kept above the melting point all the time. If it would cool down the glass tube would break.

In the mean time chlorine gas is taken out of a pressure bottle and filled in a container which has two stopcocks. The container is in liquid nitrogen and the chlorine gas is condensed in this container. The container is then connected to the apparatus. It would be in the drawing where Cl_2 is

shown. After the connection is gas tight the chlorine is slowly heated and it vaporizes. The gas is passed through $CaCl_2$ and P_4O_{10} and then condensed again in liquid nitrogen. After all the chlorine is transferred into the second cooling trap the chlorine it will be evaporated again and passed slowly through the molten salt mixture. Since the gas pressure is coming from the bottom side of the frit the salt stays above the frit. The excess chlorine gas will be collected in the NaOH solution, which will slowly turn green if the chlorine gas gets there. After all the chlorine gas has passed through the molten salt, argon is bubbled through for four hours because there should be no chlorine left in the electrolyte. A very good indication that all the chlorine gas has left the electrolyte is: the salt mixture must be completely colourless again. After the reaction is finished the vacuum is turned around and the liquid salt is filtered through the frit into the ampoule. The ampoule is then sealed under vacuum with a torch. The electrolyte can be stored for several months prior to its use.

2.1.5 Experimental apparatus

The experimental apparatus is shown in Fig.2.2. The whole tube consists of quartz. Four electrodes were used for each measurement. The most electropositive pure metal is the reference electrode. The other three electrodes are alloys. All alloys were put in quartz containers, which were fixed on a central quartz tube. The central quartz tube was movable through the O-ring seals so that the electrodes could be put into the molten electrolyte. This could hinder evaporation of alloys during the process of melting. The tungsten lead wires were used as conduction wires and sealed into the thin quartz capillaries. A Ni/NiCr thermocouple was put into the central quartz tube to measure the temperature simultaneously during the measurement. After installation, the entire cell

was evacuated and purged with argon gas, finally filled with argon to about 0.5 bar. The cell was heated in a vertical furnace. The electrodes were in a relatively higher position to the electrolyte to prevent them from evaporation before the electrolyte was melted completely.

Measurements were carried out on heating and cooling with a rate of 10 K/h. The emf was continuously measured with a voltmeter. The temperature and emf values were automatically recorded and printed every five minutes. In most cases the first cooling curve was taken to evaluate the thermodynamic properties of the measured system.

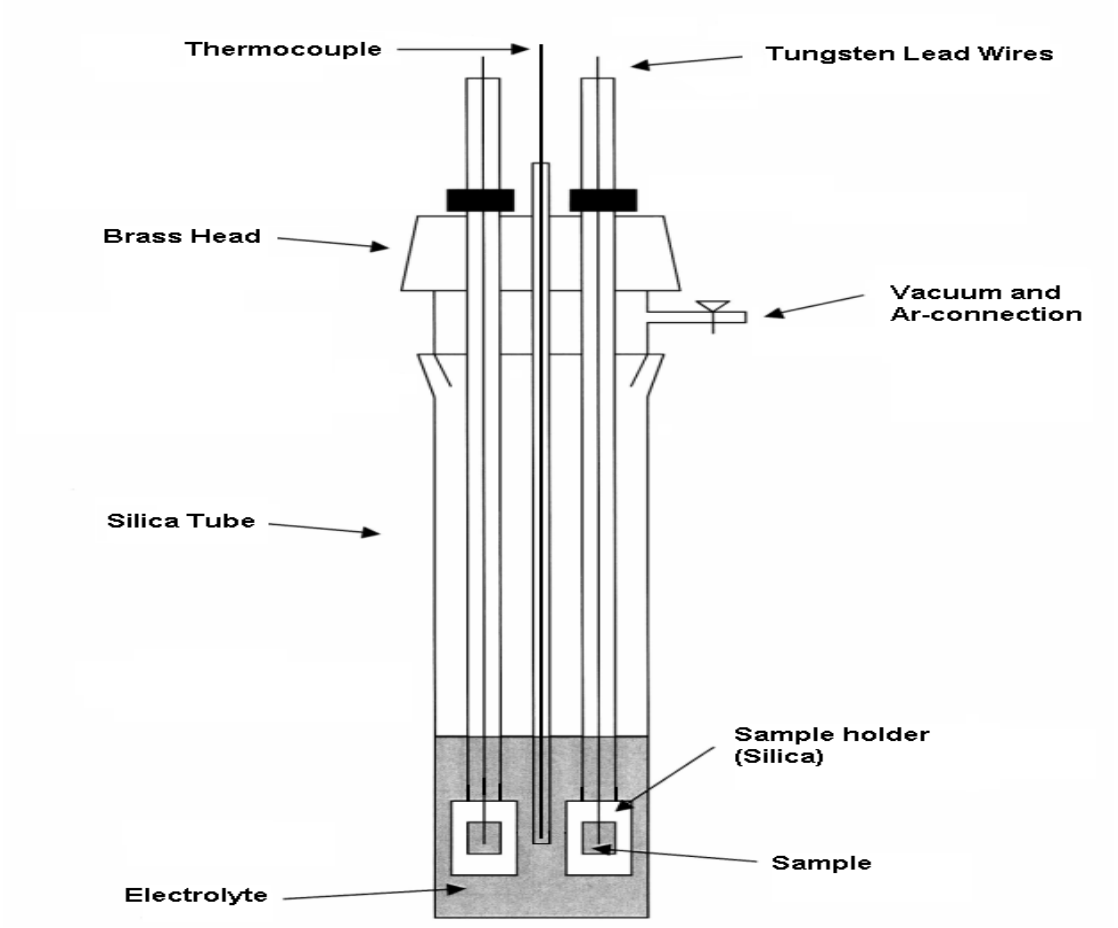

Fig. 2.2: Emf measuring equipment.

2.2 Calorimetric method

Calorimetry is the measurement of heat exchange connected with a change in the physical or chemical state. It is a very precise method to determine the enthalpy of mixing of liquid alloys and is also used to determine other integral values like the enthalpy of formation or the enthalpy of solution etc.

2.2.1 Experimental apparatus

A Calvet-type microcalorimeter (SETARAM, Lyon, France, Fig. 2.3) has been used to study the enthalpy of mixing of alloys. It is an isoperibol twin calorimeter with two separate calorimeter cells, surrounded by thermopiles with 420 pairs of thermocouples for each cell. Each thermopile is mounted as a ring formed by two concentric cylinders measuring the temperature difference between the inner and outer surface. In this way, the EMF of a thermopile gives direct information on the heat flow absorbed or released by the reaction.

The calorimeter cells are located in the large calorimeter block made of alumina and kanthal, which is surrounded by thermally isolating bricks and the electric resistance heating. As the thermopiles are connected in opposition, temperature variations of the furnace are self-compensated. So temperature differences down to 10^{-5} K can be detected. One calorimeter cell is usually permanently loaded with a block of about 25 g of alumina and serves as the reference cell. The alumina block provides similar heat capacity and thermal conductivity of the two cells in order to avoid secondary effects on the calorimeter signal. The furnace contains two further single thermocouples. One measures the sample temperature

and the other is used to control the furnace temperature with a Eurotherm 818 controller.

Fig. 2.3: Setaram Calvet-type microcalorimeter.

Fig. 2.4: Drop unit of the calorimeter.

All thermocouples are of type S (Pt/Pt-10 wt%.Rh). The furnace can be operated from room temperature up to 1100°C. The measuring cell is charged with a quartz tube that contains the sample crucible, which is made of graphite. The quartz tube is connected to the automatic drop unit. The maximum of 25 samples can be dropped into the reaction cell. Fig.2.4 shows the drop unit of the calorimeter. The automation of the isoperibol calorimeter is described in [Hayer 1987]. The entire system is gastight and can be evacuated and flushed with a protective gas. To prevent oxidation all measurements were performed under argon flow (approximately 30 cm^3/min). After each series of drops, the calorimeter was calibrated by adding 5 pieces of standard α-Al_2O_3 from NIST (National Institute of Standards and Technology, Gaithersburg, MD).

The interval between the individual drops was 40 min. The obtained signals were recorded and integrated.

The program HiQ from National Instruments is the software for evaluation and presentation of numerical data. Import, calculations, graphical presentations, and the export of data can also be automated by Programming HiQ-scripts. Data of time, Voltage (proportional to the heat flow) as well as temperature data are recorded by LabView (Laboratory Virtual Instrument Engineering Workbench) and written to a HiQ-notebook. For each period of the experiment, the notebook then contains the following data: an array of time and voltage, and the temperatures measured at the beginning of the period. The signal curve is smoothed by substituting each data point by the mean value of 25 points before and after. For each period the smoothed voltage signal is integrated over time using a horizontal base line. The base line is determined by calculating the mean of 30 values before the drop. To correct deviations of the horizontal

base line from the real signal level after the drop a triangle correction is applied. Finally, the export of integrated signal areas is made automatically by the programming scripts. The more detailed information about the calorimeter instrument and data evaluation has been given by Flandorfer et al. [2002 Flandorfer].

2.2.2. Calculation of thermodynamic properties

The measured enthalpy (integrated heat flow at constant pressure) is

$$H_{Signal} = n_i\left(H_{Sample,FT} - H_{Sample,DT}\right) + H_{Reaction} \qquad (2.16)$$

where n_i is the number of moles of the added sample, $H_{Sample,FT}$ the molar enthalpy at the respective furnace temperature (FT) of measurement and $H_{Sample,DT}$ the molar enthalpy at drop temperature (DT). The molar enthalpy differences ($H_{Sample,FT}$- $H_{Sample,DT}$) were calculated using the polynomials of pure elements from Dinsdale [1991 Dinsdale]. The approximate partial enthalpies of each drop element could be determined directly by

$$\Delta\overline{H_i} = \left(\frac{H_{Signal}}{n_i}\right) - \left(H_{Sample,FT} - H_{Sample,DT}\right) \qquad (2.17)$$

The integral enthalpy of mixing was calculated by

$$\Delta H_{Mix} = \frac{\sum H_{Reaction}}{(n+\sum n_{i)}} \qquad (2.18)$$

2.3 Differential thermal analysis (DTA)

2.3.1 Principle of differential thermal analysis

The principle of thermal analysis is based on different properties of materials which show different endothermic or exothermic reactions during heating and cooling.

The sample and a reference will be heated simultaneously and the temperature difference between the substances will be measured. DTA is a dynamic method. Heat is transferred between furnace, crucible, sample (reference) and thermocouple during the whole experiment. There are three mechanisms: convection, radiation and conduction of heat. Due to the dynamic character of the experiment, the temperature distribution is never completely homogenous. The temperature is measured at the bottom of the crucible.

2.3.2 Experimental apparatus and procedure

With our furnace temperatures up to 1873 K are possible, with a bifilar coiled heat pipe made of SiC. The thermocouple consists of PtRh10-Pt, the sensor head is made of Al_2O_3.

Pieces of the annealed samples weighing, 200–300 mg, were used for DTA measurements in evacuated and sealed quartz glass crucibles in a Netzsch DTA furnace (Netzsch, Selb, Germany) with a home-made controller system using Eurotherm components (Controller No. 3508, Eurotherm, Vienna, Austria). The measurements were performed at scanning rates of 5 K/min. Generally two heating and two cooling curves were recorded for each sample. The DTA instrument was calibrated using the high purity metals Sn, Sb and Au as standards to establish an internal calibration file.

2.3.3 Data evaluation

As the emf measurements have all taken place in the liquid state, only the melting points were determined by DTA to identify the lower temperature limit for the emf measurements. The upper limit was determined by the liquid electrolyte which would get electronic conductivity at about 1123 K. For the evaluation of the DTA measurements the last peak of the heating

curve was taken. As there were two heating curves collected with a rate of 5 K/min, the mean value of the peaks of the curves was taken as shown in Fig. 2.5.

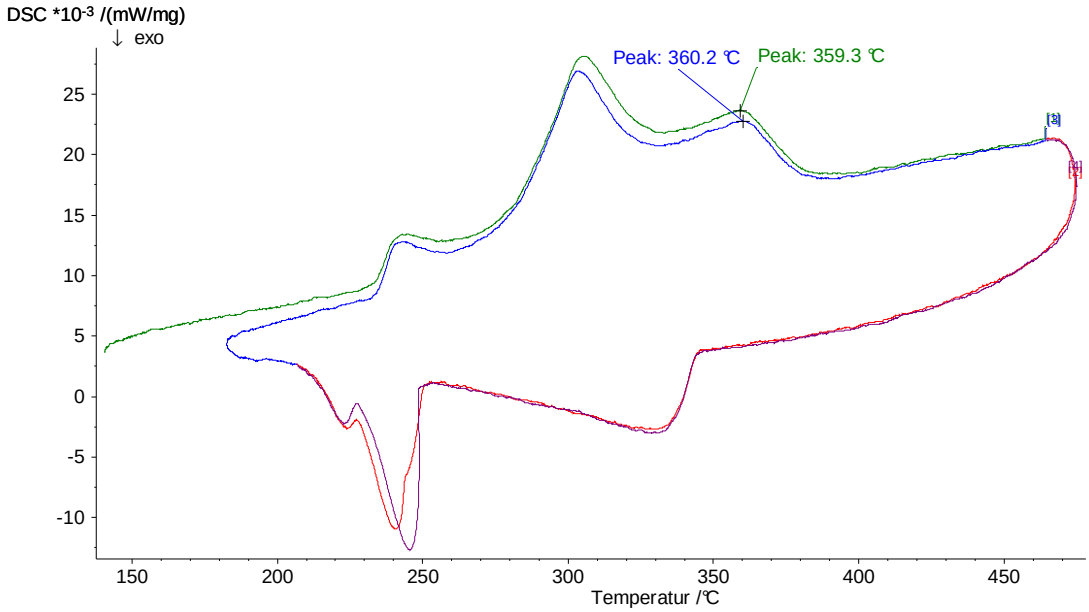

Fig. 2.5: Example of a DTA measurement.

The green and the blue line are heating curves. The purple and the red line are cooling curves. The last peak indicates the liquidus. Peaks before the liquidus are showing solid and solid liquid reactions. These were not evaluated as this was not part of the thesis.

2.4 Surface tension

Surface tension is the force acting on the surface of a liquid, tending to minimize the area of the surface; quantitatively, the force that appears to act across a line of unit length on the surface. [1974 Lapedes] In the body of a liquid, the time-averaged force exerted on any given molecule by its neighbors is zero. In the surface of a liquid the situation is quite different; beyond the free surface, there exist no molecules to counteract the forces of attraction exerted by molecules in the interior for molecules in the

surface. In consequence, molecules in the surface of a liquid experience a net attraction toward the interior of a drop. These centrally directed forces cause the droplet to assume a spherical shape, thereby minimizing both the free energy and surface area. [1989 Parker]

2.4.1 Principle of surface tension measurements

Thermodynamically, the surface tension is defined as the surface free energy per unit area. In a dynamic sense, surface tension represents the work or energy required to create one unit of additional surface at constant temperature. The dimensions of energy per unit are J/m^2 are equivalent to the dimensions of force per unit length N/m. [1988 Iida]

Sessile drop method

For the measurements, the sessile drop method has been used. It is based on the measurement of the dimensions of a stationary liquid drop, resting on a horizontal substrate. In that case the substrate is sintered aluminiumoxide. The sessile drop method has been used most extensively for measuring the surface tension of liquid metals and alloys, because of the following advantages. This method allows the determination of surface tension over a wide range of temperature compared with other methods used at high temperatures. Simultaneously the contact angle and the density can be determined.

2.4.2 Experimental apparatus

For the measurement of the surface tension a high temperature contact angle measuring system from Krüss, Germany was used consisting of the system DSA10HT (Special model) with an integrated high temperature tube furnace (LORA 1600-40-600-1) from HTM Reetz (Fig. 2.6.). A light

source was connected to the system to make the contour of the sample visible at lower temperatures before the sample starts to glow. Maximum temperatures of 1873 K can be reached with molybdenum as a heating element. During work, the heating chamber was flushed with argon to protect the molybdenum coil from oxygen. The working tube and the sample holder consist of sintered aluminum oxide. Two k-type (chromel-alumel) thermocouples are used to control the temperature of the sample. The thermocouples are inserted into the sample holder (Fig. 2.7.) to get very close to the sample. The second thermocouple serves as a controller. The program “Visk2006” was used to control the temperature.

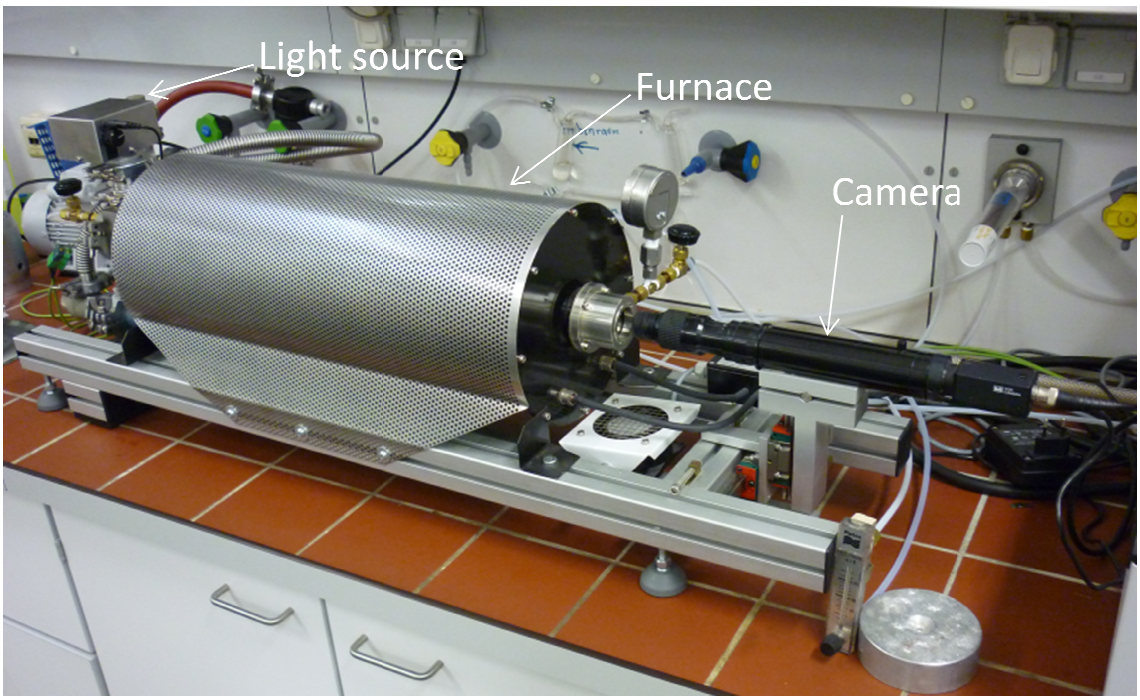

Fig. 2.6: Measuring system DSA10HT with integrated furnace LORA-1600-40-600-1.

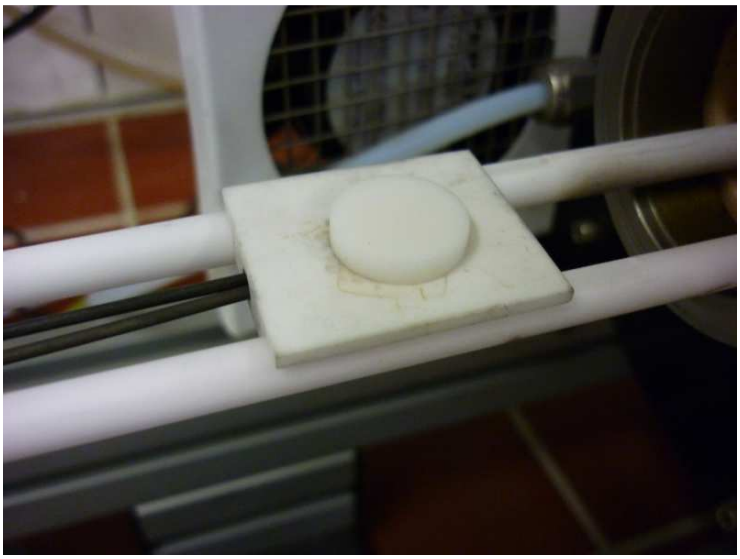

Fig. 2.7: Sample holder of the DSA10HT.

2.4.3 Data evaluation

The current way to evaluate a drop profile is based on the works of Bashforth and Adams [1892 Bashforth]. A system of differential equations is compiled based on the Young-Laplace equation for which numerical solutions are available and are used to calculate the profile of a drop. With variation of the parameters the calculated profile will be adapted to the experimental one.

The density and surface tension were determined with “Drop”, a program created by Markus Köhler in Germany. Evaluation is described in [2009 Gruner]:

In order to obtain the density and the surface tension the shape of the drop has to be analysed as shown in Fig. 2.8. The substrate line as well as the silhouette of the sample is found automatically by the evaluation software. Starting from the estimated centre of the sample, the image is radially scanned for an increase of the brightness above a certain level which is then addressed as the profile line of the sample. Assuming cylindrical symmetry the so obtained contour function $x(z)$ can be

integrated in order to obtain the volume *V* and, finally, with the sample's mass *m*, the density ρ of the droplet:

$$\rho = \frac{m}{V} = m\left[\pi \int_0^{z_{max}} dz x^2(z)\right] \tag{2.19}$$

The determination of the surface tension follows the analysis given by Rotenberg et al. [1983 Rotenberg]. The profile line is calculated by the program by numerically integrating the Laplace relation:

$$\Delta p = \sigma \cdot \left(\frac{1}{r_1} + \frac{1}{r_2}\right) = \frac{2\sigma}{R_0} + \rho g z \tag{2.20}$$

with Δp as the pressure difference across the fluid interface, σ the surface tension, g the gravitational acceleration and r_1 and r_2 as the main radii of curvature of the three-dimensional droplet shape. With R_0 as the curvature at the drop vertex, where $r_1 = r_2 = R_0$. Geometrical considerations implying cylindrical symmetry can be used to treat the radii of curvature numerically. In order to separate the influence of the density, the capillary parameter a is introduced, defined by

$$\sigma = \rho g a \tag{2.21}$$

After obtaining a theoretical profile line (shown as a blue curve in Fig. 2.8) it has to be compared with the experimental one (red curve) and the mean square deviation between the two curves is to be minimized by fitting the relative positioning of the contour functions as well as the general shape determined by the parameters a and R_0.

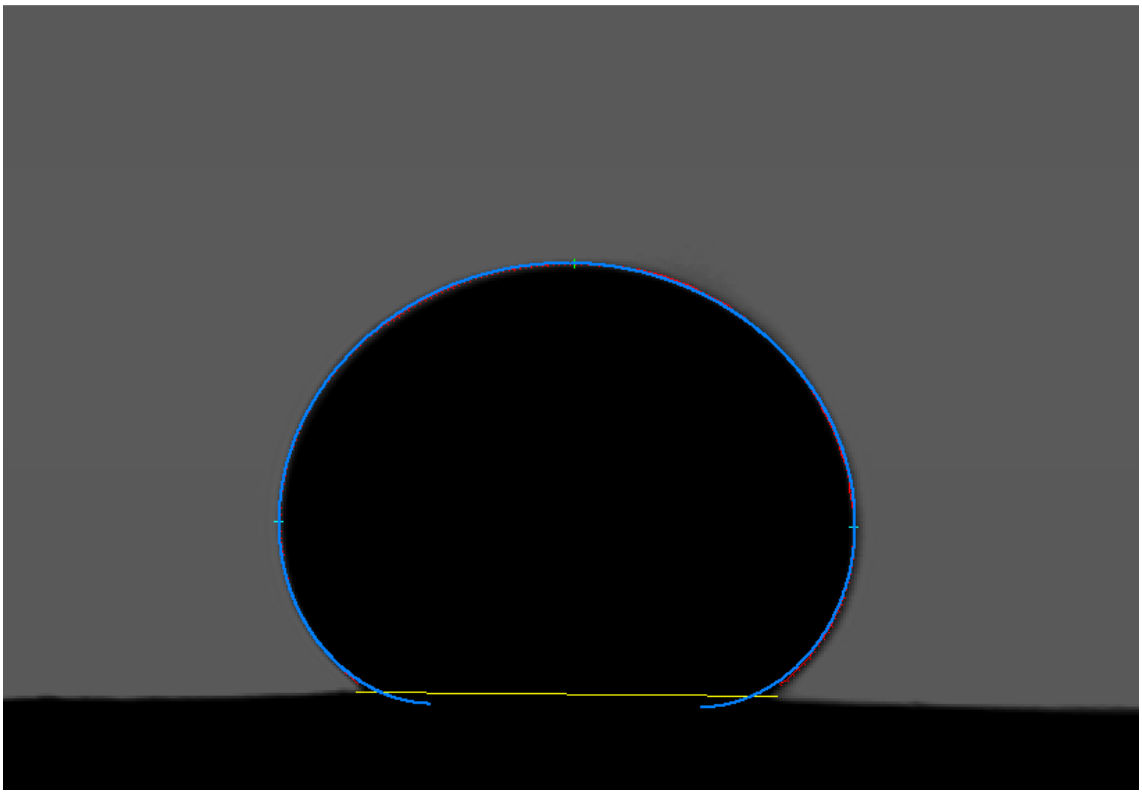

Fig. 2.8: Example of a liquid alloy.

Chapter 3: Emf investigations on the ternary Ag-Au-Sn system.

3.1 Literature review

3.1.1 Ag-Au system

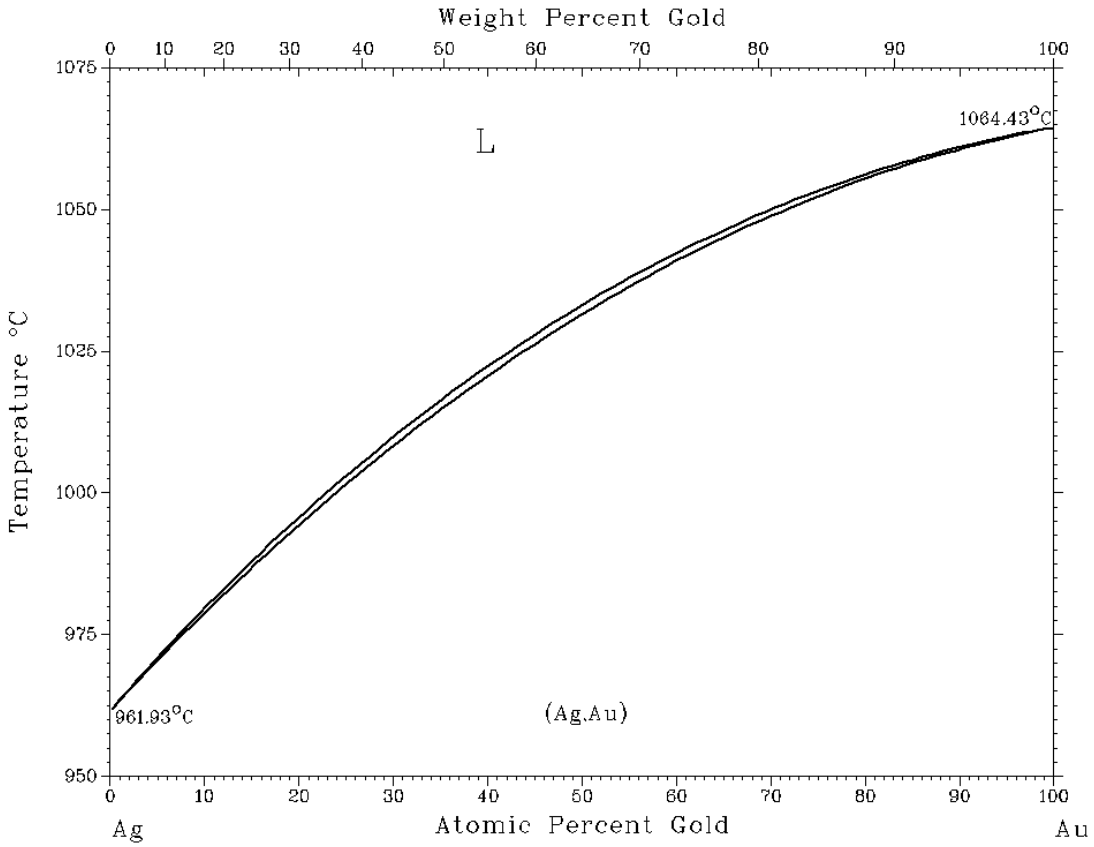

Fig. 3.1: Phase diagram of the Ag-Au system [1990 Massalski]

The Ag-Au phase diagram was evaluated by T.B.Massalski and H.Okamoto [1990 Massalski]. The very narrow liquidus-solidus gap was first predicted from thermodynamic considerations by Wagner [1954 Wagner] and first confirmed experimentally by White [1959 White]. Hultgren et al. [1973 Hultgren] selected the thermodynamic properties for liquid alloys at 1350 K. Investigations of the integral enthalpies of mixing have been performed by Topor and Kleppa [1984 Topor] and by Fitzner et al. [1999 Fitzner]. A phase diagram reassessment has been done by Park [2008 Park].

3.1.2 Ag-Sn system

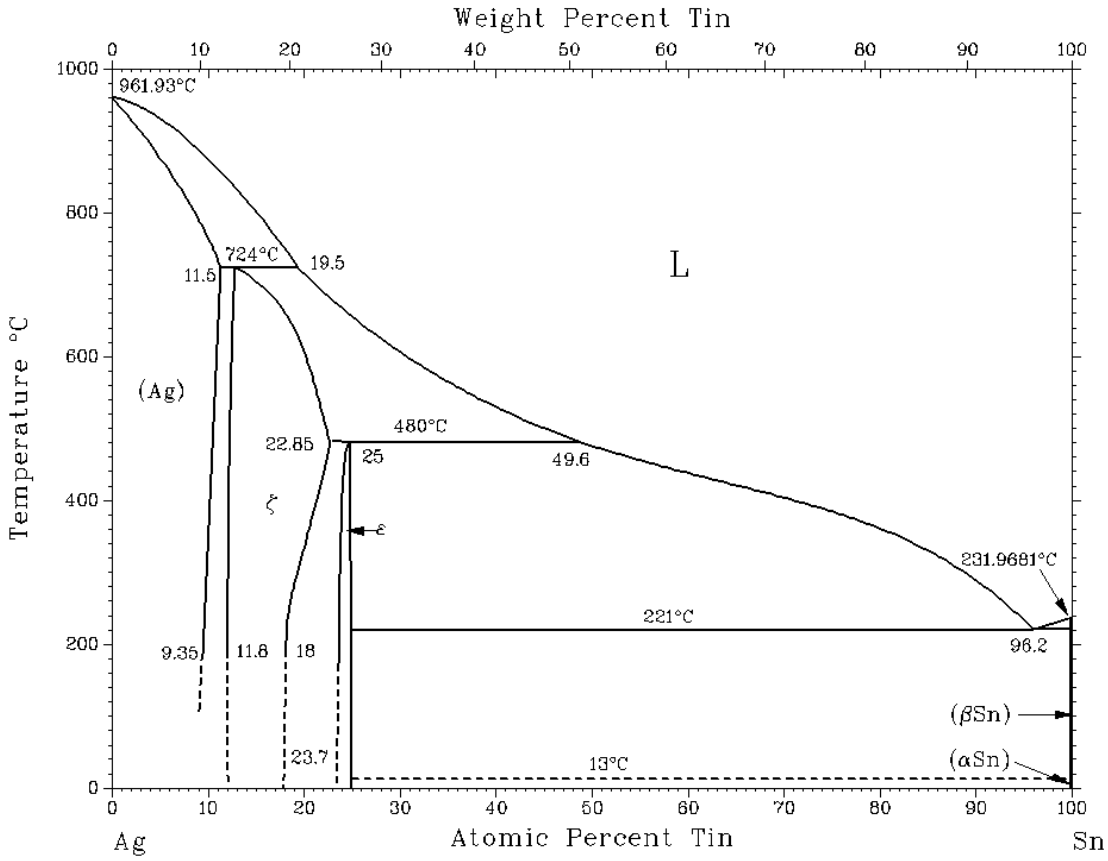

Fig. 3.2: Phase diagram of the Ag-Sn system [1990 Massalski].

Many investigations have been done on the Ag-Sn system. Thermodynamic experiments have been realized by Laurie [1966 Laurie] (emf and calorimetry) and Roy Chowdhury [1971 Roy-Chowdury] (emf). An assessment of the thermodynamic data has been done by Kubaschewski [1972 Kubaschewski]. Hultgren et al. [1973 Hultgren] selected the thermodynamic properties for liquid alloys at 900 K and at 1250 K, [1974 Farhi] (emf and calorimetry), [1976 Seetharaman] (emf), [1978 Iwase] (emf), [1987 Kameda] (emf). A thermodynamic evaluation has been done by Chevalier [1988 Chevalier] and Flandorfer did calorimetric measurements [2008 Flandorfer].

Surface tension has been determined by Moser [2001 Moser, 2001 Moser], Lee [2005 Lee, 2005 Lee] and Kucharski [2005 Kucharski].

3.1.3 Au-Sn system

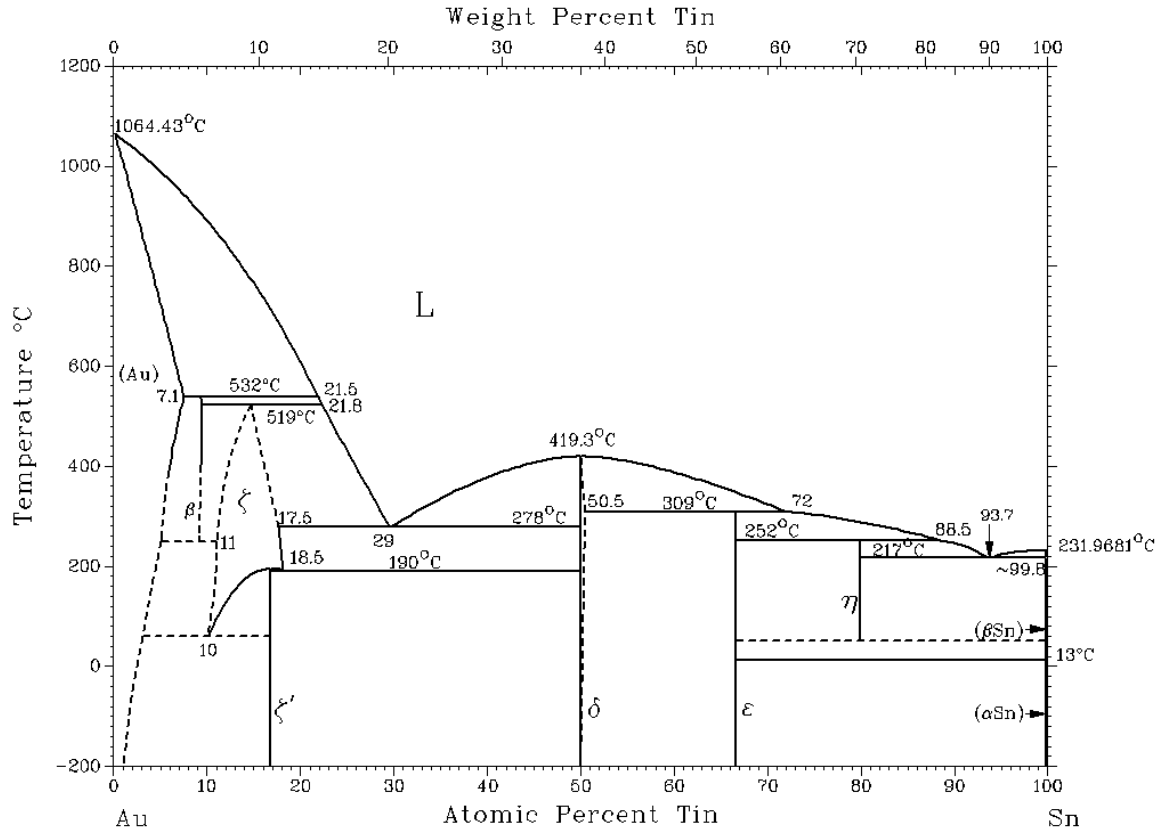

Fig. 3.3: Phase diagram of the Au-Sn system [1990 Massalski].

Many investigations have been done on the binary Au-Sn system. Kleppa did emf measurements [1950 Kleppa]. Jena did calorimetric measurements [1966 Jena]. Thermodynamic studies have been done by Petot [1972 Petot, 1972 Petot]. Hultgren et al. [1973 Hultgren] selected the thermodynamic properties for liquid alloys at 823 K. Itagaki determined the heats of mixing at 1373 K [1975 Itagaki]. Emf measurements have been done by Kameda [1977 Kameda]. Howard determined thermodynamic properties with mass spectrometry [1978 Howard]. Enthalpies of mixing were determined by Hayer [1981 Hayer].

Enthalpies of formation have been determined by Rakotomavo [1984 Rakotomavo]. A thermodynamic evaluation has been performed by Chevalier [1988 Chevalier]. Microstructural characterization has been done by Ivey [1998 Ivey], Sheen [2005 Sheen] and Tsai [2005 Tsai]. Lai studied the wetting reaction between the eutectic Au-Sn and Au foil. [2006 Lai].

3.1.4 Ag-Au-Sn system

Some information on thermal analysis is given by Evans and Prince [1974 Evans]. Enthalpies of formation were determined by Rakotomavo [1984 Rakotomavo] and Hassam [1988 Hassam]. Calorimetric measurements have been done by Li et al.[2008 Li]. A thermodynamic optimization using the CALPHAD method has been done by Wang et al. [2007 Wang] An experimental investigation and a thermodynamic assessment of phase equilibria in the Ag-Au-Sn system has been carried out by Gao et al. [2009 Gao]

3.2 Experimental procedure

Ternary alloys were prepared from high-purity metals (tin ingots, purity 99.999%; gold sheet, purity 99.95%; silver shot, purity 99.9%). Tin was a product of Johnson Matthey GmbH, Germany whereas gold and silver were products of Ögussa, Austria. To remove impurities from the silver surface, silver shots were heated for 10 min at 1083 K in a carbon crucible under vacuum. The metals were sealed into quartz capsules (for compositions see fig. 3.4) under vacuum and melted together at 1073 K. After 1 week, the alloys were quenched in ice water.

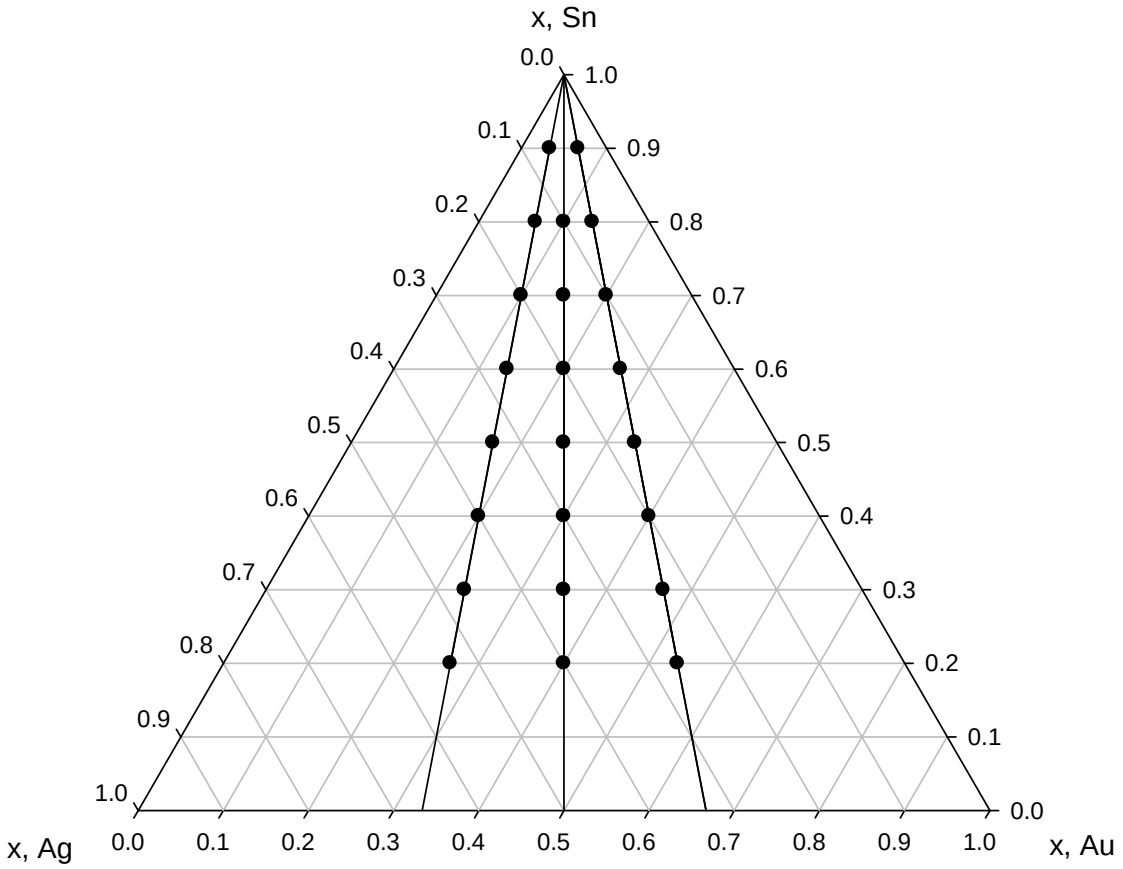

Fig. 3.4: Measured cross-sections and alloy compositions in the ternary Ag-Au-Sn system.

Before the EMF measurements started, the liquidus of the alloys was determined by differential thermal analysis so that the temperature range for EMF measurements could be determined. Samples weighing 200 mg to 300 mg were used for the DTA measurements. Evacuated, sealed quartz tubes were used for the measurements to avoid oxidation of the alloys. Two heating and cooling curves were recorded with a heating and cooling rate of 5 K/min. The average values of the melting points obtained from the two heating curves were taken and are given in Table 3.1. An EMF method with a liquid electrolyte was used to determine the activity of tin in the liquid alloys. The electrolyte consisted of the eutectic mixture of KCl (purity 99.5%) and LiCl (purity 99%) with addition of about 0.5 at.%

$SnCl_2$ (purity 98%). The $SnCl_2$ was added directly to the EMF cell before the measurement and not during the cleaning process of the electrolyte because the chlorine gas would oxidize the Sn^{2+} to Sn^{4+}. For the EMF measurements, the following cell arrangement was used:

$$W, Sn_{(l)}/KCl\text{-}LiCl\text{-}SnCl_2/Ag\text{-}Au\text{-}Sn_{(l)},W$$

3.3 Results

3.3.1 Liquidus temperatures

	Ag:Au=2:1	Ag:Au=1:1	Ag:Au=1:2
x, Sn	Liquidus *T* (K)	Liquidus *T* (K)	Liquidus *T* (K)
0.2	975	967	948
0.3	831	793	744
0.4	751	701	637
0.5	700	666	622
0.6	677	620	586
0.7	648	603	559
0.8	581	571	525
0.9	514	490	485

Table 3.1: Liquidus temperatures for the Ag:Au 2:1, 1:1 and 1:2 cross-section.

3.3.2 Measured emf values

Table 3.2: Measured emf data of liquid Ag-Au-Sn alloys.

Cross-section Ag:Au=2:1

x, Sn	emf (mV)
0.2	79.34+0.0602·*T*(±0.05)
0.3	16.53+0.0685·*T*(±0.68)
0.4	-12.74+0.0728·*T*(±0.21)
0.5	-5.67+0.0421·*T*(±0.05)
0.5[*1]	-6.38+0.0423·*T*(±0.45)
0.6	-9.95+0.0390·*T*(±0.12)
0.7	-7.08+0.0253·*T*(±0.29)
0.8	-0.81+0.0103·*T*(±0.02)
0.9	-1.25+0.0056·*T*(±0.08)

[*1]Remeasured

Cross-section Ag:Au=1:1

x, Sn	emf (mV)
0.2	107.08+0.0552·*T*(±0.49)
0.3	17.05+0.0837·*T*(±0.74)
0.4	6.68+0.0606·*T*(±0.26)
0.5	-2.29+0.0509·*T*(±0.04)
0.6	-4.11+0.0372·*T*(±0.03)
0.7	0.83+0.0171·*T*(±0.10)
0.8	-0.42+0.0113·*T*(±0.05)
0.9	-0.05+0.0046·*T*(±0.03)

Cross-section Ag:Au=1:2

x, Sn	emf (mV)
0.2	126.76+0.0436·*T*(±0.49)
0.3	41.65+0.0760·*T*(±0.59)
0.4	12.78+0.0649·*T*(±0.49)
0.5	7.71+0.0429·*T*(±0.81)
0.6	4.52+0.0280·*T*(±0.78)
0.7	-1.11+0.0197·*T*(±0.26)
0.8	0.26+0.0071·*T*(±0.56)
0.9	-1.54+0.0041·*T*(±0.04)

Our investigation started from the binary Ag-Au system by adding Sn. The activity of Sn was measured along three cross-sections. The T versus EMF curves at each composition exhibited straight lines, expressed by Eq.2.2. From the EMF data, the activity of tin, the partial Gibbs free energy, and the partial molar enthalpies and entropies were calculated and are given in Table 3.3. The integrated thermodynamic quantities are listed in Table 3.4. The activities of Sn in the ternary Ag-Au-Sn system and in the Ag-Sn [1987 Kameda] and Au-Sn system [1977 Kameda] at 973 K are shown in Fig.3.5. In the Ag-Sn system, the activities show a negative deviation from Raoult's law up to 37 at.% Sn, after which it becomes positive. At the Ag:Au 2:1 cross-section, the activity of Sn is less than in the Ag-Sn system. It was observed that the value for the activity at 50% Sn is more positive than expected. The sample of Ag:Au 2:1 and 50 at.% Sn was measured twice but gave nearly identical results (see table 3.2 and 3.3). We have no explanation for the more positive value of the activity of Sn at this composition. At the Ag:Au 1:1 cross-section, the negative deviation from

Raoult´s law increases. This is also observed for the activities at the Ag:Au 1:2 cross-section from 20 at.% to 70 at.% Sn. However, at 80 at.% and 90 at.% Sn, positive deviation from Raoult´s law was observed.

3.3.3. Partial molar quantities of tin in liquid Ag-Au-Sn alloys.

Table 3.3.: Partial molar quantities of tin in liquid Ag-Au-Sn alloys.

Cross-section Ag:Au=2:1

x, Sn	a	ln γ	α-function	$\overline{\Delta G}$ (J/mol)	$\overline{\Delta H}$ (J/mol)	$\overline{\Delta S}$ (J/K·mol)
0.2	0.041	-1.5847	-2.6241	-26607	-15310	11.61
0.3	0.1394	-0.7664	-1.5663	-15949	-3190	13.22
0.4	0.2512	-0.4652	-1.2962	-11188	2458	14.05
0.5	0.4308	-0.1490	-0.5916	-6804	1094	8.12
0.5[*1]	0.4333	-0.1443	-0.5773	-6774	1230	8.23
0.6	0.5098	-0.1629	-1.0216	-5455	1921	7.53
0.7	0.6593	-0.0599	-0.5212	-3265	1367	4.88
0.8	0.8040	0.0050	0.1212	-1766	156	1.99
0.9	0.9026	0.0029	0.2641	-832	241	1.08

[*1]Remeasured

Cross-section Ag:Au=1:1

x, Sn	a	ln γ	α-function	$\overline{\Delta G}$ (J/mol)	$\overline{\Delta H}$ (J/mol)	$\overline{\Delta S}$ (J/K·mol)
0.2	0.0217	-2.2210	-3.4739	-30993	-20664	10.65
0.3	0.0922	-1.1798	-2.4086	-19288	-3290	16.15
0.4	0.2097	-0.6458	-1.7948	-12639	-1289	11.69
0.5	0.3242	-0.4332	-1.7341	-9114	442	9.82
0.6	0.4655	-0.2538	-1.5901	-6190	794	7.18
0.7	0.6546	-0.0671	-0.7465	-3429	-160	3.30
0.8	0.7770	-0.0292	-0.7300	-2042	80	2.18
0.9	0.8991	-0.0010	-0.0943	-861	9	0.89

Cross-section Ag:Au=1:2

x, Sn	a	ln γ	α-function	$\overline{\Delta G}$ (J/mol)	$\overline{\Delta H}$ (J/mol)	$\overline{\Delta S}$ (J/K·mol)
0.2	0.0177	-2.4248	-3.7911	-32649	-24461	8.41
0.3	0.0631	-1.5591	-3.1853	-22367	-8037	14.67
0.4	0.1636	-0.8940	-2.4891	-14662	-2466	12.52
0.5	0.3068	-0.4884	-1.9587	-9569	-1488	8.28
0.6	0.4654	-0.2540	-1.5872	-6187	-872	5.40
0.7	0.6452	-0.0815	-0.9030	-3543	214	3.80
0.8	0.8283	0.0348	0.8722	-1523	-51	1.37
0.9	0.9435	0.0472	4.7141	-471	297	0.79

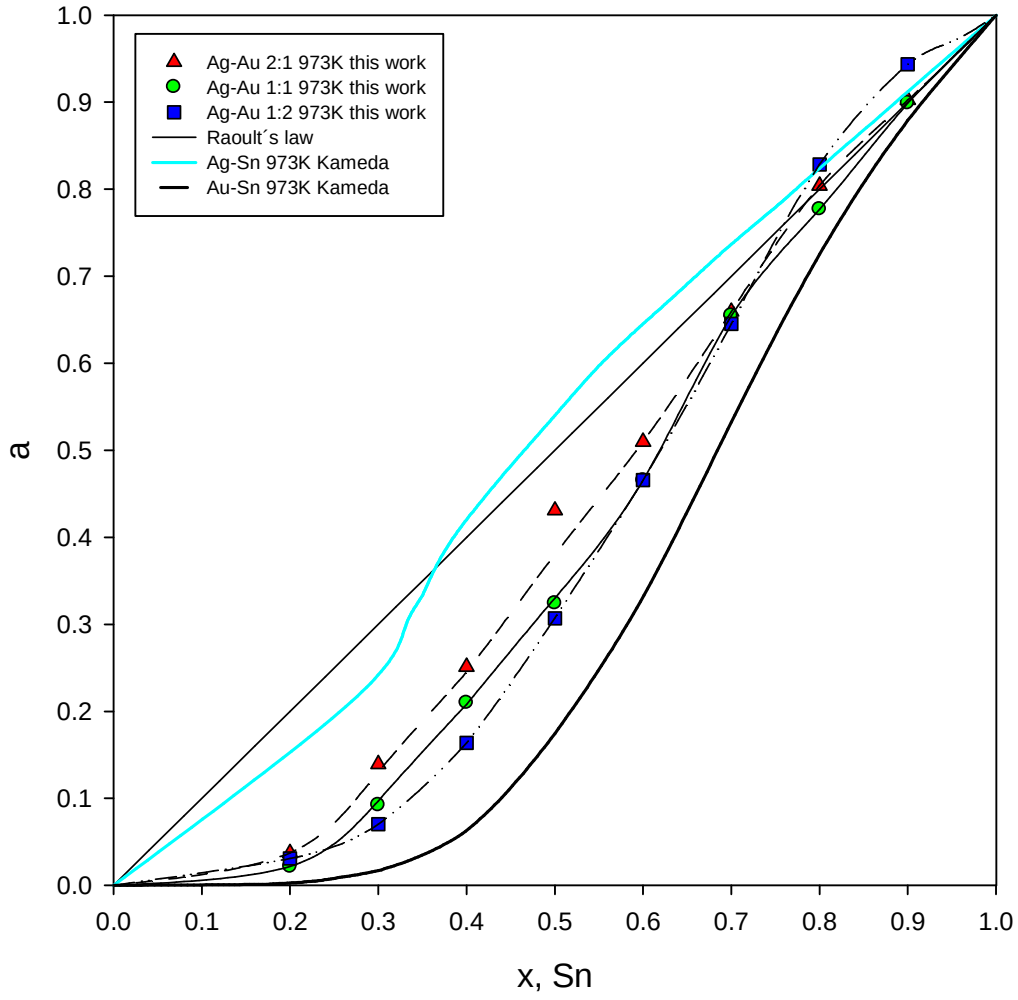

Fig. 3.5: Activities of Sn in Ag-Au-Sn alloys and the binary Ag-Sn [1987 Kameda] and Au-Sn [1977 Kameda] systems.

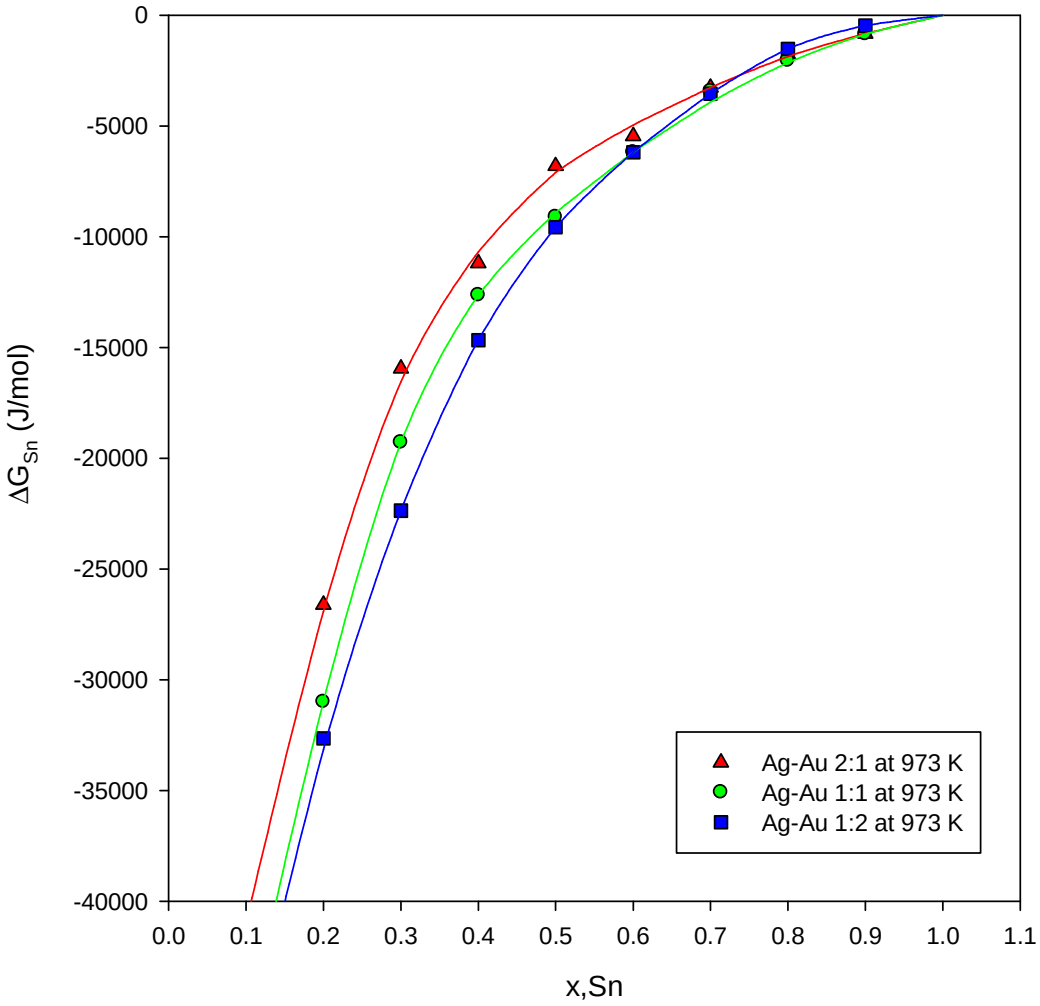

Fig. 3.6: Partial Gibbs energies for the Ag:Au 2:1, 1:1 and 1:2 cross-sections at 973 K.

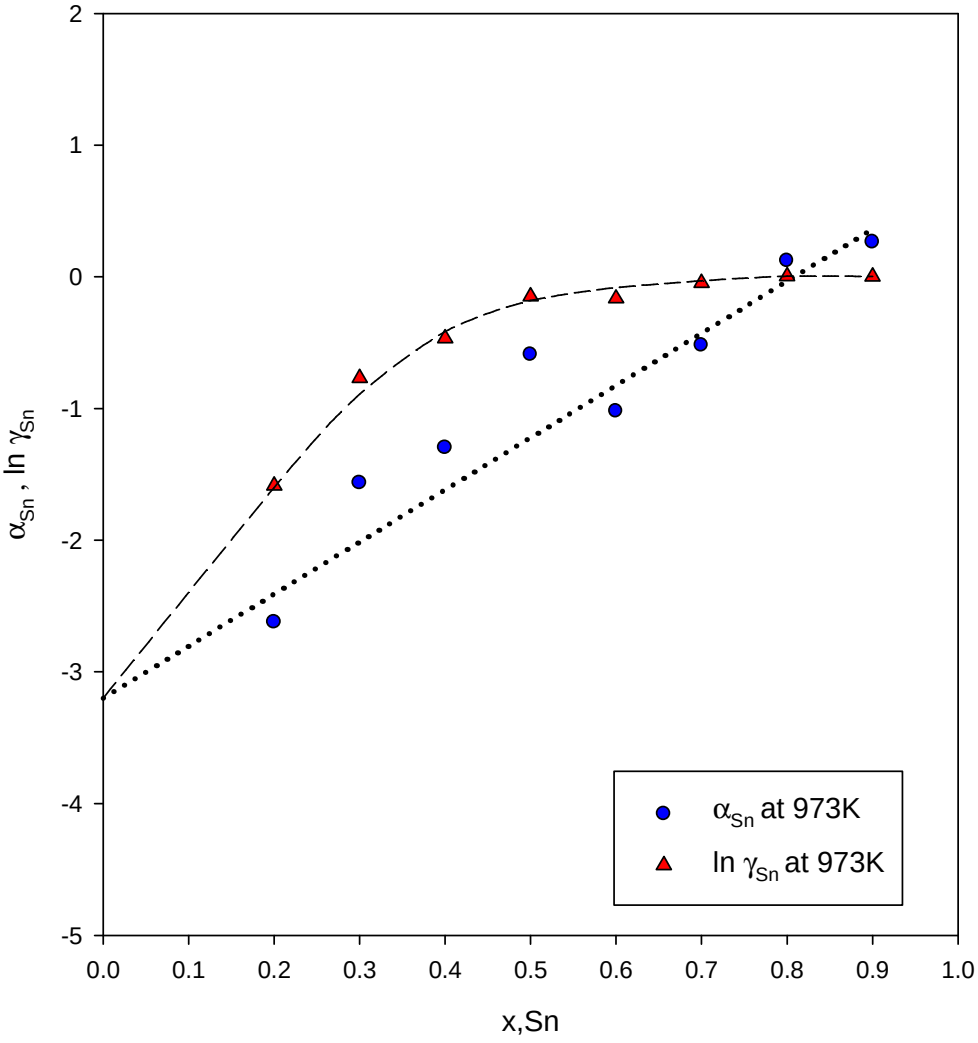

Fig. 3.7: α and ln γ for the Ag:Au 2:1 cross-section at 973 K.

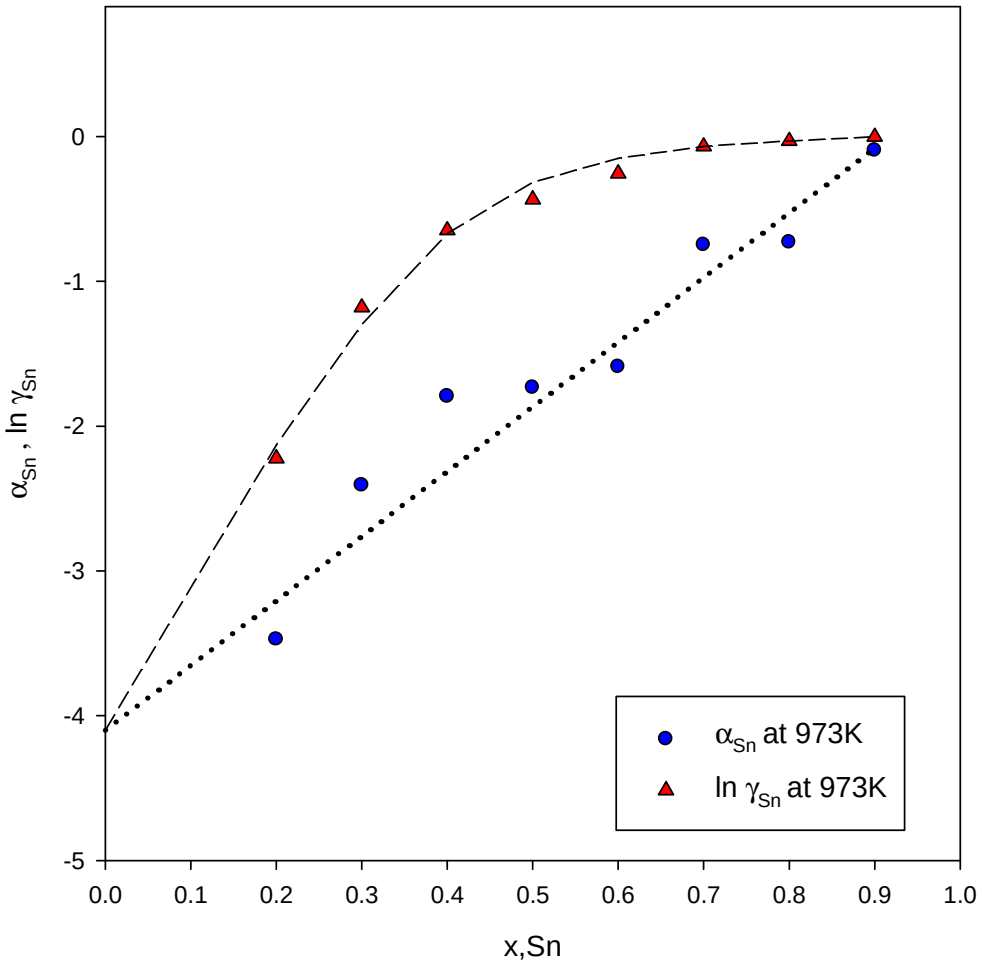

Fig. 3.8: α and ln γ for the Ag:Au 1:1 cross-section at 973 K.

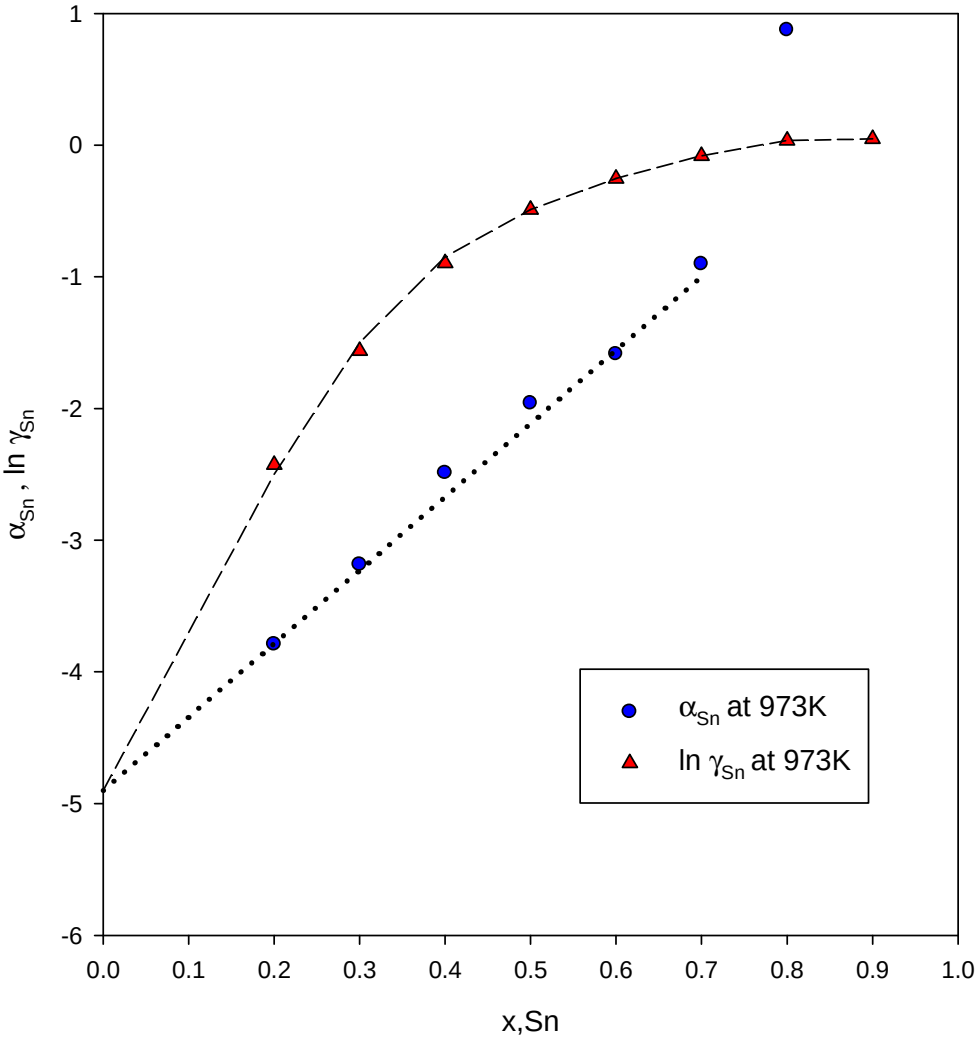

Fig. 3.9: α and ln γ for the Ag:Au 1:2 cross-section at 973 K.

The values for a and ln γ are shown in Fig.3.7-Fig.3.9 and extrapolated to $x_{Sn}=0$ to get the first value for the integration of the alpha function. Regarding the apparent fluctuations of the alpha values, ln γ has also been used for the extrapolation towards $x_{Sn}=0$ in order to confirm the extrapolation of the alpha function.

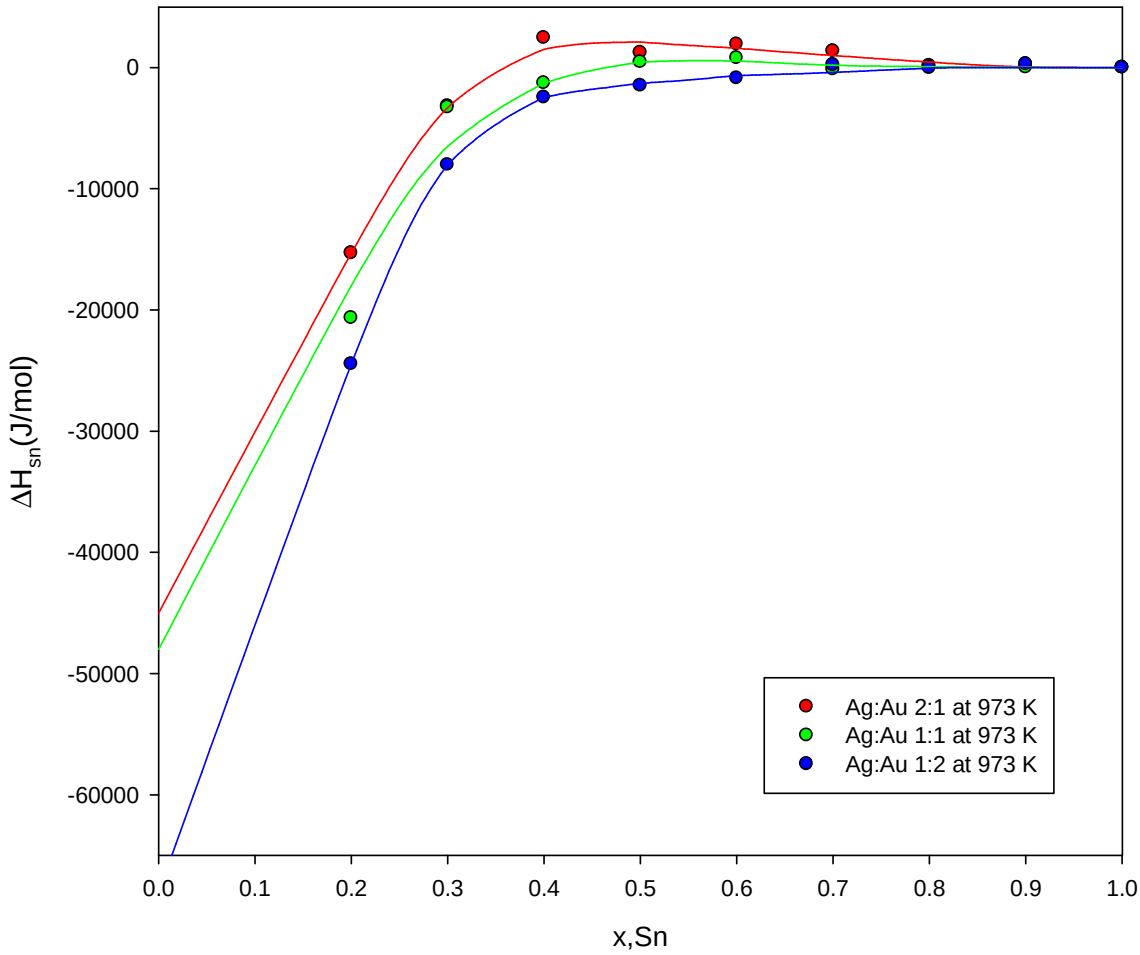

Fig. 3.10: Partial enthalpies of mixing of tin for the Ag:Au 2:1, 1:1 and 1:2 cross-sections at 973 K.

3.3.4 Integral molar quantities of tin in liquid Ag-Au-Sn alloys

Based on the partial quantities of tin, the integral enthalpy of mixing and the excess Gibbs free energy for liquid Ag-Au-Sn alloys were calculated along the constant molar ratios of Ag:Au = 2:1, 1:1 and 1:2 applying equations 2.11 and 2.12 to the Ag-Au-Sn system:

$$\Delta H = (1 - x_{Sn})[\Delta H_{Sn=0} + \int_0^{x_{Sn}} \frac{\Delta \overline{H}_{Sn}}{(1-X_{Sn})^2} dx_{Sn}]_{x_{Ag}/x_{Au}}$$

$$\Delta G^{xs} = (1 - x_{Sn})[\Delta G^{xs}_{Sn=0} + \int_0^{x_{Sn}} \frac{\Delta \overline{G^{xs}_{Sn}}}{(1-X_{Sn})^2} dx_{Sn}]_{x_{Ag}/x_{Au}}$$

And with introducing the alpha-function (see eq.2.14) leading to:

$$\Delta G^{xs} = (1 - x_{Sn})[\Delta G^{xs}_{Sn=0} + RT \int_0^{x_{Sn}} \alpha \, dx_{Sn}]_{x_{Ag}/x_{Au}}$$

For the integration of the excess Gibbs free energy in the ternary system, the constant starting values of $\Delta G^{xs}_{Sn=0}$ in the Ag-Au system were taken from the data compiled by Hultgren et al. [1973 Hultgren] and calculated to the temperature used for the measurements by combining the enthalpy ΔH with the excess entropy term $T\Delta S^{xs}$, assuming that ΔH and ΔS^{xs} are constant. The constant starting values of $\Delta H_{Sn=0}$ were taken from Fitzner at al. [1999 Fitzner]. All integral molar quantities were determined for 973 K. The integral entropy was derived from the equation

$$\Delta G = \Delta H - T\Delta S$$

Table 3.4: Integral molar quantities of tin in liquid Ag-Au-Sn alloys

Cross-section Ag:Au=2:1

x, Sn	ΔG (J/mol)	ΔG^{xs} (J/mol)	ΔH (J/mol)	ΔS (J/K·mol)
0	-6849	-1700	-3862	3.07
0.2	-13205	-5038	-8526	4.81
0.3	-14101	-5570	-8787	5.46
0.4	-13990	-5456	-7711	6.45
0.5	-13111	-4928	-6411	6.89
0.6	-11708	-4204	-5158	6.73
0.7	-9827	-3340	-3886	6.11
0.8	-7337	-2259	-2584	4.88
0.9	-4259	-1114	-1276	3.07

Cross-section Ag:Au=1:1

x, Sn	ΔG (J/mol)	ΔG^{xs} (J/mol)	ΔH (J/mol)	ΔS (J/K·mol)
0	-7408	-1800	-4323	3.17
0.2	-14876	-6050	-9840	5.18
0.3	-16082	-7200	-10193	6.05
0.4	-16013	-7204	-8959	7.25
0.5	-15128	-6717	-7528	7.81
0.6	-13599	-5911	-5988	7.82
0.7	-11341	-4717	-4408	7.13
0.8	-8434	-3264	-2870	5.72
0.9	-4856	-1665	-1420	3.53

Cross-section Ag:Au=1:2

x, Sn	ΔG (J/mol)	ΔG^{xs} (J/mol)	ΔH (J/mol)	ΔS (J/K·mol)
0	-6672	-1520	-3766	2.99
0.2	-15008	-6840	-11606	3.5
0.3	-16507	-8002	-12032	4.6
0.4	-16735	-8201	-11181	5.71
0.5	-15916	-7733	-9697	6.39
0.6	-14265	-6761	-7942	6.5
0.7	-11859	-5373	-5987	6.03
0.8	-8662	-3584	-3930	4.86
0.9	-4711	-1566	-1887	2.9

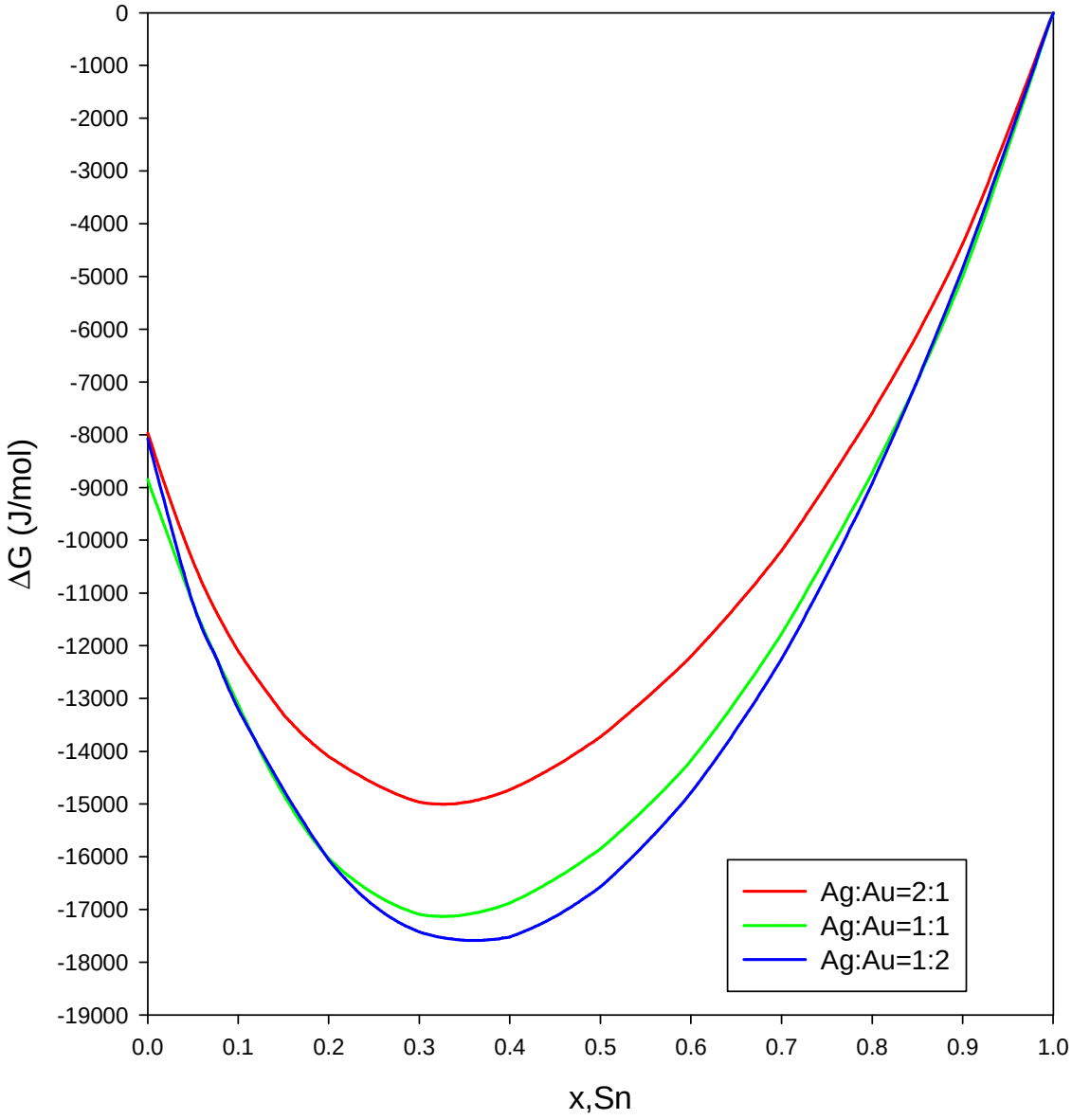

Fig. 3.11: Integral Gibbs free energy curves ΔG (J/mol) for the Ag:Au 2:1, 1:1 and 1:2 cross-sections at 973 K.

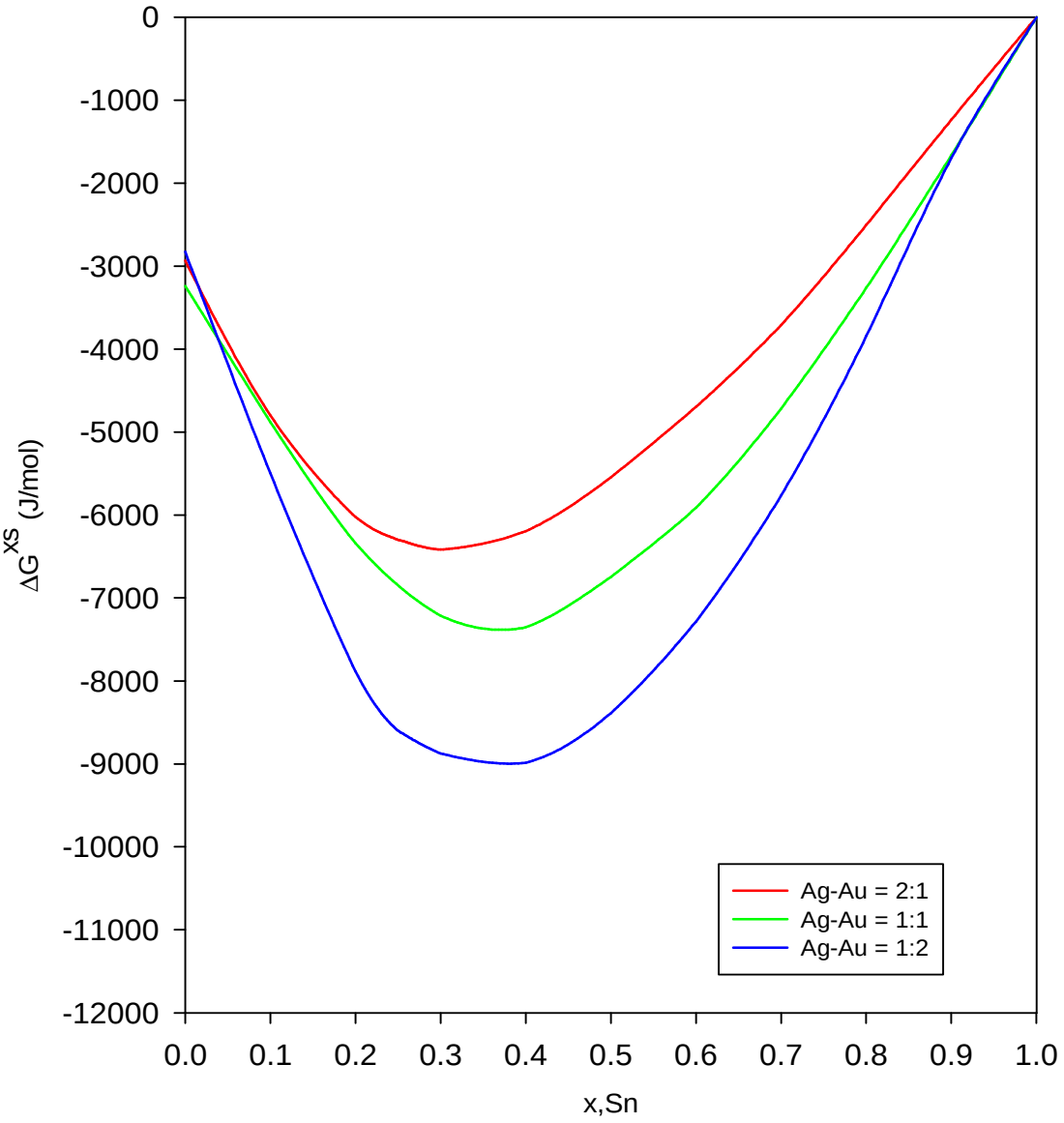

Fig. 3.12: Integral excess Gibbs free energy ΔG^{xs} (J/mol) for the Ag:Au: 2:1, 1:1, and 1:2 cross-sections at 973 K.

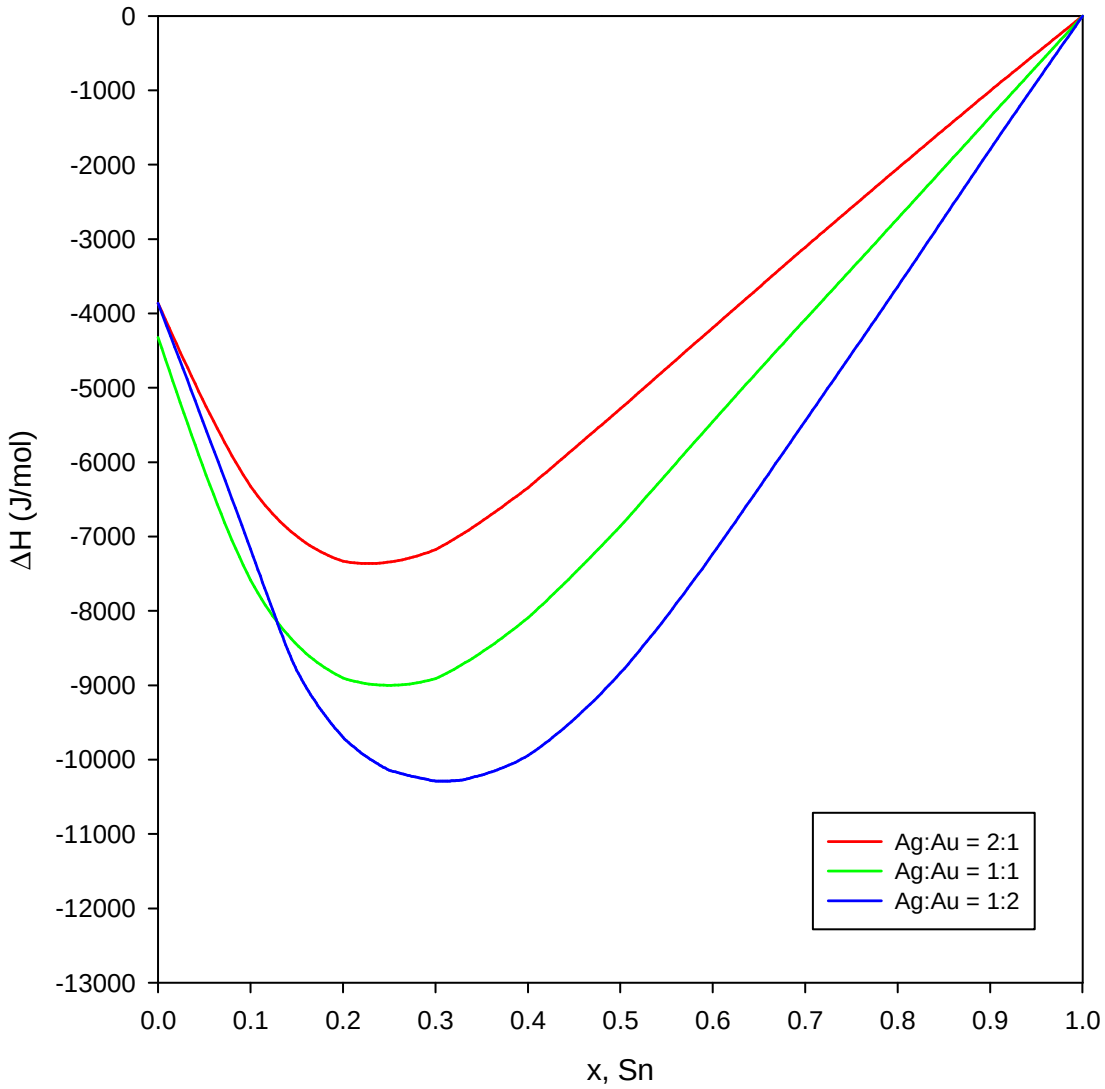

Fig. 3.13: Integral enthalpy of mixing ΔH (J/mol) for the Ag:Au: 2:1, 1:1, and 1:2 cross-sections at 973 K.

The integral Gibbs free energy values become more negative from the Ag-rich side (Ag:Au 2:1) to the Au-rich side (Ag:Au 1:2). The curves are shown in Fig. 3.11. The trend for the excess Gibbs energy curves is the same (Fig.3.12). It has been observed that the minimum ΔG and ΔG^{xs} is shifted to higher tin content from the Ag-rich to the Au-rich side. The integrated enthalpies of mixing are shown in Fig. 3.13. The minimum ΔH is also shifted to higher tin content from the Ag-rich to the Au-rich side.

The excess Gibbs free energies for the Ag-Sn and the Au-Sn system for plotting the iso-Gibbs free energy curves and the iso-excess Gibbs free energy curves in the ternary Ag-Au-Sn system were calculated from the EMF of the measurements of Kameda which covered the temperature range of 686 K to 983 K for the Ag-Sn system [1987 Kameda] and the temperature range of 944 K to 1256 K for the Au-Sn system [1977 Kameda]. The values for Ag-Au system were taken from Hultgren [1973 Hultgren]. The interaction parameters for the Gibbs free energy and the Gibbs free excess energy were calculated by using a Redlich–Kister fit. For the calculation of the interaction parameters for the enthalpy of mixing for the Au-Sn system the data from Hultgren et al. [1973 Hultgren] were taken, and for the Ag-Sn system the interaction parameters were determined from the work of Flandorfer et al. [2008 Flandorfer]. For the Ag-Au system the data compiled from Hultgren [1973 Hultgren] were taken. The iso-Gibbs free energy curves and the Iso-excess Gibbs free energy curves are plotted in Fig. 3.14 and Fig. 3.15., respectively. The plotted iso-enthalpy curves are shown in Fig. 3.16. All iso-curves shown herein were calculated using Redlich–Kister–Muggianu polynomials.

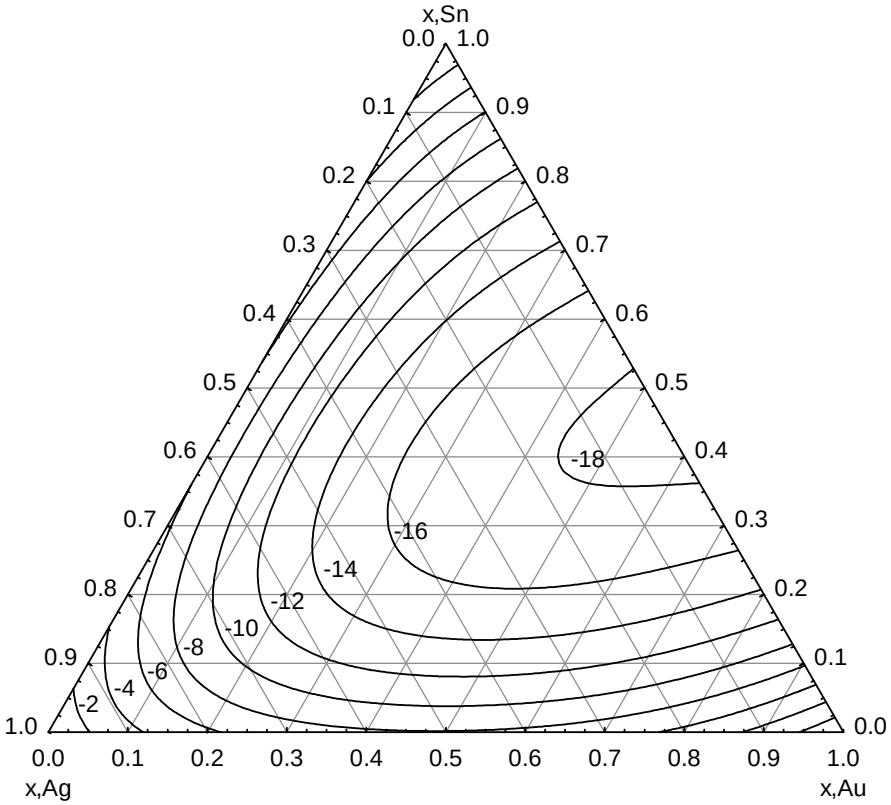

Fig. 3.14: Iso-Gibbs free energy curves (kJ/mol) for the Ag-Au-Sn system at 973 K.

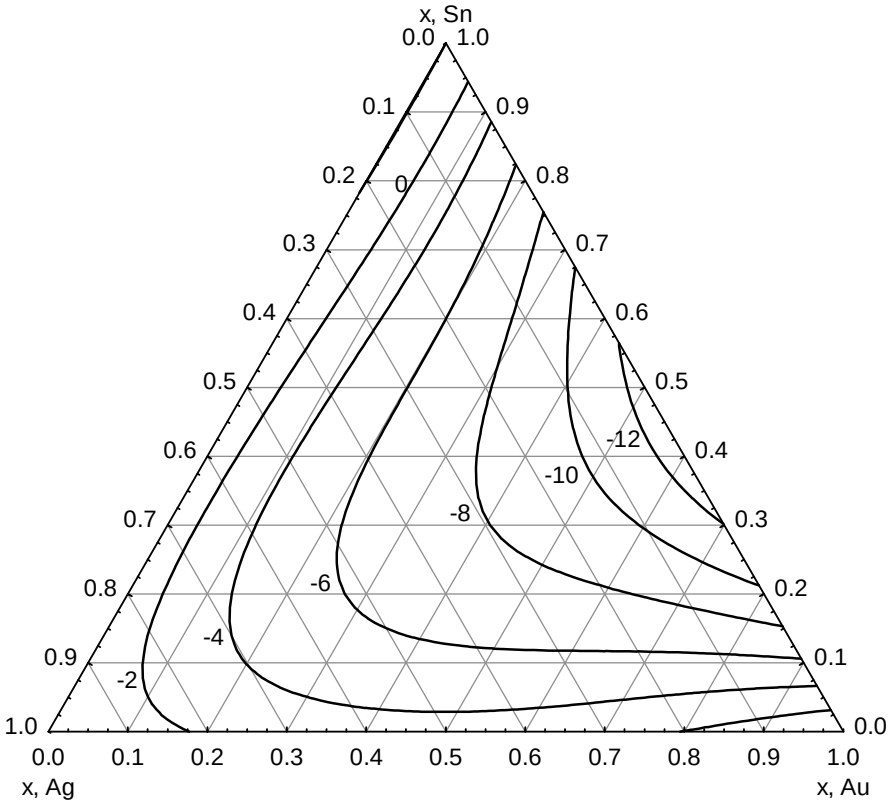

Fig. 3.15: Iso-excess Gibbs free energy curves (kJ/mol) for the Ag-Au-Sn system at 973 K.

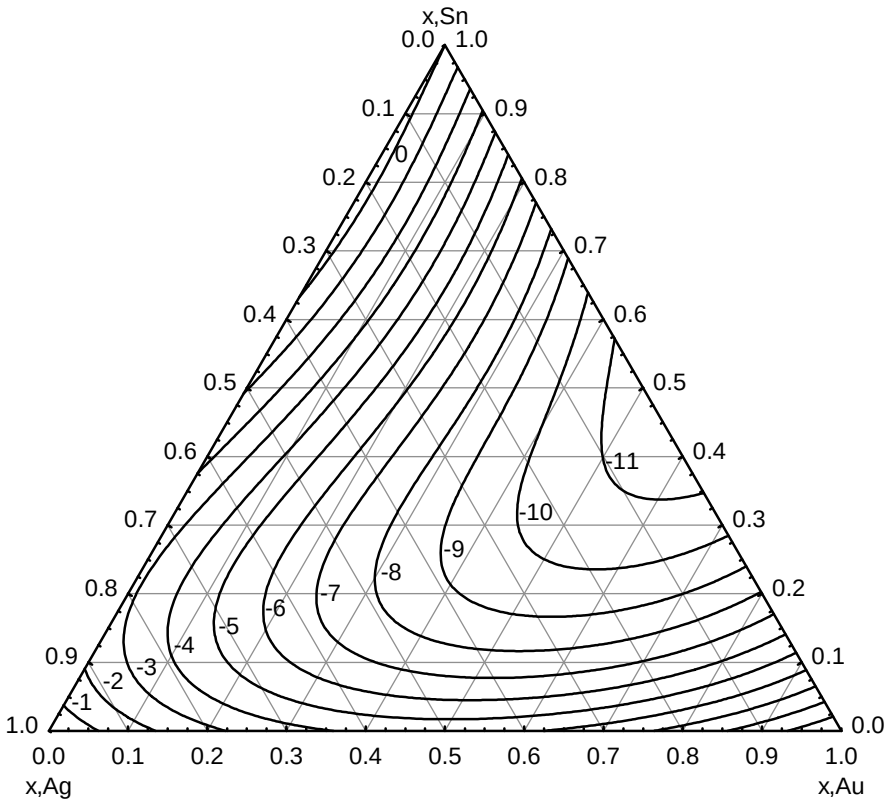

Fig. 3.16: Iso-enthalpy curves (kJ/mol) for the Ag-Au-Sn system at 973 K.

3.3.5. Comparison with calorimetric measurements

The integrated enthalpies of mixing, measured with the emf method, compared with data from Li [2008 Li] obtained by calorimetric measurements are shown in Fig. 3.19.. The raw data of the calorimetric measurements were used to calculate via Redlich–Kister–Muggianu polynomials the enthalpy values for the cross-sections that were measured with the EMF method. The minimum ΔH is also shifted to higher tin content from the Ag-rich to the Au-rich side. As shown in Fig. 3.19., the ΔH values determined with the EMF method are in very good agreement with the data obtained by calorimetric measurements.

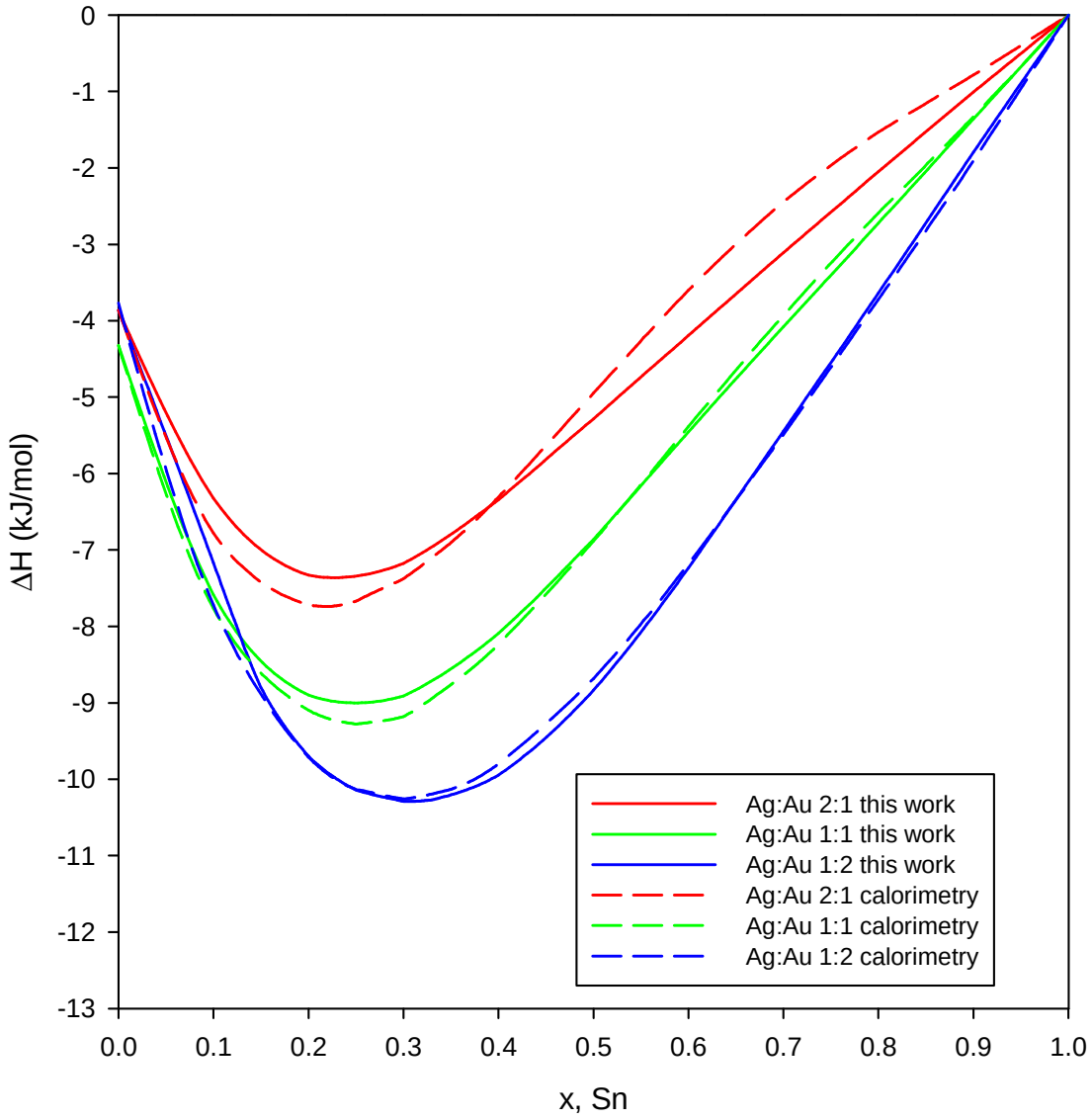

Fig. 3.17: Comparison of the Integral enthalpy of mixing ΔH for the Ag:Au = 2:1, 1:1, and 1:2 cross-sections at 973 K determined by emf method with calorimetric method [2008 Li].

3.3.6. Conclusion

Using an appropriate galvanic cell, the activities and partial free energies of Sn in liquid Ag-Au-Sn alloys were determined as a function of concentration and temperature. Thermodynamic properties were obtained for 27 alloys. Their compositions were situated on three cross-sections with the constant ratios of Ag:Au = 2:1, 1:1, and 1:2. The integral

properties for the ternary system were calculated at 973 K by Gibbs-Duhem integration. Comparisons of experimental results from the emf method with calorimetric measurements show, that the enthalpies of mixing determined by the emf method are in good agreement with the results Li [2008 Li] obtained by calorimetric measurements.

Chapter 4: Emf investigations on the ternary Au-Sb-Sn system

4.1. Literature review

4.1.1. Au-Sb system

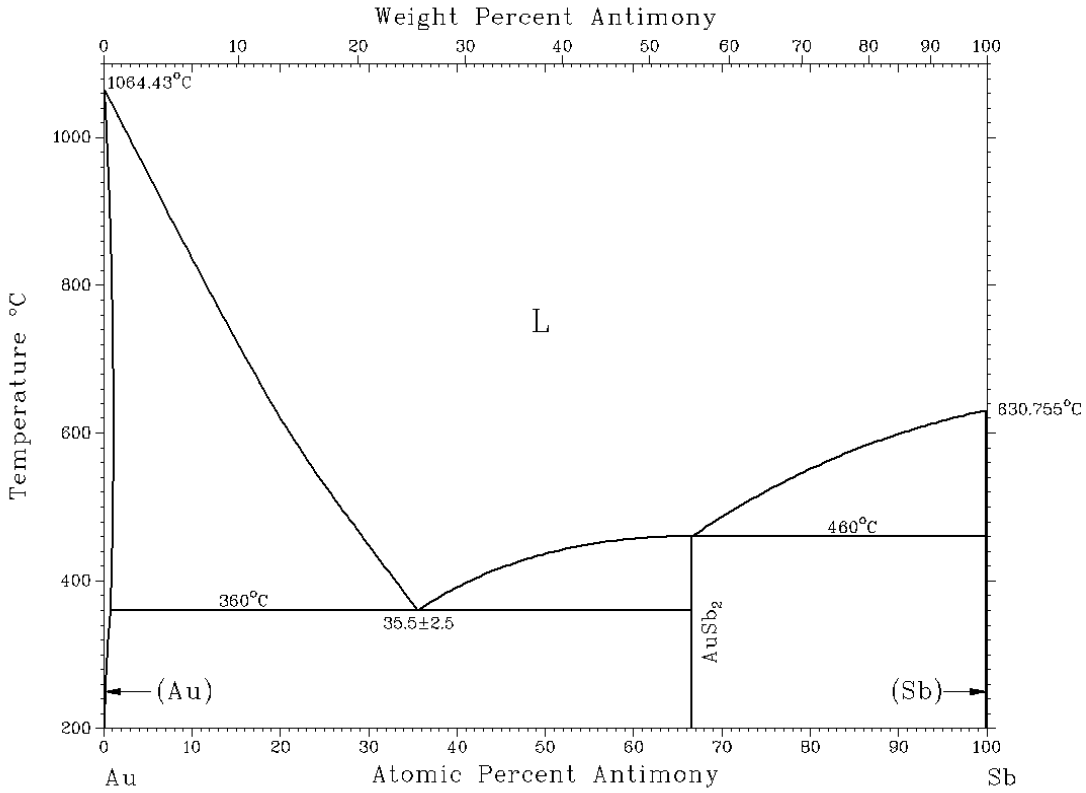

Fig. 4.1: Phase diagram of the Au-Sb system [1990 Massalski].

A review with an assessed phase diagram was first given by Massalski in 1984 [1984 Okamoto]. The heat of formation of the $AuSb_2$ compound was measured by Jena [1968 Jena]. Emf measurements have been performed by Kameda [1974 Kameda] and vapour pressure measurements by Hino [1975 Hino]. Itagaki did measurements on the heats of fusion [1976 Itagaki]. Chevalier [1989 Chevalier] did a thermodynamic evaluation. Anres [1994 Anres] investigated the heat of content of solid and liquid $AuSb_2$ compounds. Calorimetric investigations over a wide temperature range were done by Hayer [1995 Hayer].

4.1.2 Sb-Sn system

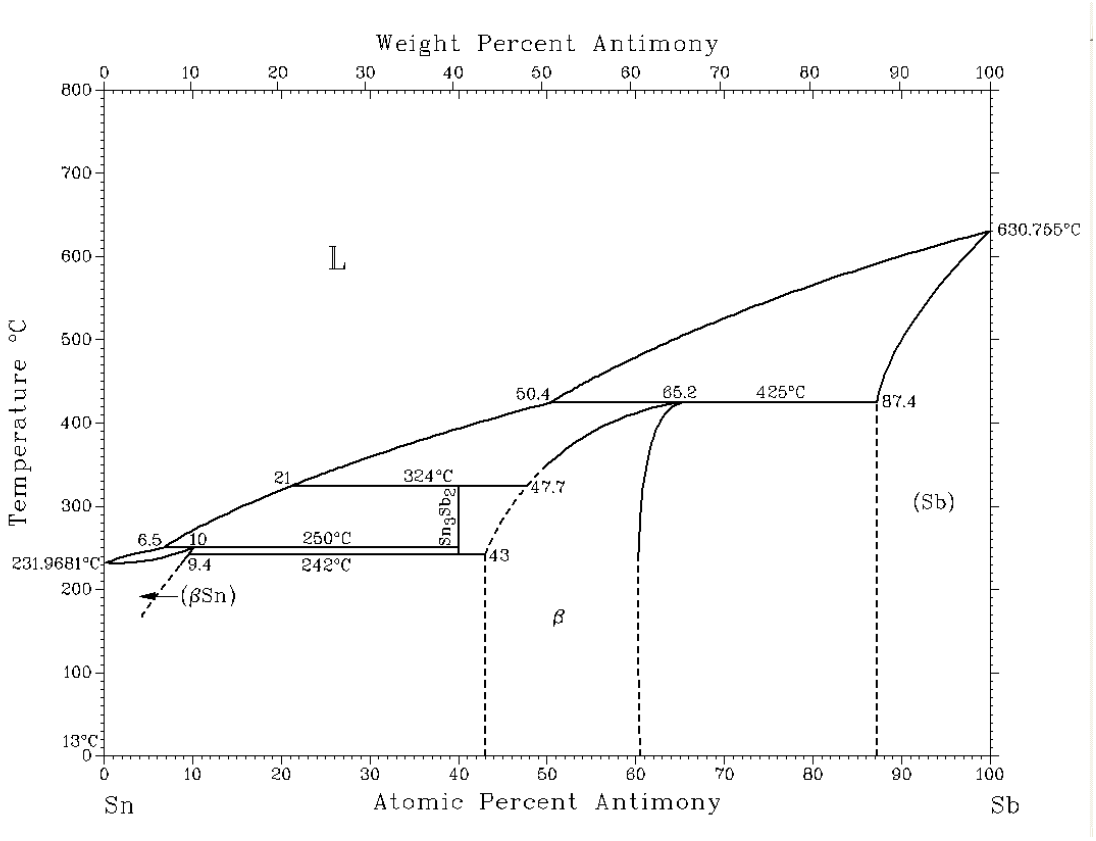

Fig. 4.2: Phase diagram of the Sb-Sn system [1990 Massalski].

Measurements on the heats of mixing have been done by Yazawa [1968 Yazawa]. Hultgren et al. [1973 Hultgren] selected the thermodynamic properties for liquid alloys at 905 K. Many calorimetric investigations have been done by Sommer [1983 Sommer]. Badawi did some calorimetric studies on the enthalpy of formation [1987 Badawi] and the enthalpy of mixing [1989 Badawi]. Emf measurements have been done on a few compositions by Vassiliev [1997 Vassiliev]. Studies on phase equilibria have been done by Chen [2008 Chen]. An experimental study on the density and surface tension has been done by Plevachuk [2010 Plevachuk].

4.1.3 Au-Sb-Sn system

Thermodynamic calculations on phase equilibria have been done by Kim [2002 Kim].

4.2 Experimental procedure

Ternary alloys were prepared from high-purity metals (tin ingots, purity 99.999%; antimony ingot, purity 99.99%; gold sheet, purity 99.95%). Tin and antimony were product of Johnson Matthey GmbH, Germany whereas gold was product of Ögussa, Austria. The metals were sealed into quartz capsules under vacuum and melted together at 1073 K. After 1 week, the alloys were quenched in ice water.

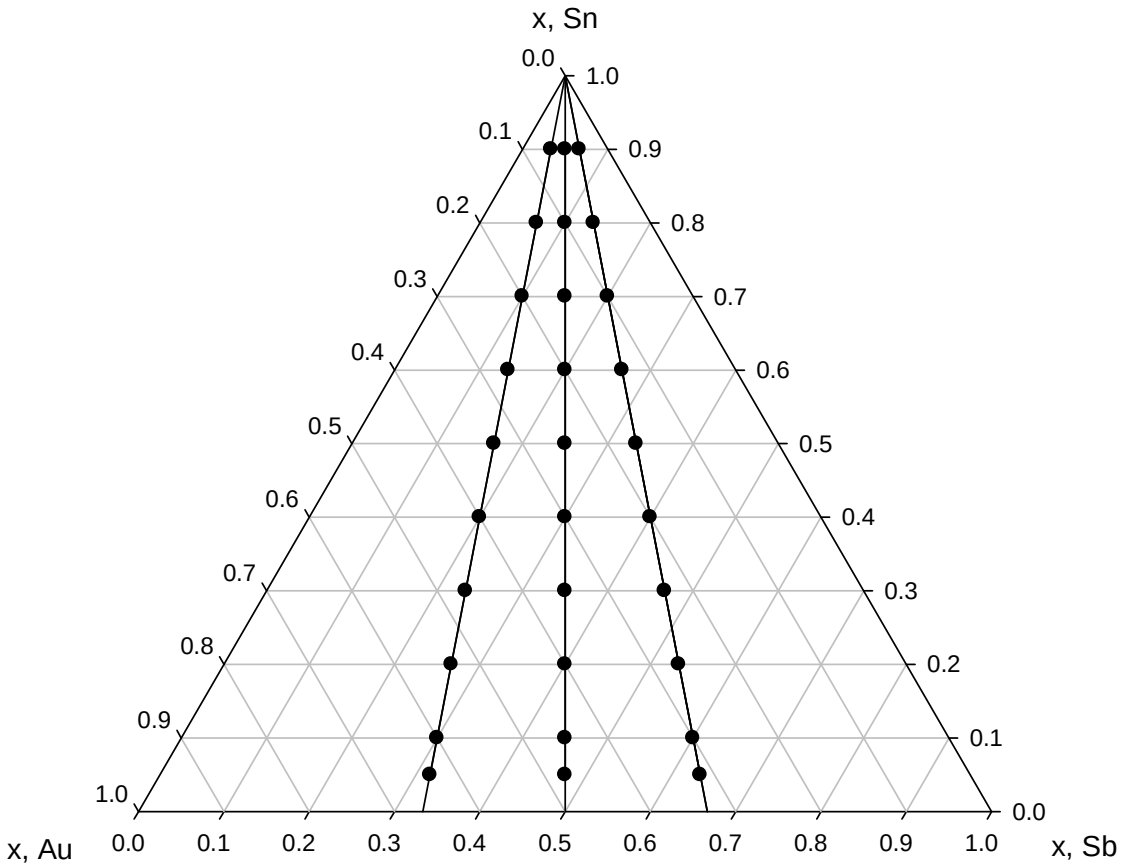

Fig. 4.3: Measured cross-sections and alloy compositions in the ternary Au-Sb-Sn system.

Before EMF the measurements started, the liquidus of the alloys was determined by differential thermal analysis so that the temperature range for EMF measurements could be determined. Samples weighing 200 mg to 300 mg were used for the DTA measurements. Evacuated, sealed quartz tubes were used for the measurements to avoid oxidation of the alloys. Two heating and cooling curves were recorded with a heating and cooling rate of 5 K/min. The average values of the melting points obtained from the two heating curves were taken and are given in Table 4.1: An EMF method with liquid electrolyte was used to determine the activity of tin in the liquid alloys. The electrolyte consisted of the eutectic mixture of KCl (purity 99.5%) and LiCl (purity 99%) with addition of about 0.5 at.% $SnCl_2$ (purity 98%).

For the EMF measurements, the following cell arrangement was used:

$$W, Sn_{(l)}/KCl\text{-}LiCl\text{-}SnCl_2/Au\text{-}Sb\text{-}Sn_{(l)}, W$$

4.3 Results

4.3.1 Liquidus temperatures

	Au:Sb=2:1	Au:Sb=1:1	Au:Sb=1:2
x, Sn	Liquidus *T* (K)	Liquidus *T* (K)	Liquidus *T* (K)
0	813	723	683
0.05	644	714	748
0.1	679	720	736
0.2	669	718	754
0.3	681	710	738
0.4	673	680	711
0.5	651	630	668
0.6	596	615	633
0.7	571	599	623
0.8	536	524	594
0.9	518	518	526

Table 4.1: Liquidus temperatures for the Au:Sb 2:1, 1:1 and 1:2 cross-section.

4.3.2. Measured emf values

Table 4.2.: Measured emf data of liquid Ag-Au-Sn alloys.

Cross-section Au:Sb 2:1

x, Sn	emf (mV)
0.05	141.1+0.1199·T(±0.10)
0.1	120.71+0.105·T(±0.35)
0.2	97.69+0.0614·T(±0.15)
0.3	70.83+0.0472·T(±0.09)
0.4	44.64+0.037·T(±0.11)
0.5	30.72+0.0271·T(±0.06)
0.6	15.27+0.0222·T(±0.18)
0.7	5.37+0.0185·T(±0.07)
0.8	2.28+0.0098·T(±0.15)
0.9	1.77+0.0033·T(±0.03)

Cross-section Au:Sb 1:1

x, Sn	emf (mV)
0.05	112.31+0.1073·T(±0.19)
0.1	97.1+0.0816·T(±0.10)
0.2	69.76+0.0652·T(±0.11)
0.3	51.46+0.0498·T(±0.09)
0.4	36.84+0.0341·T(±0.05)
0.5	23.39+0.0281·T(±0.04)
0.6	7.71+0.0296·T(±0.08)
0.7	5.8+0.0164·T(±0.01)
0.8	-2.19+0.0179·T(±0.03)
0.9	-1.06+0.0071·T(±0.03)

Cross-section Au:Sb 1:2

x, Sn	emf (mV)
0.05	73.85+0.1202·T(±0.07)
0.1	73.46+0.0853·T(±0.10)
0.2	50.63+0.0692·T(±0.09)
0.3	37.63+0.051·T(±0.06)
0.4	27+0.038·T(±0.17)
0.5	20.96+0.0228·T(±0.13)
0.6	9.65+0.0208·T(±0.25)
0.7	7.14+0.0109·T(±0.12)
0.8	0.12+0.013·T(±0.07)
0.9	2.05+0.0029·T(±0.06)

4.3.3. Partial molar quantities of tin in liquid Au-Sb-Sn alloys

Our investigation started from the binary Au-Sb system by adding Sn. The activity of Sn was measured along three cross-sections. The T versus EMF curves at each composition exhibited straight lines, expressed by Eq.2.2. From the EMF data, the activity of tin, the partial Gibbs free energy, and the partial molar enthalpies and entropies were calculated and are given in Table 4.3. The integrated thermodynamic quantities are listed in Table 4.4. The activities of Sn in the ternary Au-Sb-Sn system and in the Au-Sn [1977 Kameda] and Sb-Sn [1973 Hultgren et al.] system at 873 K are shown in Fig.4.4.

The partial molar quantities, activities and the alpha-function are listed in table 4.3. The values for the alpha-function are obtained by:

$$\alpha = \frac{\ln \gamma}{(1 - x_{Sn})^2}$$

Table 4.3: Partial molar quantities of tin in liquid Ag-Au-Sn alloys.

Cross-section Au:Sb=2:1

x, Sn	a	ln γ	α-function	$\overline{\Delta G}$ (J/mol)	$\overline{\Delta H}$ (J/mol)	$\overline{\Delta S}$ (J/mol·K)
0.05	0.0015	-3.5066	-3.92	-47427	-27228	23.14
0.1	0.0035	-3.3524	-4.128	-40982	-23293	20.26
0.2	0.0179	-2.4135	-3.77	-29195	-18851	11.85
0.3	0.0509	-1.7739	-3.621	-21620	-13668	9.11
0.4	0.1293	-1.1293	-3.137	-14847	-8614	7.14
0.5	0.2356	-0.7525	-3.01	-10493	-5928	5.23
0.6	0.398	-0.4105	-2.565	-6687	-2947	4.28
0.7	0.5643	-0.2155	-2.394	-4153	-1036	3.57
0.8	0.7497	-0.0649	-1.623	-2091	-440	1.89
0.9	0.8837	-0.0183	-1.828	-897	-342	0.64

Cross-section Au:Sb=1:1

x, Sn	a	ln γ	α-function	$\overline{\Delta G}$ (J/mol)	$\overline{\Delta H}$ (J/mol)	$\overline{\Delta S}$ (J/mol·K)
0.05	0.0042	-2.4769	-2.7483	-39749	-21672	20.71
0.1	0.0114	-2.1716	-2.6823	-32484	-18737	15.75
0.2	0.0345	-1.7574	-2.7474	-24445	-13462	12.58
0.3	0.0801	-1.3205	-2.6937	-18320	-9930	9.61
0.4	0.1702	-0.8545	-2.3737	-12854	-7109	6.58
0.5	0.2797	-0.5809	-2.3234	-9247	-4514	5.42
0.6	0.4099	-0.3810	-2.3821	-6474	-1488	5.71
0.7	0.5858	-0.1781	-1.9794	-3882	-1119	3.16
0.8	0.6996	-0.1341	-3.3518	-2593	423	3.45
0.9	0.8723	-0.0313	-3.1242	-992	205	1.37

Cross-section Au:Sb=1:2

x, Sn	a	ln γ	α-function	$\overline{\Delta G}$ (J/mol)	$\overline{\Delta H}$ (J/mol)	$\overline{\Delta S}$ (J/mol·K)
0.05	0.0086	-1.7603	-1.9471	-34500	-14251	23.19
0.1	0.0196	-1.6296	-2.0124	-28545	-14176	16.46
0.2	0.0522	-1.3432	-2.0978	-21428	-9770	13.35
0.3	0.1126	-0.9799	-2.0002	-15853	-7261	9.84
0.4	0.2019	-0.6837	-1.8985	-11612	-5210	7.33
0.5	0.3374	-0.3933	-1.573	-7886	-4045	4.4
0.6	0.4775	-0.2284	-1.4279	-5366	-1862	4.01
0.7	0.6422	-0.0862	-0.9569	-3214	-1378	2.1
0.8	0.7372	-0.0818	-2.044	-2213	-23	2.51
0.9	0.8854	-0.0164	-1.6384	-884	699	2.47

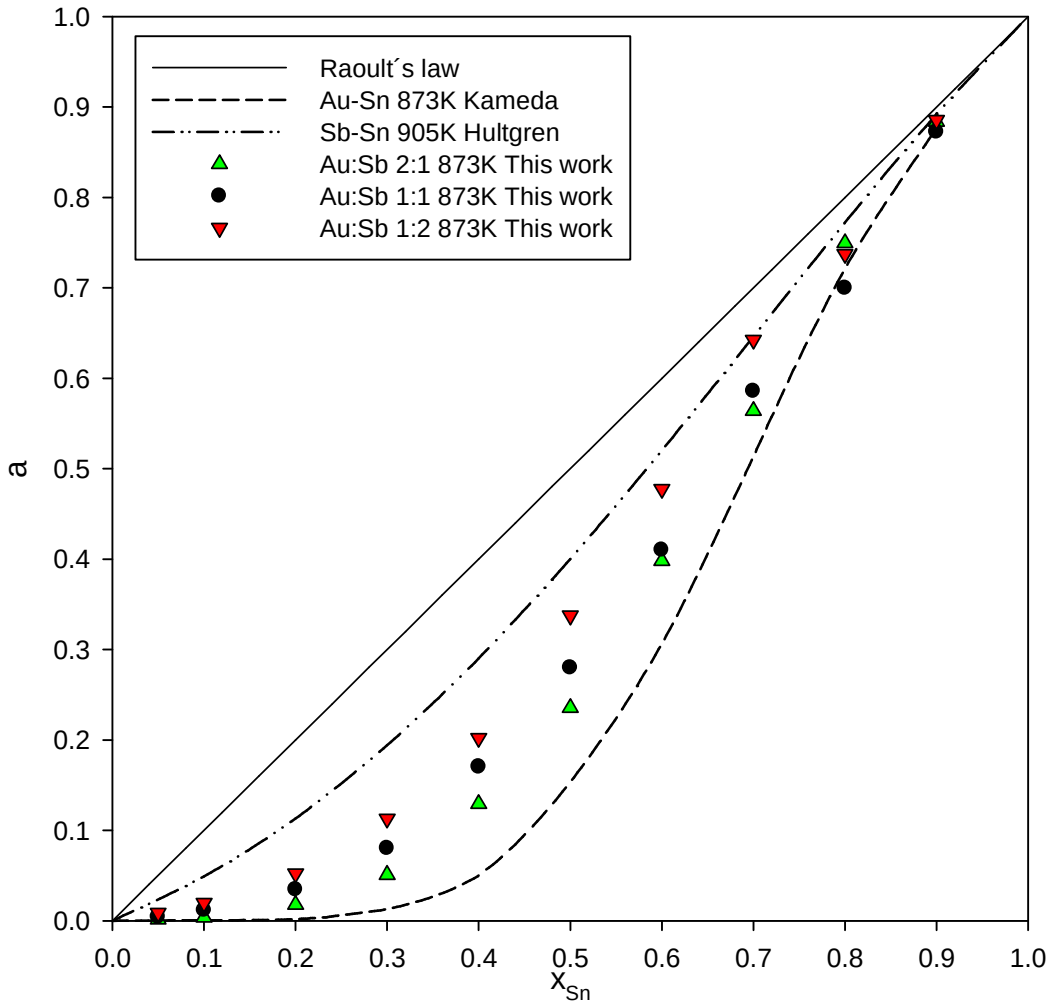

Fig. 4.4: Activities of Sn in Au-Sb-Sn alloys and the binary Au-Sn [1977 Kameda] and Sb-Sn [1973 Hultgren] systems.

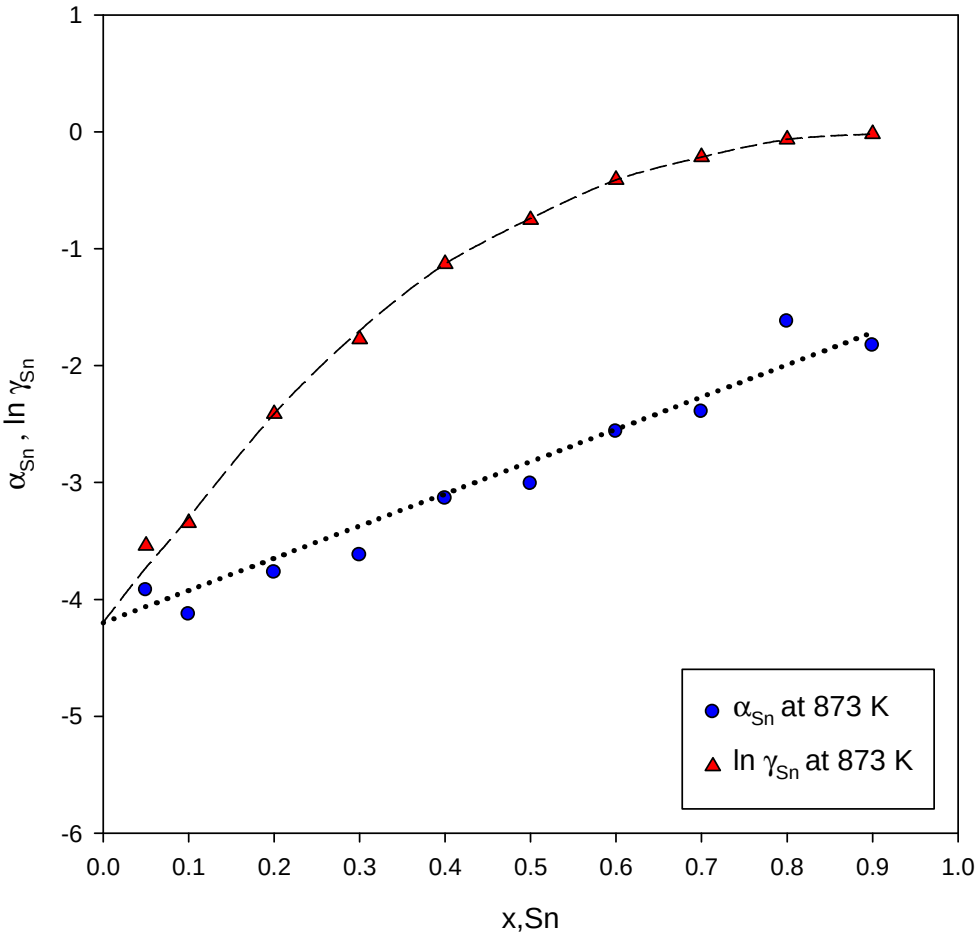

Fig. 4.5: α and ln γ for the Au:Sb 2:1 cross-section at 873 K.

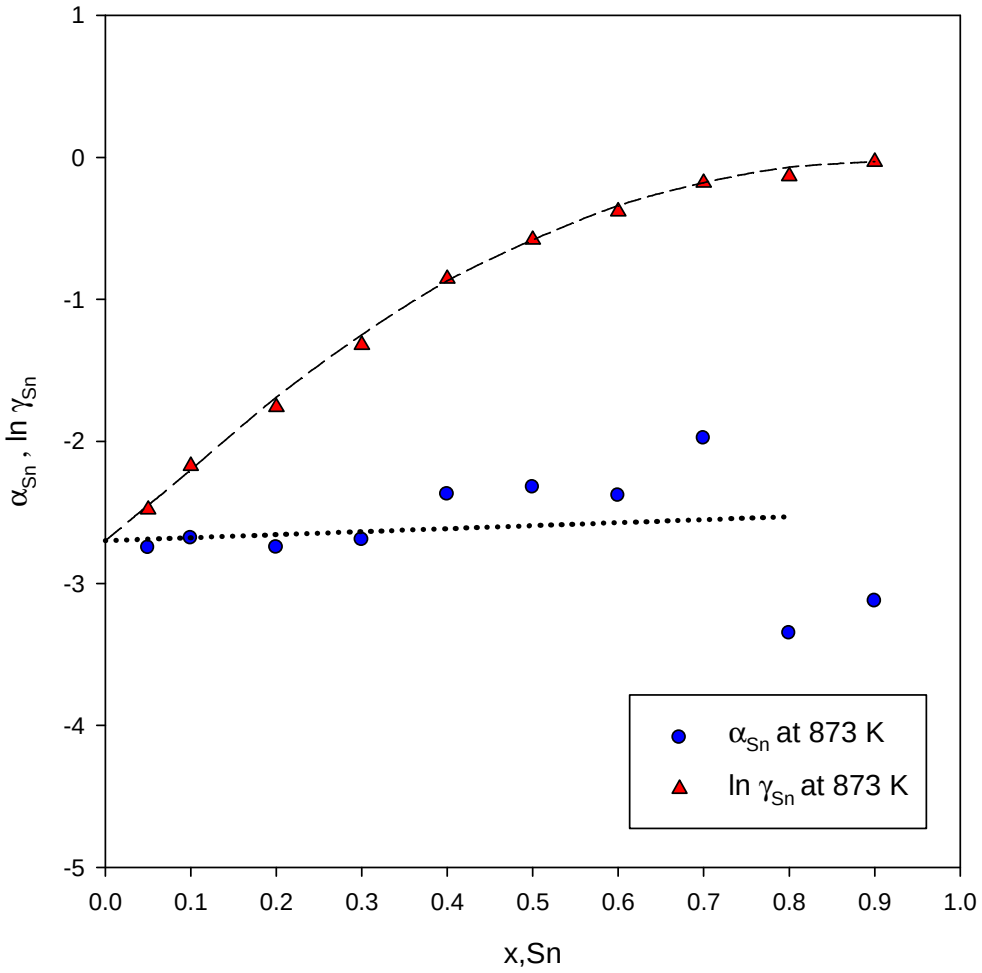

Fig. 4.6: α and ln γ for the Au:Sb 1:1 cross-section at 873 K.

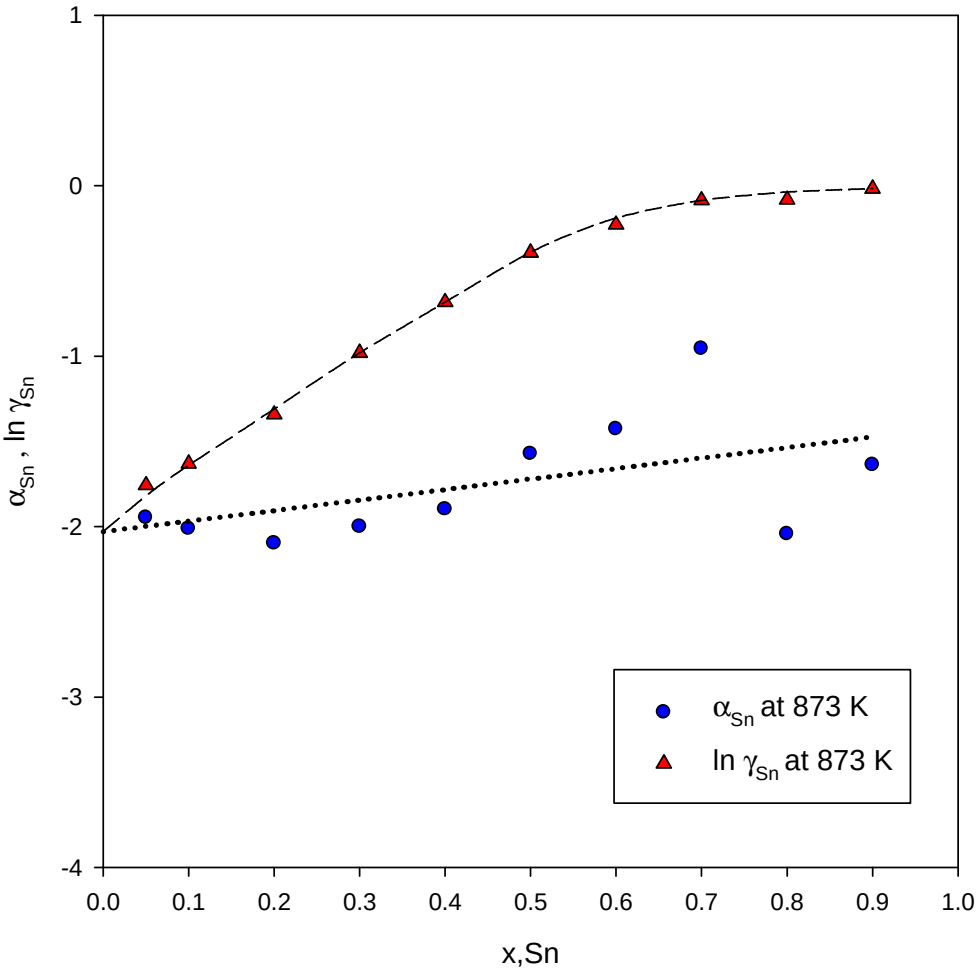

Fig. 4.7: α and ln γ for the Au:Sb 1:2 cross-section at 873 K.

The values for a and ln γ are shown in Fig.4.5-Fig.4.7 and extrapolated to x_{Sn}=0 to get the first value for the integration of the alpha function. Both quantities have been used for the extrapolation because at x_{Sn}=0 the values have to be the same and with higher content of Sn the fluctuations of the alpha values are getting larger. The extrapolation of ln γ towards x_{Sn}=0 is necessary in some cases to confirm the extrapolation of the alpha function.

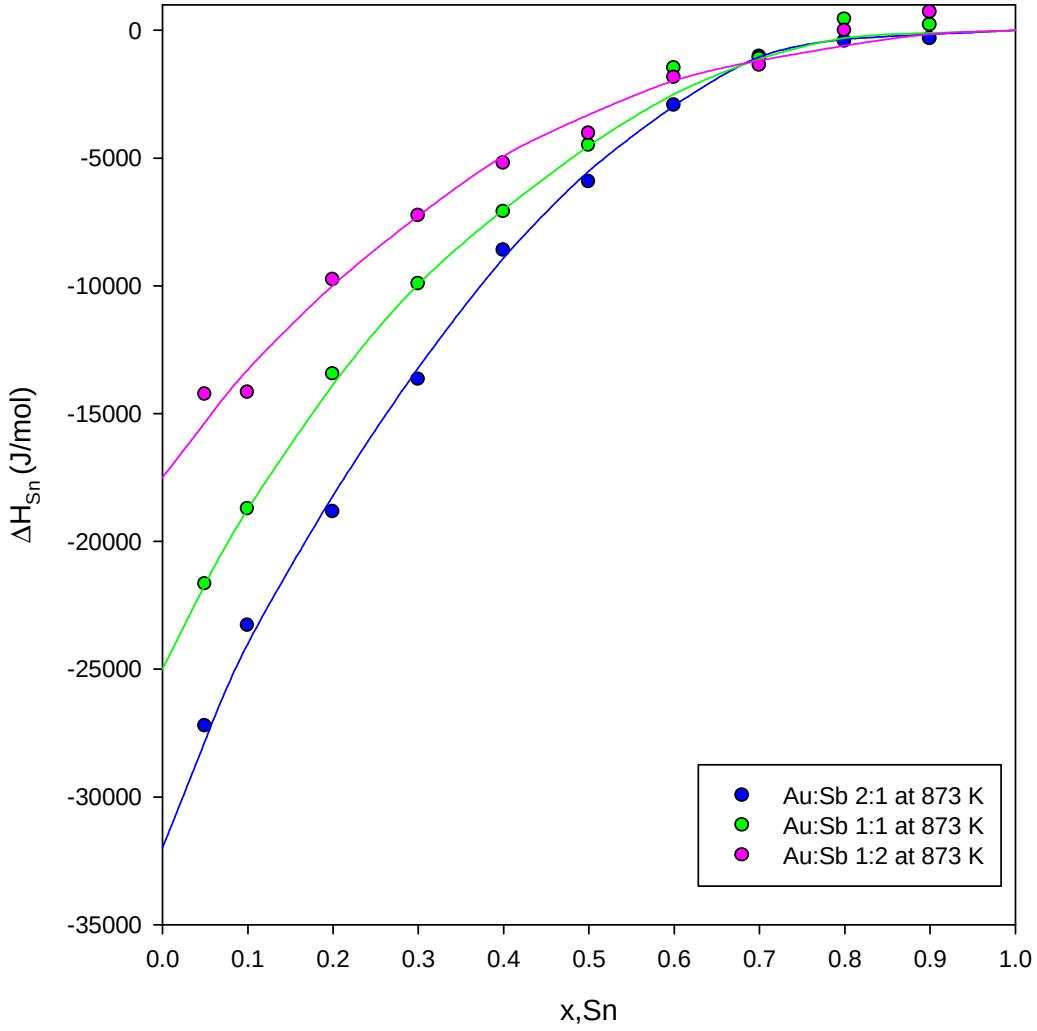

Fig. 4.8: Partial enthalpies of mixing for the Au:Sb 2:1, 1:1 and 1:2 cross-sections at 873 K.

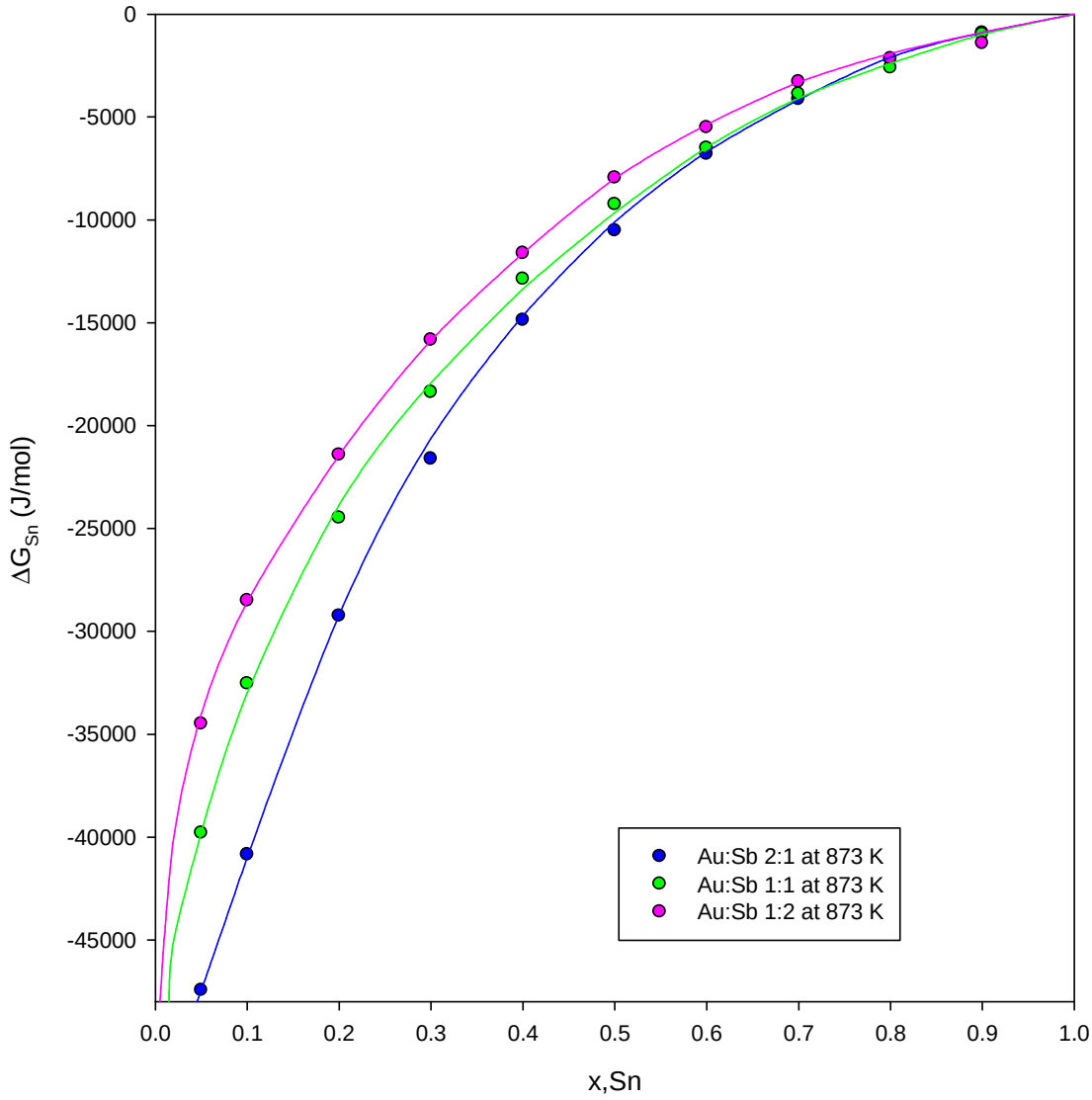

Fig. 4.9: Partial Gibbs Energies of the Au:Sb 2:1, 1:1 and 1:2 cross-sections at 873 K.

4.3.4. Integral molar quantities of tin in liquid Au-Sb-Sn alloys

Based on the partial quantities of tin, the integral enthalpy of mixing and the excess Gibbs free energy for liquid Au-Sb-Sn alloys were calculated along the constant molar ratios of Au:Sb = 2:1, 1:1 and 1:2 applying equations 2.11 and 2.12 to the Au-Sb-Sn system:

$$\Delta H = (1 - x_{Sn})[\Delta H_{Sn=0} + \int_0^{x_{Sn}} \frac{\Delta \overline{H}_{Sn}}{(1-X_{Sn})^2} dx_{Sn}]_{x_{Au}/x_{Sb}}$$

$$\Delta G^{xs} = (1 - x_{Sn})[\Delta G^{xs}_{Sn=0} + \int_0^{x_{Sn}} \frac{\Delta \overline{G^{xs}_{Sn}}}{(1-X_{Sn})^2} dx_{Sn}]_{x_{Au}/x_{Sb}}$$

And accordingly

$$\Delta G^{xs} = (1 - x_{Sn})[\Delta G^{xs}_{Sn=0} + RT \int_0^{x_{Sn}} \alpha \, dx_{Sn}]_{x_{Au}/x_{Sb}}$$

For the integration of the excess Gibbs free energy in the ternary system, the constant starting values of $\Delta G^{xs}_{Sn=0}$ in the Au-Sb system were taken from own measurements, which will be shown in chapter 5. The values from Kameda were not taken because of several problems, occurred during his measurements. Because of high volatility of $SbCl_3$ the emf became unstable leading to lower values which then recovered by adding $SbCl_3$ through an addition port. Nevertheless Kameda reported unstable values at Sb=20% which was the lowest measured concentration which is very important for the extrapolation to Sb=>0 and the integration. To reduce the volatility the salt mixture of KCl-LiCl-$SbCl_3$ was tempered at 110°C for several weeks to form compounds. The procedure of the preparation is described in Chapter 5. Another reason not to trust the values from Kameda´s measurements were the results of the enthalpy of mixing which Okamoto [1984 Okamoto] reported from the calculated values of Hino [1975 Hino], where the enthalpies of mixing determined by

the emf measurements of Kameda [1974 Kameda] and his own [1975 Hino] vapor pressure measurements served as a basis. There was reported that the enthalpy of mixing in the Au-Sb system is highly temperature dependent. A minimum of the integral enthalpy of mixing with more than – 10 kJ/mol was reported at 733 K while the minimum at 1373 K was more negative than -20 kJ/mol. Contrary to that investigation Hayer [1995 Hayer] didn´t find any temperature dependence while doing calorimetric experiments at several temperatures with values not exceeding -4 kJ/mol. So the constant starting values of $\Delta H_{Sn=0}$ were taken from Hayer al. [1995 Hayer]. All integral molar quantities were determined for 873 K. The integral entropy was derived from the equation

$$\Delta G = \Delta H - T\Delta S$$

Table 4.4: Integral molar quantities of tin in liquid Au-Sb-Sn alloys.

Cross-section Au:Sb=2:1

x, Sn	ΔG (J/mol)	ΔG^{xs} (J/mol)	ΔH (J/mol)	ΔS (J/K·mol)
0	-9706	-4868	-2437	8.43
0.05	-11854	-6024	-3719	9.32
0.1	-13539	-7022	-4849	9.95
0.2	-15863	-8534	-6638	10.57
0.3	-17013	-9345	-7816	10.54
0.4	-17139	-9482	-8254	10.18
0.5	-16358	-9017	-8240	9.30
0.6	-14756	-8023	-8100	7.62
0.7	-12377	-6557	-7298	5.82
0.8	-9219	-4663	-4237	5.71
0.9	-5278	-2457	-2344	3.36

Cross-section Au:Sb=1:1

x, Sn	ΔG (J/mol)	ΔG^{xs} (J/mol)	ΔH (J/mol)	ΔS (J/K·mol)
0	-10281	-5032	-2590	8.81
0.05	-11940	-5720	-3644	9.50
0.1	-13193	-6306	-4513	9.94
0.2	-14838	-7181	-5778	10.38
0.3	-15622	-7666	-6501	10.45
0.4	-15578	-7674	-6773	10.09
0.5	-14794	-7248	-6589	9.40
0.6	-13378	-6481	-5818	8.66
0.7	-11279	-5336	-4690	7.55
0.8	-8582	-3944	-3301	6.05
0.9	-5070	-2457	-1725	3.83

Cross-section Au:Sb=1:2

x, Sn	ΔG (J/mol)	ΔG^{xs} (J/mol)	ΔH (J/mol)	ΔS (J/K·mol)
0	-8799	-3945	-2096	7.68
0.05	-10263	-4433	-2740	8.62
0.1	-11364	-4847	-3301	9.24
0.2	-12830	-5502	-4165	9.93
0.3	-13523	-5855	-4698	10.11
0.4	-13524	-5867	-4905	9.87
0.5	-12861	-5519	-4854	9.17
0.6	-11584	-4851	-4519	8.09
0.7	-9718	-3898	-3853	6.72
0.8	-7373	-2817	-2922	5.10
0.9	-4364	-1542	-1711	3.04

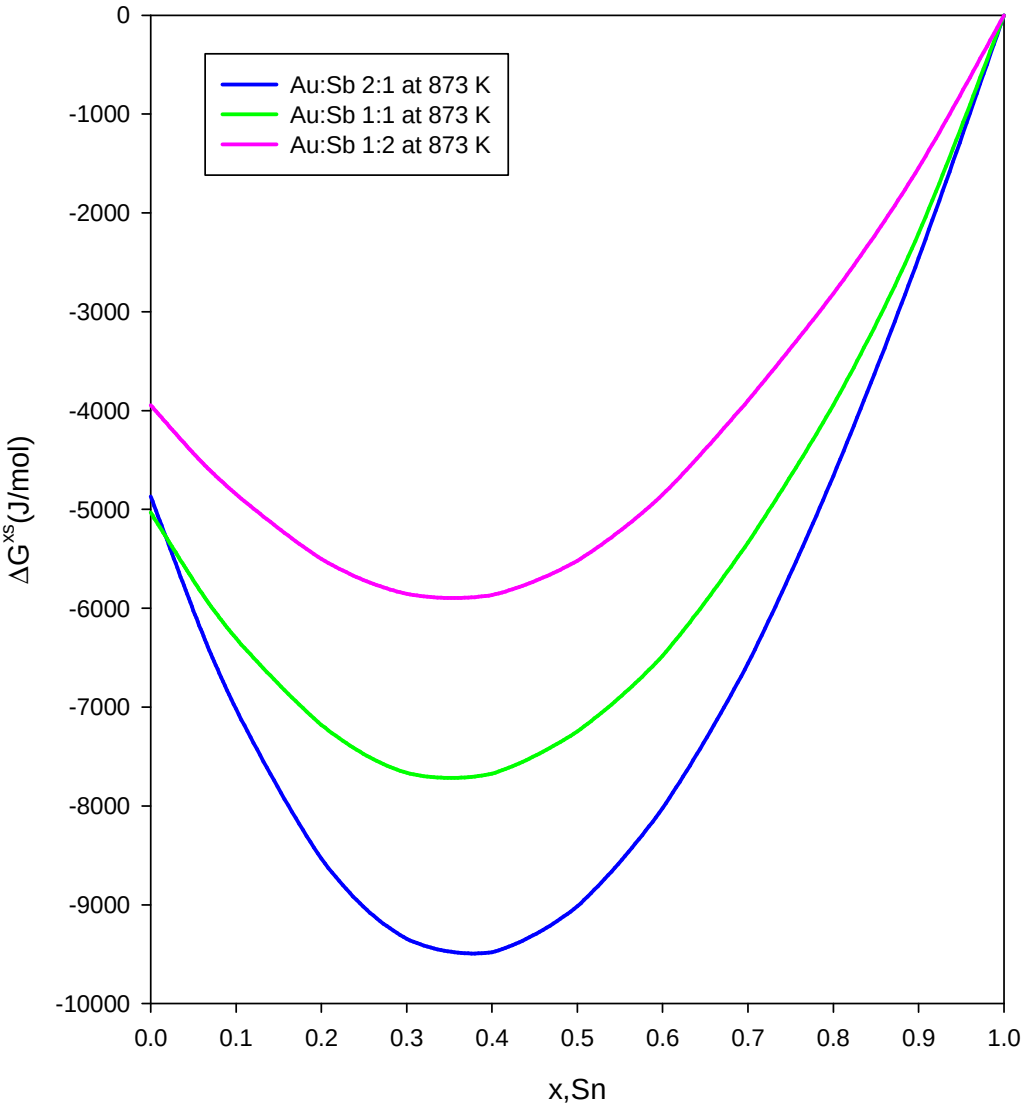

Fig. 4.10.: Integral excess Gibbs free energy ΔG^{xs} for the Au:Sb: 2:1, 1:1, and 1:2 cross-sections at 873 K.

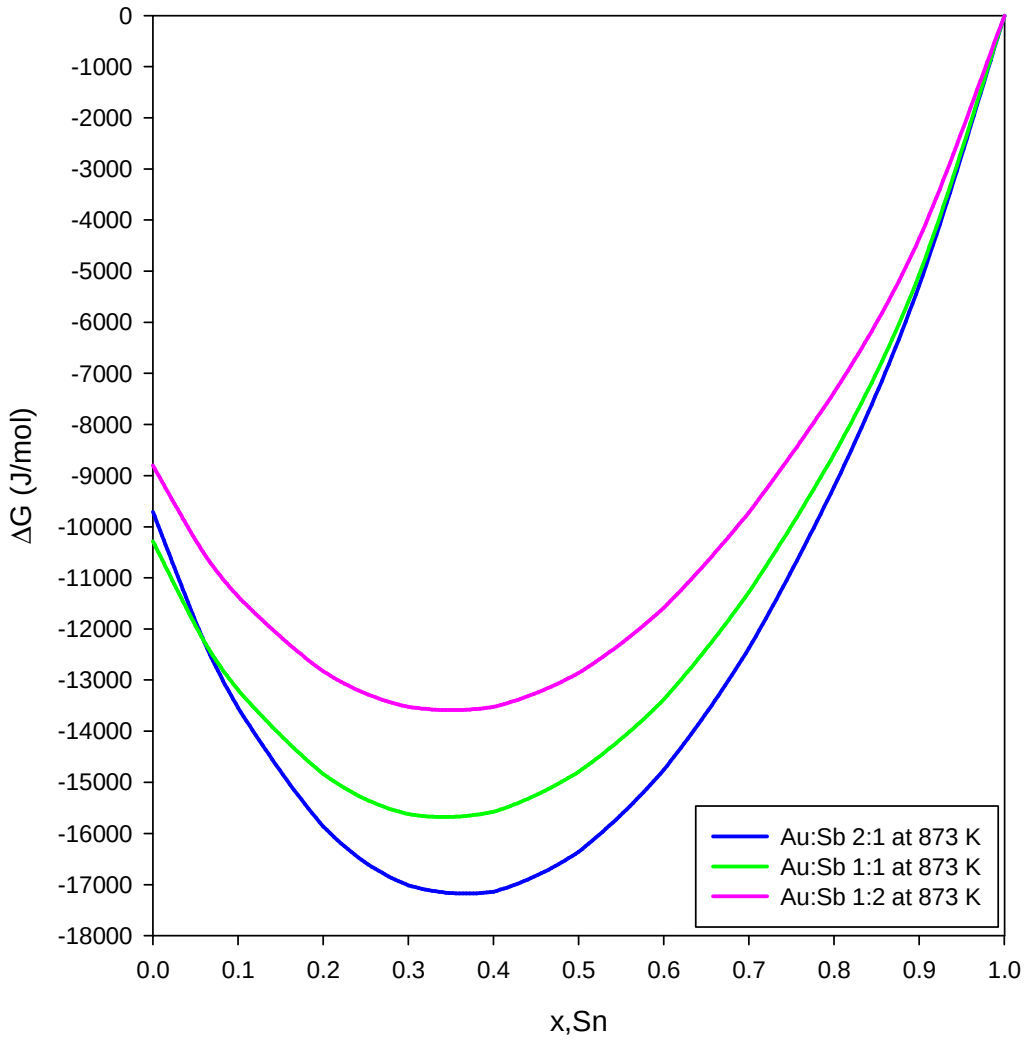

Fig. 4.11: Integral Gibbs free energy curves ΔG (J/mol) for the Au:Sb 2:1, 1:1 and 1:2 cross-sections at 873 K.

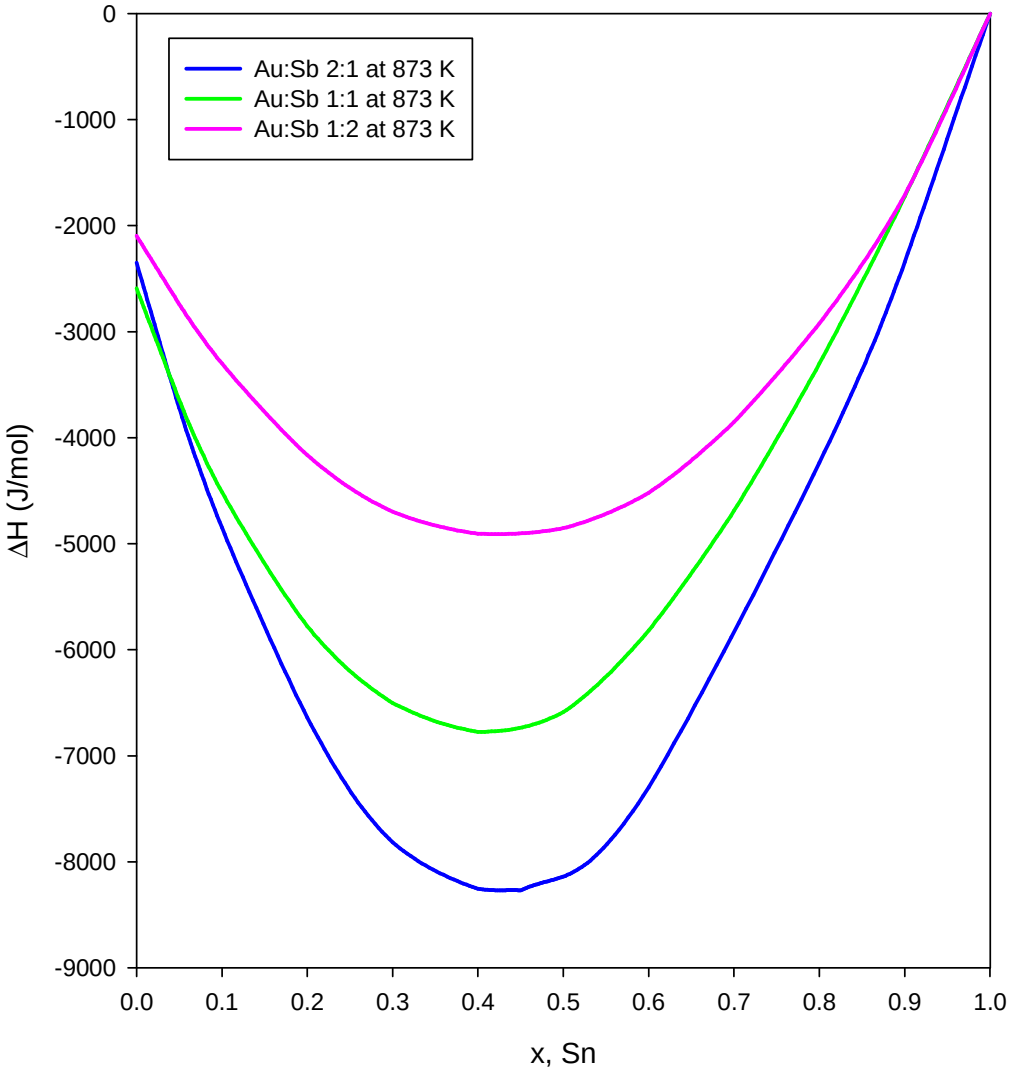

Fig. 4.12: Integral enthalpy of mixing ΔH (J/mol) for the Au:Sb: 2:1, 1:1, and 1:2 cross-sections at 873 K.

The excess Gibbs free energy values become more negative from the Sb-rich side (Au:Sb 1:2) to the Au-rich side (Au:Sb 2:1). The curves are shown in Fig. 4.10. The trend for the Gibbs energy curves (Fig.4.11) and the enthalpies of mixing is the same (Fig.4.12).

The excess Gibbs free energies for the Au-Sn system for plotting the iso-excess Gibbs free energy curves and the iso-Gibbs free energy curves in the ternary Au-Sb-Sn system were calculated from the EMF of the measurements of Kameda which covered the temperature range of 944 K to 1256 K for the Au-Sn system [1977 Kameda]. The values for the Sb-Sn were taken from Hultgren [1973 Hultgren]. For the Au-Sb system own data were taken. The interaction parameters for the Gibbs free energy and the Gibbs free excess energy were calculated by using a Redlich–Kister fit. For the calculation of the interaction parameters for the enthalpy of mixing for the Au-Sn system the data from Hayer et al. [1981 Hayer] were taken, and also for the Au-Sb system [1995 Hayer]. For the Sb-Sn system the data from Sommer et al. [1983 Sommer] were taken. The iso-Gibbs free energy and the iso-excess Gibbs free energy curves are plotted in Fig. 4.13 and Fig. 4.14, respectively. The plotted iso-enthalpy curves are shown in Fig. 4.15. All iso-curves shown herein were calculated using Redlich–Kister–Muggianu polynomials.

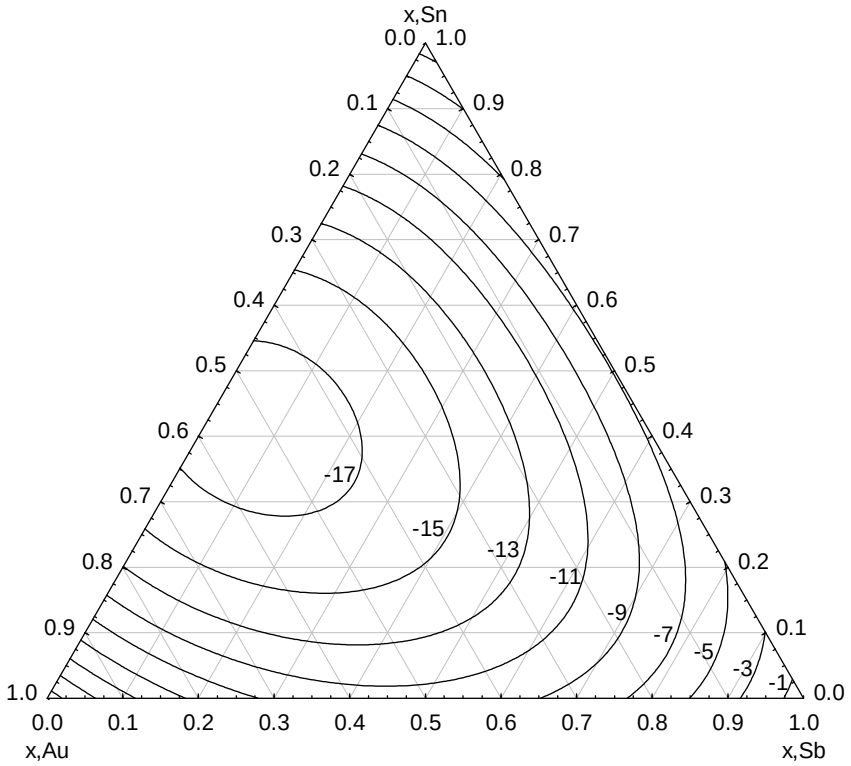

Fig. 4.13: Iso-Gibbs curves (kJ/mol) of the ternary Au-Sb-Sn system at 873 K determined by emf- measurements.

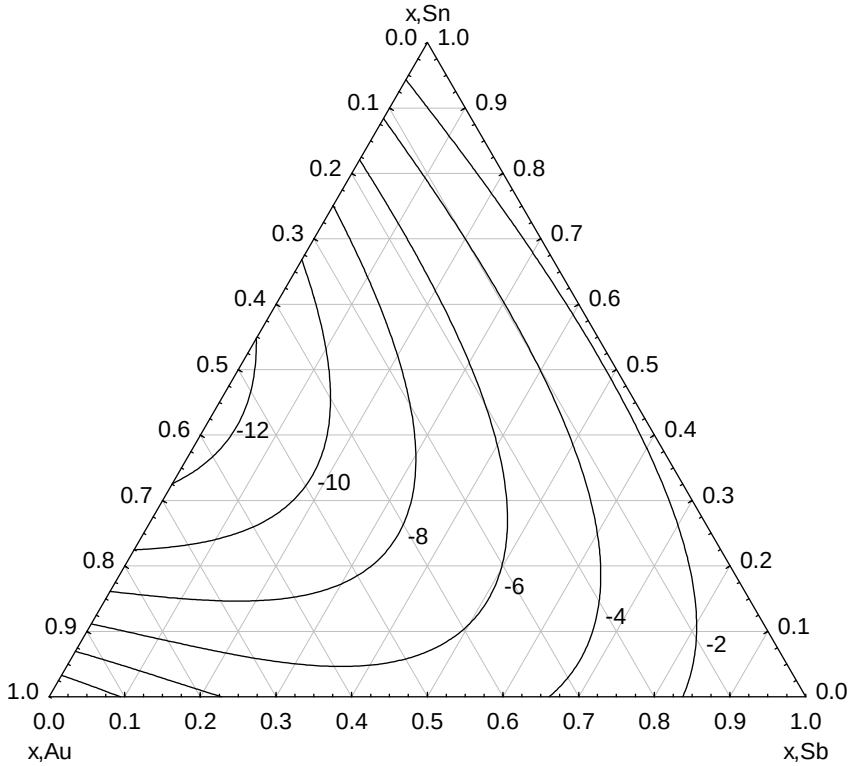

Fig. 4.14: Iso-excess Gibbs curves (kJ/mol) of the ternary Au-Sb-Sn system at 873K determined by emf measurements.

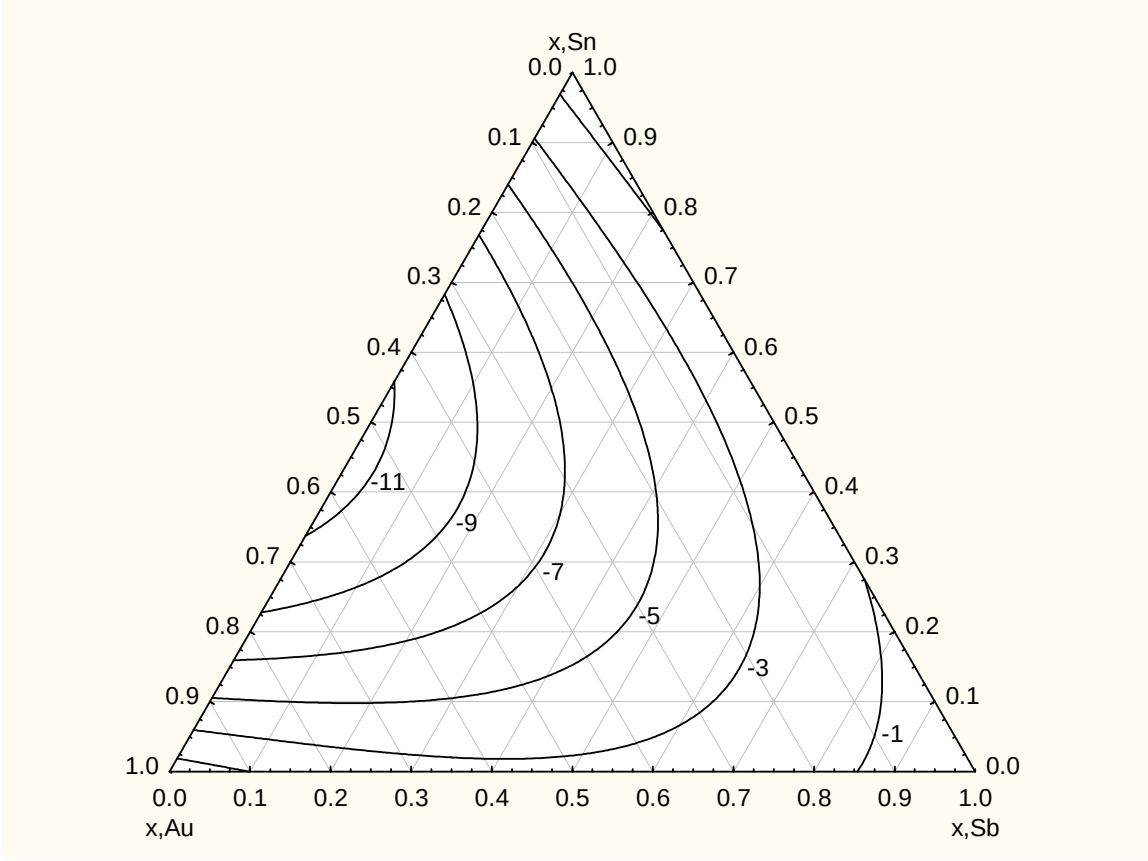

Fig. 4.15: Iso-enthalpy curves (kJ/mol) of the ternary Au-Sb-Sn system at 873 K determined by emf measurements.

4.3.5. Conclusion

Using an appropriate galvanic cell, the activities and partial free energies of Sn in liquid Au-Sb-Sn alloys were determined as a function of concentration and temperature. Thermodynamic properties were obtained for 33 alloys. Their compositions were situated on three cross-sections with the constant ratios of Au:Sb = 2:1, 1:1, and 1:2. The integral properties for the ternary system were calculated at 873 K by Gibbs-Duhem integration.

Chapter 5: Emf investigations on the binary Au-Sb system.

The emf values for the Au-Sb system were remeasured because no reliable data were found in literature like the emf measurements from Kameda [1974 Kameda]. A detailed description has been given in chapter 4.3.4.

5.1 Experimental procedure

Binary alloys were prepared from high-purity metals (antimony ingot, purity 99.99%; gold sheet, purity 99.95%). Antimony was product of Johnson Matthey GmbH, Germany whereas gold was product of Ögussa, Austria. The metals were sealed into quartz capsules under vacuum and melted together at 1073 K. After 1 week, the alloys were quenched in ice water. An EMF method with liquid electrolyte was used to determine the activity of antimony in the liquid alloys. The electrolyte consisted of the eutectic mixture of KCl (purity 99.5%) and LiCl (purity 99%) with addition of about 0.5 at.% $SbCl_3$ (purity 98%). After the purification of the eutectic mixture of KCl and LiCl the electrolyte was powdered together with $SbCl_3$ inside the glove box to avoid impurities from air. Then the electrolyte was sealed under vacuum into a glass ampoule and then put into a furnace at 110°C for 2 month. The reason for that procedure was to get a compound of LiCl and $SbCl_3$ (see phase diagram [1923 Kendall] in Fig.5.1) to stabilize the electrolyte during the heating time before the measurements started to avoid evaporation. Thus only the starting values for the Gibbs energy were necessary for the integrations, the measurements have been done at one specific temperature. As the melting point of pure antimony is 904 K the chosen temperature was 913 K to be sure that antimony was liquid during the measurements.

For the EMF measurements, the following cell arrangement was used:

W, $Sb_{(l)}$/KCl-LiCl-$SbCl_3$/Au-$Sb_{(l)}$,W

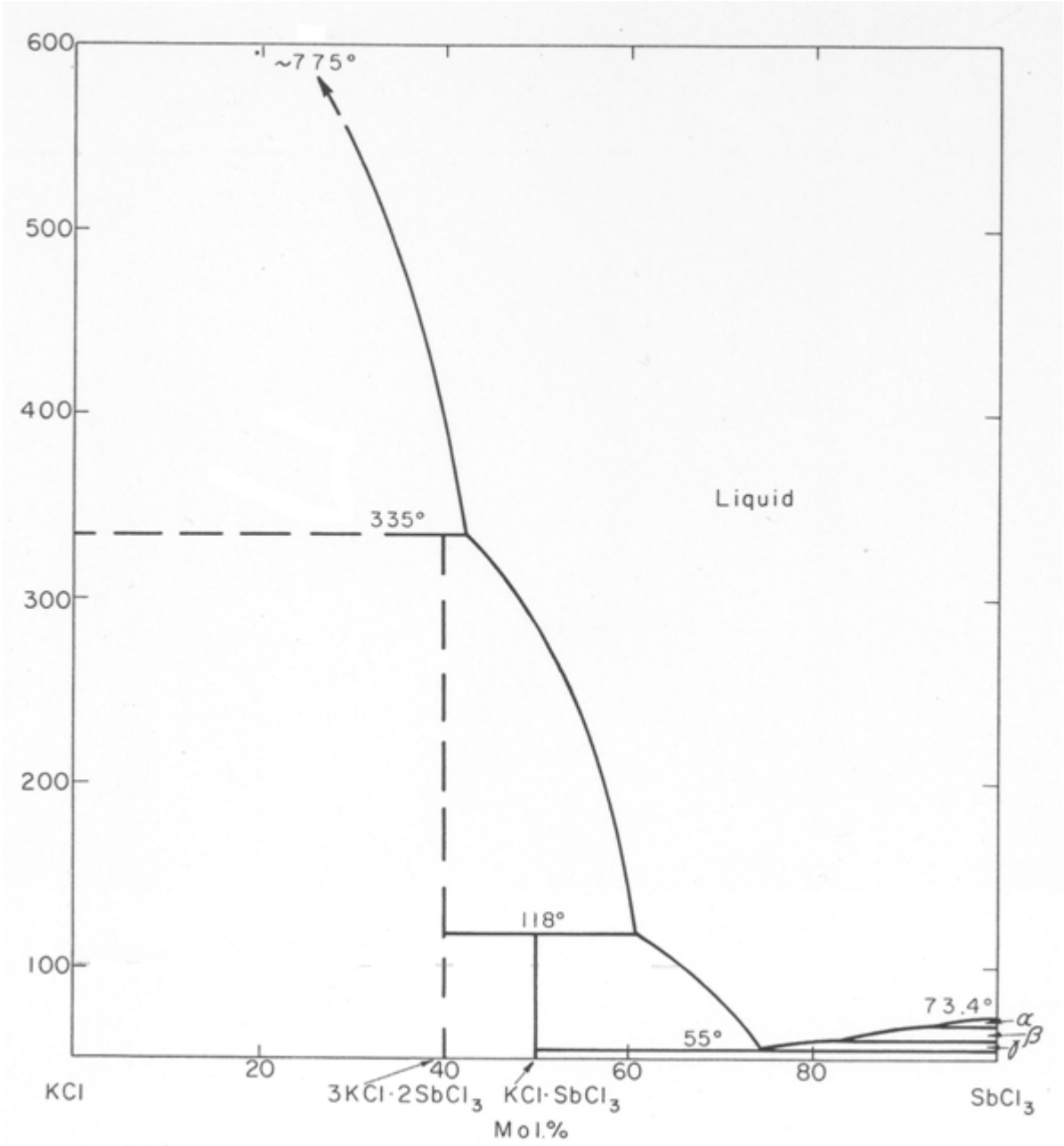

Fig. 5.1.: Phase diagram of the KCl-$SbCl_3$ system [1923 Kendall].

5.2 Results

5.2.1 Liquidus temperatures

x, Sb	Liquidus *T* (K)
0.25	801
0.325	683
0.4	657
0.5	706
0.65	733
0.8	831

Table 5.1: Liquidus temperatures [1990 Massalski] for the Au-Sb system.

5.2.2. Measured emf values

x, Sb	emf (mV)
0.25	73.2
0.325	60.8
0.4	46
0.5	28.4
0.65	15.9
0.8	5.34

Table 5.2.: Measured emf data of liquid Au-Sb alloys at 913 K.

5.2.3. Partial molar quantities of tin in liquid Au-Sb alloys at 913 K.

x, Sb	a	ln γ	α-function	$\overline{\Delta G}$ (J/mol)
0.25	0.0615	-2.8016	-2.5161	-21188
0.325	0.0989	-2.3270	-2.6406	-17599
0.4	0.1737	-1.7606	-2.3453	-13315
0.5	0.3389	-1.0870	-1.5752	-8221
0.65	0.5460	-0.1778	-1.4514	-4602
0.8	0.8159	0.0188	-0.4700	-1546

Table 5.3: Partial molar quantities of tin in liquid Au-Sb alloys at 913 K.

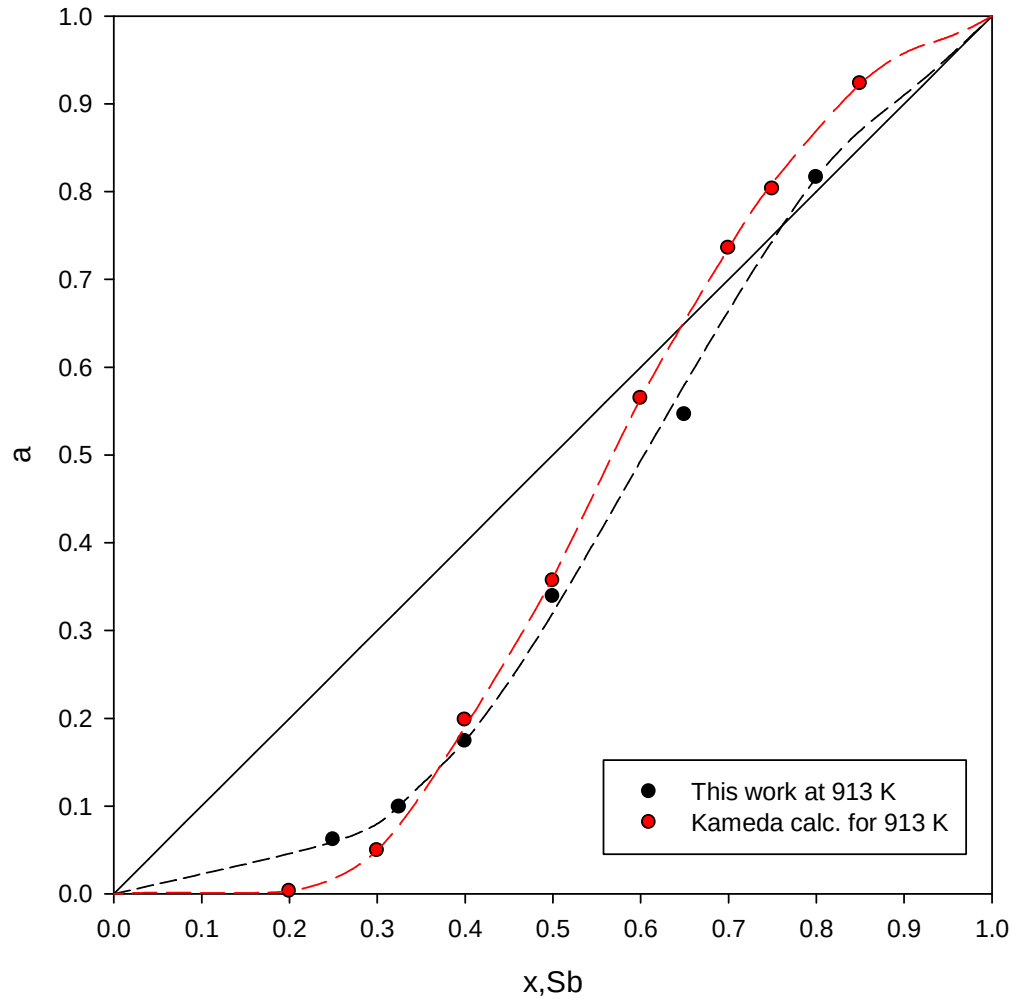

Fig. 5.2: Activities of Sb in Au-Sb alloys in the binary Au-Sb system.

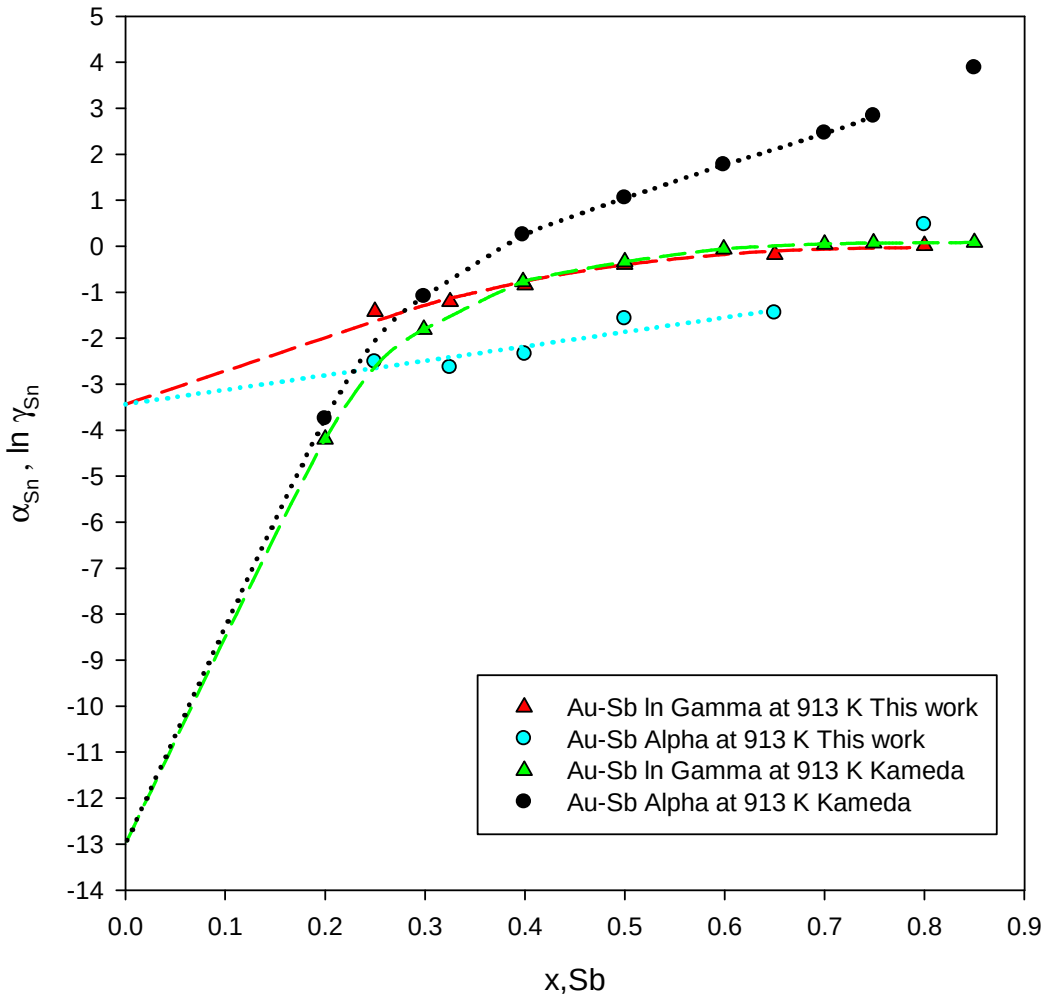

Fig. 5.3: α and ln γ for the Au-Sb system at 913 K.

The new measurements show much less negative values for the alpha function and the logarithm of gamma than the values Kameda found [1974 Kameda] resulting in much less negative values for the excess Gibbs energies. This seems logical when comparing the integral enthalpies of mixing Hayer [1995 Hayer] measured with the values Hino [1975 Hino] calculated from Kameda´s measurements. There, Hayer found no temperature dependencies and a minimum of about -2.6 kJ/mol while Hino calculated from his and Kameda´s measurements values more negative than -20 kJ/mol and found strong temperature dependencies for the enthalpies of mixing. To estimate the first value for the Gibbs-Duhem

integration, the values for ln γ and α were extrapolated for Sb=0. As it is not necessary to use all values for the extrapolation to estimate the value for α at Sb=0 at.%, values were not used at high concentrations of antimony were the fluctuations were to large like at Sb=80 at.%.

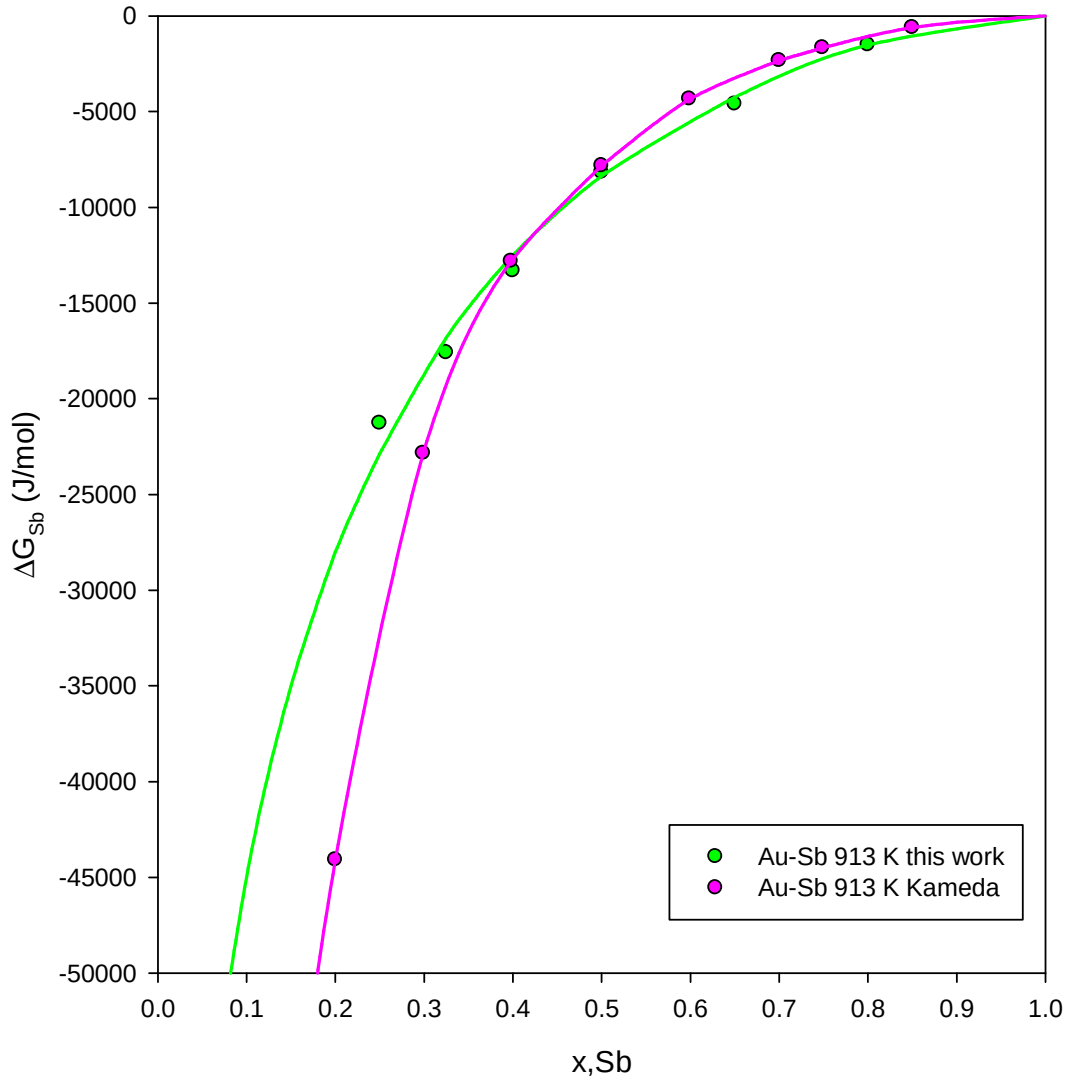

Fig. 5.4: Partial Gibbs energies for the Au-Sb system at 913 K.

In Fig. 5.4 the partial Gibbs energies from my own measurements are compared with this from Kameda. In Kameda´s work, the values are getting much more negative at low concentrations of antimony.

5.2.4. Integral molar quantities of tin in liquid Au-Sb alloys at 913 K.

x, Sb	ΔG (J/mol)	ΔG^{xs} (J/mol)
0.25	-8507	-4239
0.325	-9592	-4806
0.4	-10232	-5123
0.5	-10275	-5013
0.65	-9027	-4113
0.8	-6260	-2462

Table 5.4.: Integral molar quantities of tin in liquid Au-Sb alloys at 913 K.

The integrated Gibbs energies in this work are less negative than these found in Kameda´s work. Also the minimum is shifted to 45 at.% antimony compared to Kameda´s work, where the minimum can be found from the calculations at about 33 at.% of antimony.

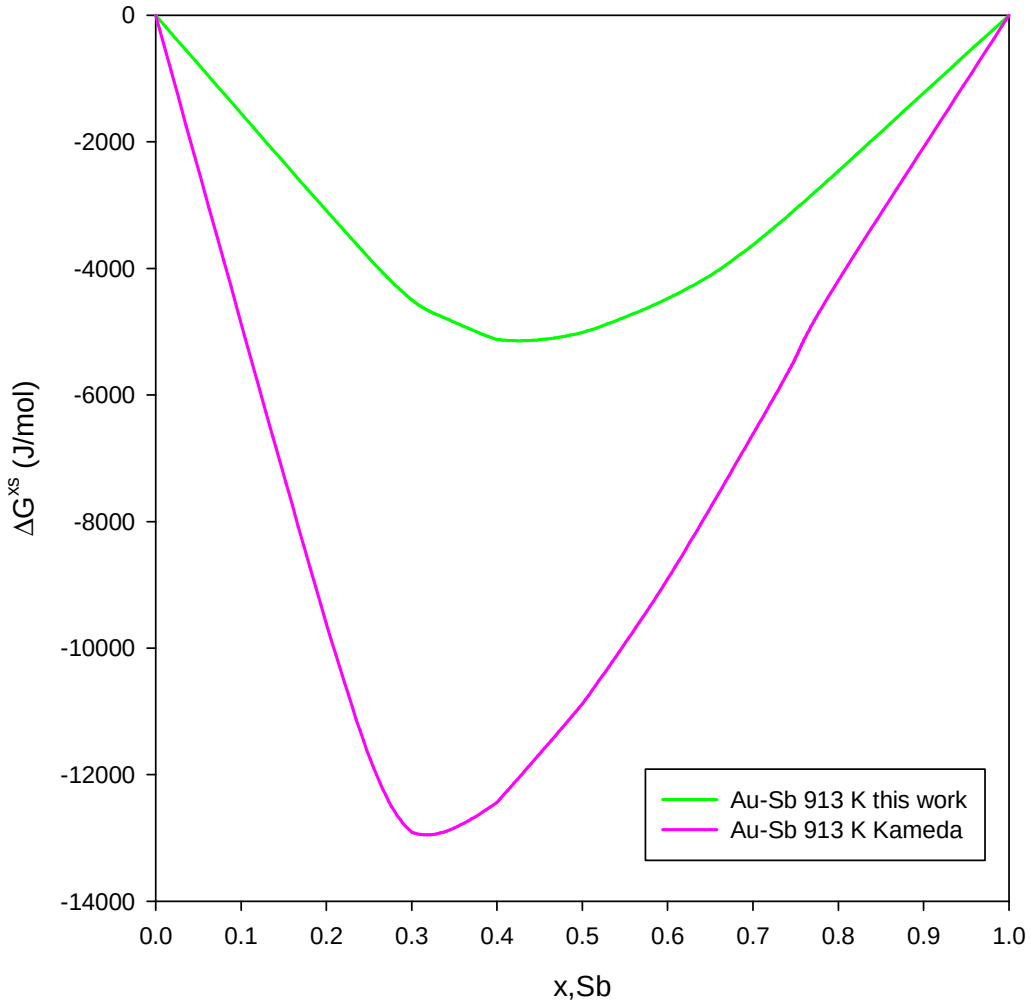

Fig. 5.5: Integral excess Gibbs free energy ΔG^{xs} for the Au-Sb system at 913 K.

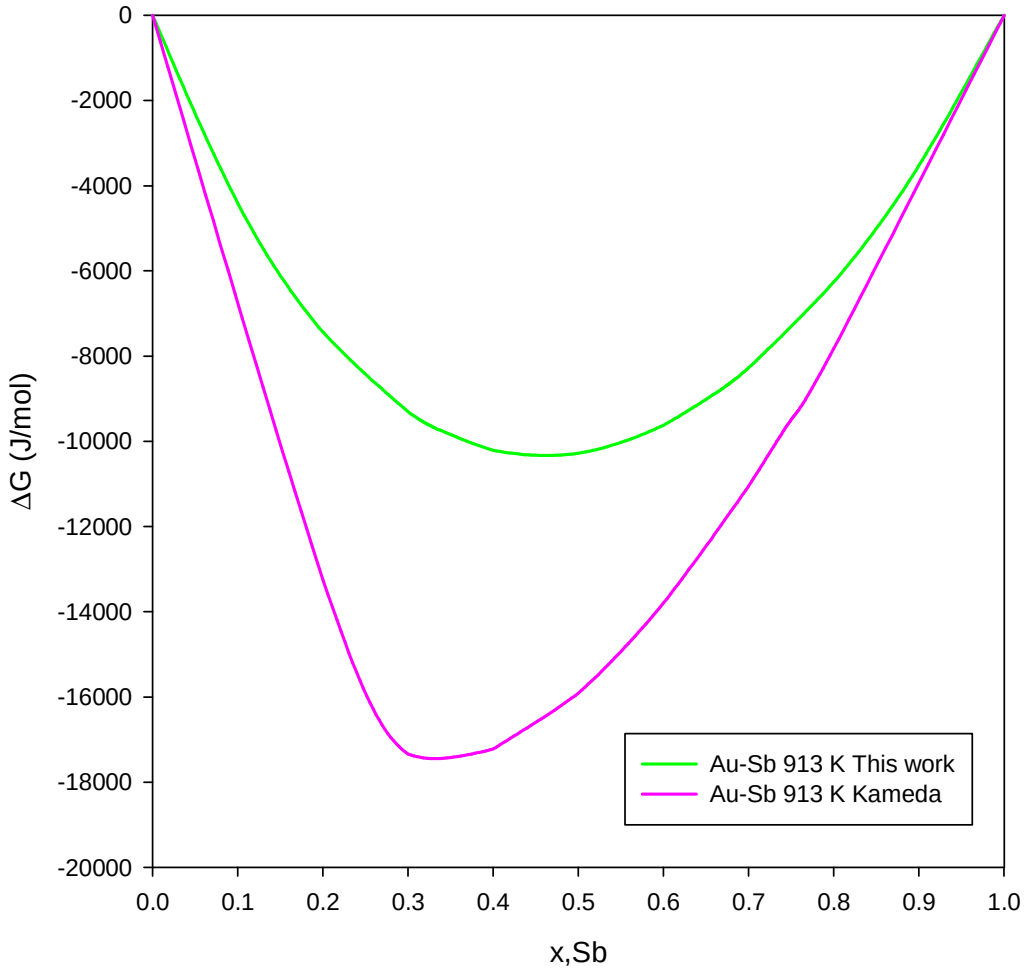

Fig. 5.6.: Integral Gibbs free energy ΔG for the Au-Sb system at 913 K.

5.2.5. Conclusion

The Au-Sb system was measured at 913 K with an emf method using a liquid electrolyte. Integral Gibbs energies were calculated by Gibbs-Duhem integration. The obtained values were less negative than the ones obtained by Kameda. The values were stable at all compositions during the measurements at 913 K.

Chapter 6: Calorimetric investigations on the ternary Au-Sb-Sn system

6.1. Experimental procedure

Same qualities of the metals were used as for the emf measurements. The integral enthalpies of mixing in the ternary system Au–Sb–Sn were determined at six cross-sections (Fig.6.1) at 873 K and at three cross-sections at 1073 K to check if there are temperature dependencies. The investigations were carried out at six cross-sections at 873 K with constant molar ratios of Au:Sn = 2:1, 1:1, 1:2 with Sb added in the concentration range between 0 and 60 at.% and Sb:Sn = 2:1, 1:1, 1:2 with Au added in the concentration between 0 and 50 at.%. Then three cross-sections were investigated at 1073 K with constant molar ratios of Au:Sn = 2:1, 1:1, 1:2 with Sb added in the concentration range between 0 and 60 at.%.

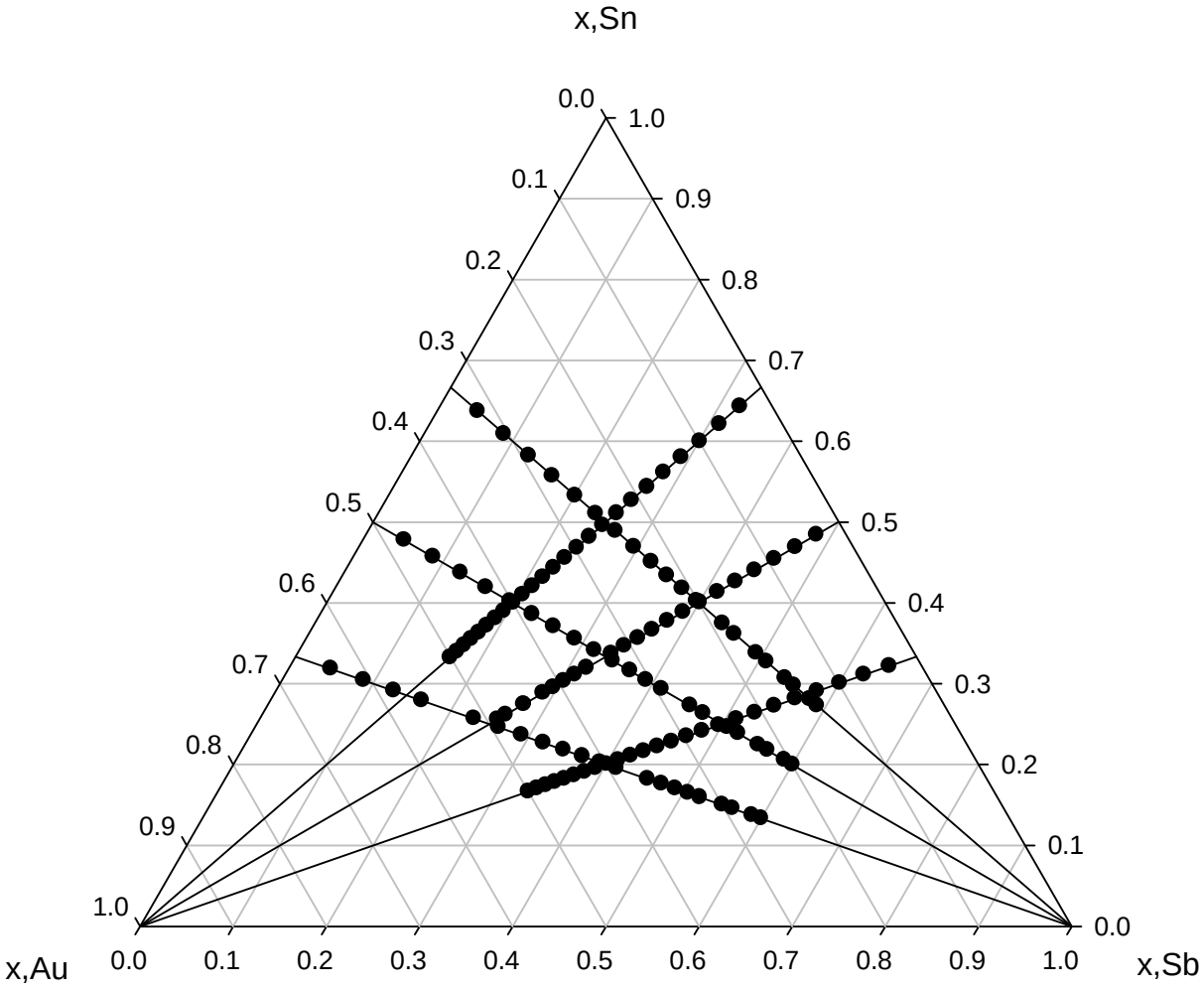

Fig. 6.1: Measured cross-sections in the ternary Au-Sb-Sn system.

6.2. Results

6.2.1. Integral enthalpies of mixing

The partial and integral values for the enthalpy of mixing are listed in tables 6.1 and 6.2. Illustrations are given in Fig. 6.2-6.8.

Table 6.1: Partial and integral enthalpies of mixing of liquid Au-Sb-Sn alloys at 600°C, standard states: pure liquid components.

Cross-section Au:Sn = 1:1, starting value: n(Au) = 2.9360 mmol

n(Sb) = 2.9396 mmol ; ΔH_M=-11484 J/mol

n Sb (mmol)	x,Sb	$\Delta\overline{H_{Sb}}$ (J/mol)	ΔH_M(J/mol)
0.2771	0.0450	5286	-10729
0.5565	0.0865	4490	-10068
0.8454	0.1258	4131	-9457
1.1344	0.1618	3667	-8916
1.4347	0.1963	3253	-8416
1.7370	0.2282	2893	-7967
2.0475	0.2584	2689	-7550
2.3880	0.2890	2620	-7131
2.7287	0.3171	2396	-6753
3.0713	0.3433	2384	-6403
3.4219	0.3680	2190	-6079
3.7744	0.3911	2083	-5781
4.1401	0.4134	1700	-5508
4.8910	0.4543	1010	-5054
5.2713	0.4729	1453	-4832
6.0470	0.5072	875	-4460
6.4389	0.5229	943	-4288
7.2263	0.5515	1191	-3959
7.6216	0.5647	953	-3815
8.4191	0.5890	950	-3549
8.8275	0.6004	963	-3424

Cross-section Au:Sn = 2:1, starting value: n(Au) = 3.7681 mmol

n(Sn) = 1.8881 mmol ; ΔH_M=-10960 J/mol

n Sb (mmol)	x,Sb	$\Delta\overline{H_{Sb}}$ (J/mol)	ΔH(J/mol)
0.2707	0.0457	6039	-10184
0.5453	0.0879	5054	-9509
0.8210	0.1268	3818	-8942
1.1002	0.1628	3008	-8448
1.6897	0.2300	2595	-7562
2.0061	0.2618	2263	-7156
2.3245	0.2913	2038	-6789
2.6536	0.3193	1769	-6450
2.9864	0.3455	1896	-6129
3.3193	0.3698	1810	-5834
3.6537	0.3925	1603	-5567
3.9904	0.4137	1468	-5322
4.6994	0.4538	550	-4920
5.0546	0.4719	1314	-4713
5.4197	0.4893	1286	-4515
5.7884	0.5058	881	-4341
6.1593	0.5213	1186	-4168
6.9097	0.5499	1068	-3855
7.2949	0.5633	976	-3712
8.0855	0.5884	535	-3467
8.4882	0.6001	978	-3341

Cross-section Au:Sn = 1:2, starting value: n(Au) = 2.0404 mmol

n(Sn) = 4.0762 mmol ; ΔH_M=-9328 J/mol

n Sb (mmol)	x,Sb	$\Delta\overline{H_{Sb}}$ (J/mol)	ΔH(J/mol)
0.2828	0.0442	2814	-8791
0.5778	0.0863	2706	-8285
0.8853	0.1264	2189	-7825
1.2025	0.1643	2668	-7370
1.5367	0.2008	1904	-6965
1.8717	0.2343	1893	-6594
2.2181	0.2661	1707	-6249
2.5696	0.2958	1900	-5919
2.9221	0.3233	1443	-5632
3.2763	0.3488	1618	-5358
3.6403	0.3731	1497	-5103
4.0136	0.3962	1300	-4867
4.7721	0.4383	1339	-4434
5.1553	0.4574	1015	-4249
5.9409	0.4927	1248	-3891
6.3389	0.5089	957	-3736
7.1524	0.5390	1178	-3435
7.5609	0.5528	865	-3306
8.3913	0.5784	396	-3094
8.8085	0.5902	931	-2982

Cross-section Sb:Sn = 1:1, starting value: n(Sb) = 3.1557 mmol

n(Sn) = 3.1558 mmol ; ΔH_M=-1483 J/mol

n Au (mmol)	x,Au	$\Delta\overline{H_{Au}}$ (J/mol)	ΔH(J/mol)
0.2052	0.0315	-20644	-2086
0.4155	0.0618	-20338	-2657
0.6372	0.0917	-19915	-3208
0.8598	0.1199	-19191	-3704
1.0916	0.1475	-18300	-4161
1.3242	0.1734	-18292	-4591
1.5633	0.1985	-17437	-4981
1.8039	0.2223	-16813	-5332
2.0482	0.2450	-16465	-5657
2.2933	0.2665	-15740	-5945
2.5399	0.2869	-15072	-6199
2.7874	0.3063	-14441	-6423
3.0398	0.3251	-14304	-6636
3.5611	0.3607	-13170	-6981
3.8266	0.3774	-12561	-7127
4.0936	0.3934	-11666	-7243
4.3608	0.4086	-11383	-7347
4.6283	0.4231	-10847	-7433
5.1752	0.4505	-10349	-7572
5.7382	0.4762	-9338	-7654
6.0233	0.4883	-8827	-7681

Cross-section Sb:Sn = 2:1, starting value: n(Sb) = 4.2012 mmol

n(Sn) = 2.1017 mmol ; ΔH_M=-1190 J/mol

n Au (mmol)	x,Au	$\Delta\overline{H_{Au}}$ (J/mol)	ΔH(J/mol)
0.2255	0.0345	-16406	-1715
0.4545	0.0673	-16172	-2206
0.6871	0.0983	-15982	-2664
0.9232	0.1278	-15073	-3069
1.1619	0.1556	-14990	-3451
1.4067	0.1825	-14269	-3794
1.6528	0.2077	-13965	-4109
1.8994	0.2316	-13556	-4393
2.1479	0.2542	-12838	-4641
2.3967	0.2755	-12273	-4859
2.6460	0.2957	-11936	-5056
2.8972	0.3149	-11273	-5226
3.1496	0.3332	-11012	-5381
3.4062	0.3508	-10802	-5524
3.6641	0.3676	-10584	-5655
3.9227	0.3836	-9788	-5759
4.1816	0.3988	-9196	-5844
4.4407	0.4133	-9448	-5931
4.7021	0.4273	-8624	-5995
4.9636	0.4406	-8486	-6053
5.2256	0.4533	-8058	-6099
5.4887	0.4655	-7934	-6139
5.7523	0.4772	-7529	-6170
6.0226	0.4886	-7288	-6194
6.2954	0.4997	-7020	-6212

Cross-section Sb:Sn = 1:2, starting value: n(Sb) = 2.1046 mmol

n(Sn) = 4.1916 mmol ; ΔH_M=-1328 J/mol

n Au (mmol)	x,Au	$\Delta\overline{H_{Au}}$ (J/mol)	ΔH(J/mol)
0.2241	0.0344	-25087	-2145
0.4551	0.0674	-24024	-2893
0.6921	0.0990	-24126	-3613
0.9304	0.1287	-22969	-4252
1.1732	0.1571	-22124	-4833
1.4166	0.1837	-22380	-5386
1.6623	0.2089	-20945	-5867
1.9091	0.2327	-20065	-6294
2.1568	0.2551	-19180	-6671
2.4071	0.2766	-19311	-7035
2.6574	0.2968	-17855	-7337
2.9079	0.3159	-17373	-7610
3.1595	0.3341	-17234	-7866
3.4128	0.3515	-15974	-8078
3.6667	0.3680	-15550	-8268
3.9272	0.3841	-14617	-8430
4.1885	0.3995	-14093	-8571
4.4512	0.4142	-13383	-8689
4.7142	0.4282	-12849	-8788
4.9788	0.4416	-12965	-8886
5.2435	0.4544	-12011	-8958
5.5082	0.4666	-11050	-9005
5.7748	0.4784	-10953	-9048
6.0436	0.4898	-10687	-9084
6.3138	0.5007	-10542	-9115

Table 6.2: Partial and integral enthalpies of mixing of liquid Au-Sb-Sn alloys at 800°C, standard states: pure liquid components.

Cross-section Au:Sn = 1:1, starting value: n(Au) = 2.9370 mmol

n(Sn) = 2.9354 mmol ; ΔH_M=-11484 J/mol

n Sb (mmol)	x,Au	$\Delta\overline{H_{Au}}$ (J/mol)	ΔH(J/mol)
0.3069	0.0497	4916	-10670
0.6358	0.0977	4356	-9910
0.9653	0.1412	2999	-9288
1.2958	0.1808	3304	-8708
1.6312	0.2174	2861	-8190
1.9691	0.2511	2683	-7722
2.3073	0.2821	2478	-7300
2.6457	0.3106	2350	-6917
2.9912	0.3375	2000	-6569
3.3386	0.3625	1542	-6263
3.6897	0.3859	1320	-5985
4.0430	0.4078	1562	-5716
4.3969	0.4282	1667	-5461
4.7517	0.4473	1305	-5235
5.1092	0.4652	1149	-5028
5.4675	0.4821	1322	-4827
5.8261	0.4980	1245	-4641
6.1865	0.5130	1152	-4468
6.5494	0.5272	906	-4311
6.9176	0.5409	1149	-4154
7.2863	0.5537	917	-4012
7.6588	0.5660	794	-3879

8.0354	0.5778	669	-3756
8.4163	0.5890	718	-3637
8.8067	0.5999	689	-3522

Cross-section Au:Sn = 2:1, starting value: n(Au) = 3.7702 mmol

n(Sn) = 1.8881 mmol ; ΔH_M=-10960 J/mol

n Au (mmol)	x,Au	$\Delta\overline{H_{Au}}$ (J/mol)	ΔH(J/mol)
0.3008	0.0505	5604	-10124
0.6016	0.0961	3975	-9445
0.9050	0.1379	1102	-8956
1.2158	0.1769	3290	-8402
1.5278	0.2126	2714	-7917
1.8448	0.2459	3284	-7444
2.1620	0.2765	2390	-7043
2.4874	0.3054	2171	-6673
2.8172	0.3324	1952	-6337
3.1504	0.3576	1904	-6025
3.4852	0.3812	1870	-5664
4.1715	0.4244	1493	-5216
4.5195	0.4441	1495	-4986
4.8683	0.4625	2060	-4752
5.2192	0.4798	300	-4589
5.5708	0.4961	1716	-4391
5.9282	0.5116	1383	-4212
6.2877	0.5263	1826	-4030
6.6514	0.5403	2632	-3833

7.0154	0.5535	-72	-3725
7.3810	0.5661	493	-3607
7.7494	0.5780	-943	-3534
8.1200	0.5893	1096	-3409

Cross-section Au:Sn = 1:2, starting value: n(Au) = 2.0389 mmol

n(Sn) = 4.0694 mmol ; ΔH_M=-9328 J/mol

n Sb (mmol)	x,Sb	$\Delta\overline{H_{Au}}$ (J/mol)	ΔH(J/mol)
0.3281	0.0510	3094	-8695
0.6614	0.0977	2502	-8144
1.0051	0.1413	2256	-7641
1.3518	0.1812	1741	-7205
1.7002	0.2177	2002	-6794
2.0530	0.2515	1843	-6421
2.4062	0.2826	1187	-6105
2.7606	0.3113	1891	-5786
3.1151	0.3377	1707	-5498
3.4760	0.3627	1429	-5237
3.8385	0.3859	1230	-5001
4.2034	0.4076	1230	-4781
4.5699	0.4280	861	-4587
4.9425	0.4473	1467	-4383
5.3160	0.4653	1111	-4203
5.6941	0.4825	727	-4045
6.0729	0.4985	888	-3892
6.4523	0.5137	1047	-3743

6.8327	0.5280	1193	-3598
7.2182	0.5416	664	-3474
7.6041	0.5545	759	-3355
7.9915	0.5668	-553	-3278
8.3804	0.5784	715	-3171
8.7729	0.5895	725	-3068
9.1655	0.6001	812	-2969

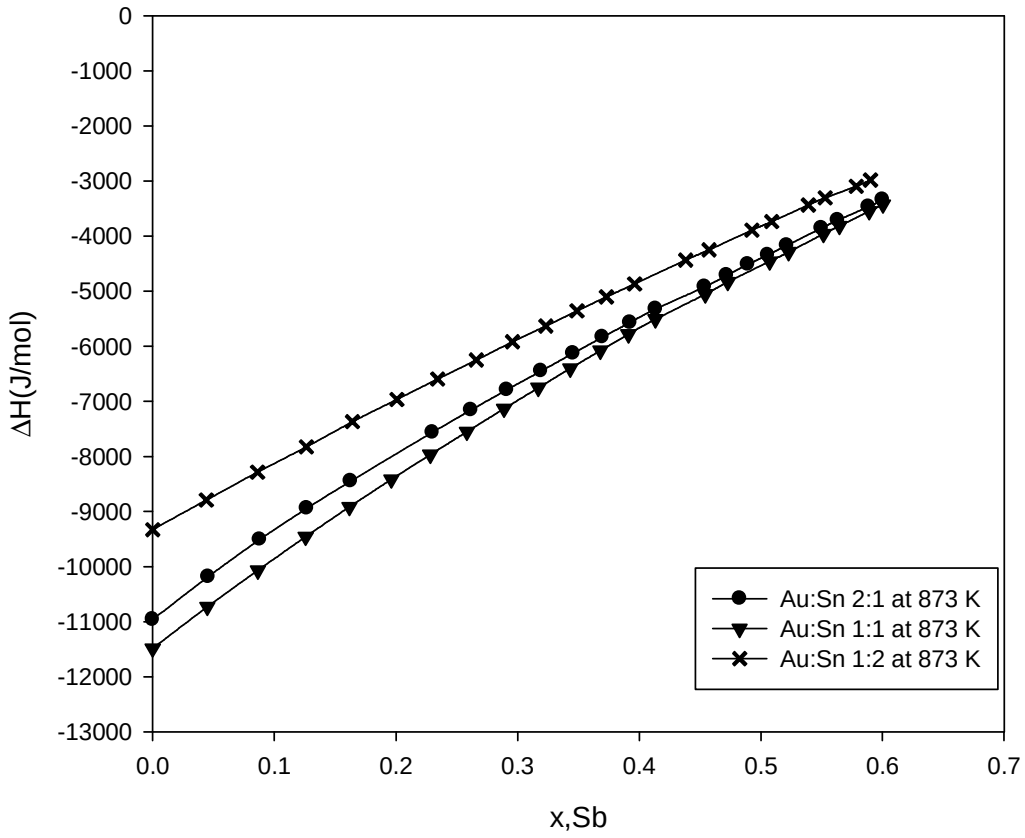

Fig. 6.2: Integral enthalpies of mixing of liquid Au-Sb-Sn alloys at 873 K, pure antimony dropped into molten Au-Sn alloys.

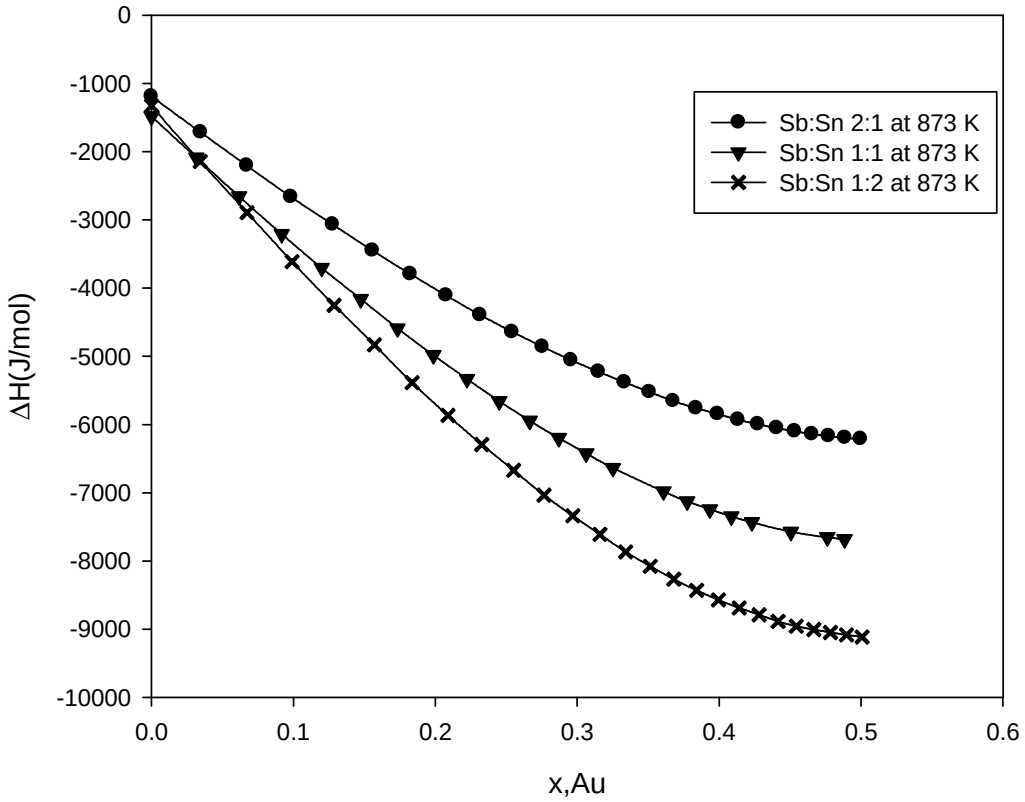

Fig. 6.3: Integral enthalpies of mixing of liquid Au-Sb-Sn alloys at 873 K, pure gold dropped into molten Sb-Sn alloys.

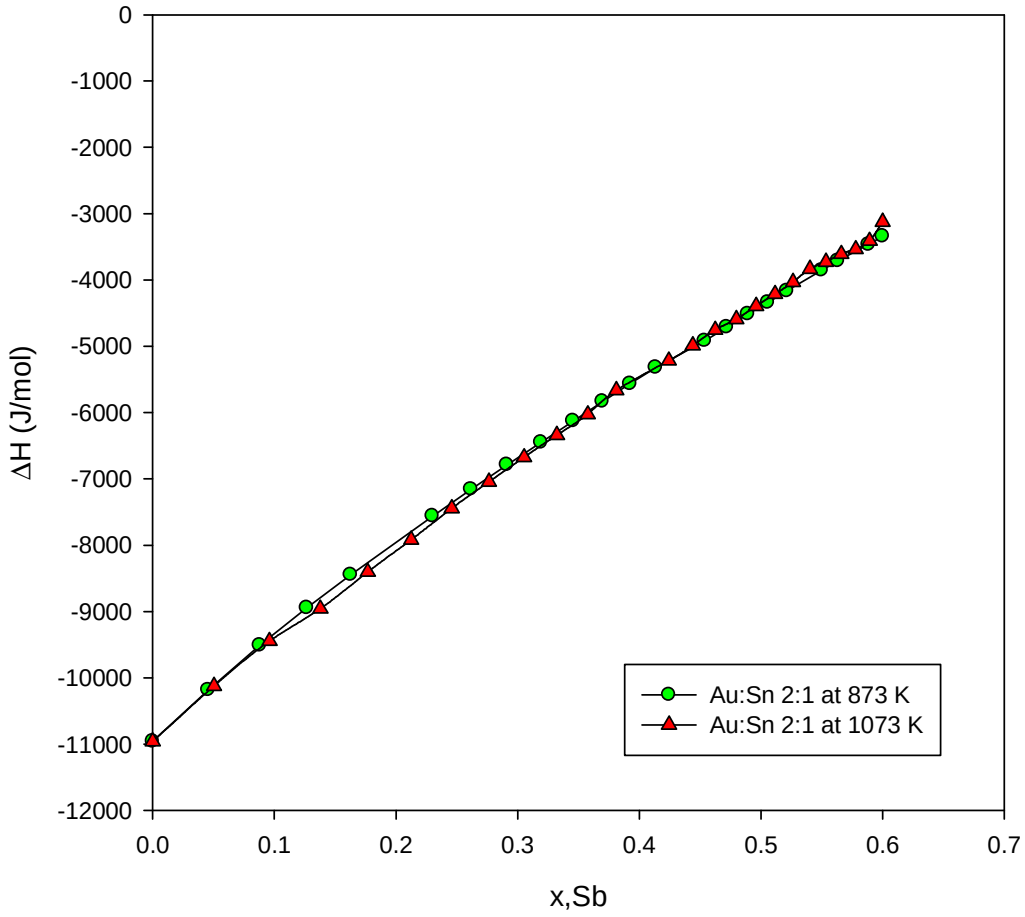

Fig. 6.4: Integral enthalpies of mixing of liquid Au-Sb-Sn alloys at the Au:Sn=2:1 cross-section at 873 K and 1073 K, pure antimony dropped into molten Au-Sn alloys.

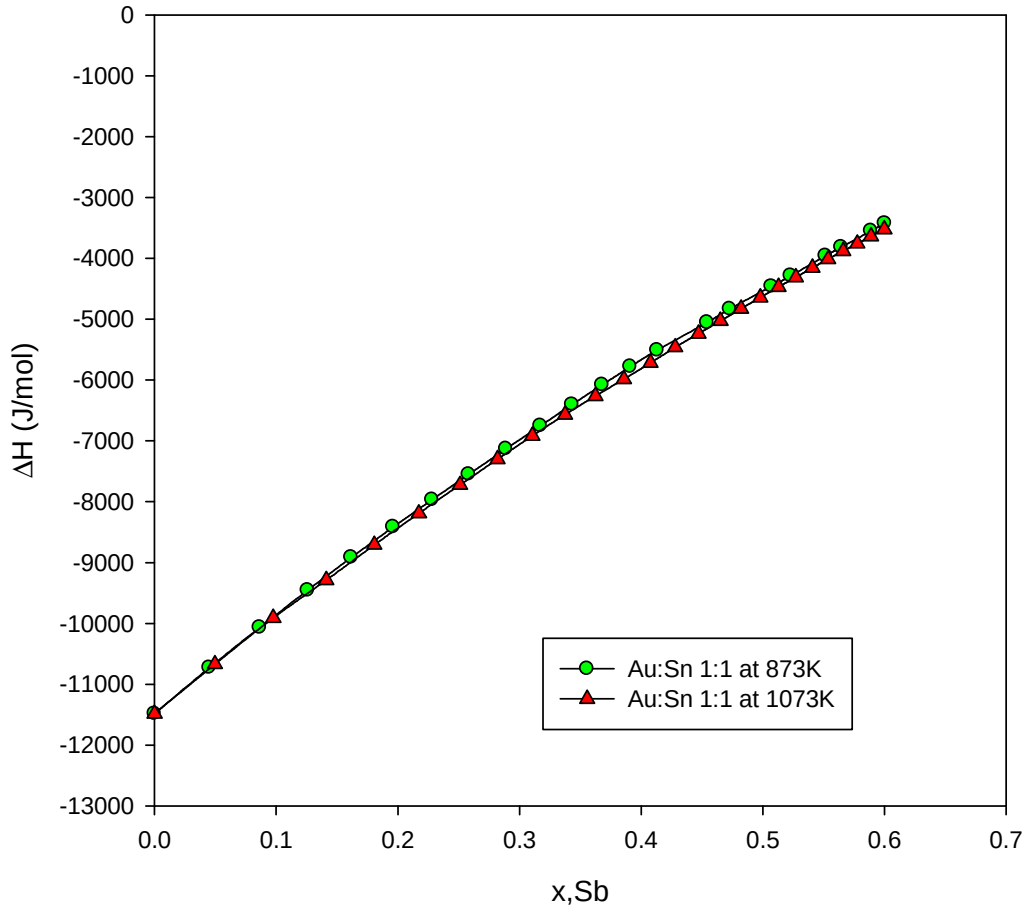

Fig. 6.5: Integral enthalpies of mixing of liquid Au-Sb-Sn alloys at the Au:Sn=1:1 cross-section at 873 K and 1073 K, pure antimony dropped into molten Au-Sn alloys.

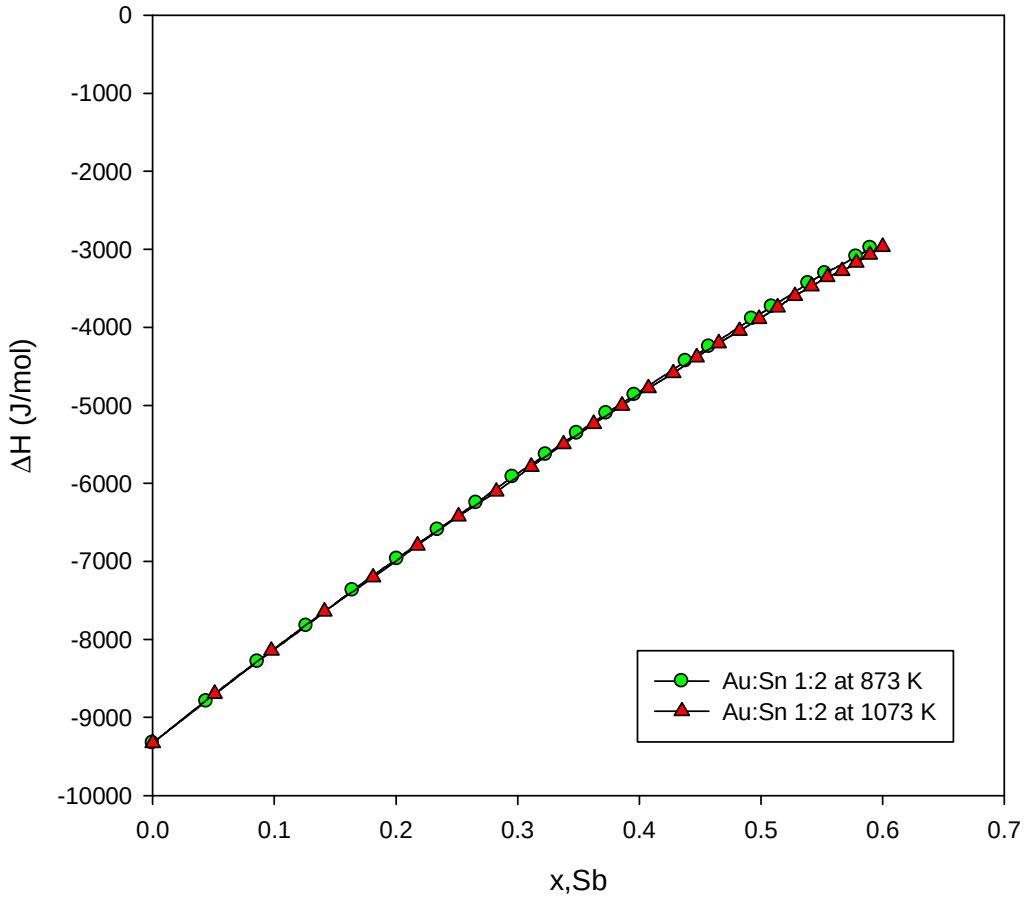

Fig. 6.6: Integral enthalpies of mixing of liquid Au-Sb-Sn alloys at the Au:Sn=1:2 cross-section at 873 K and 1073 K, pure antimony dropped into molten Au-Sn alloys.

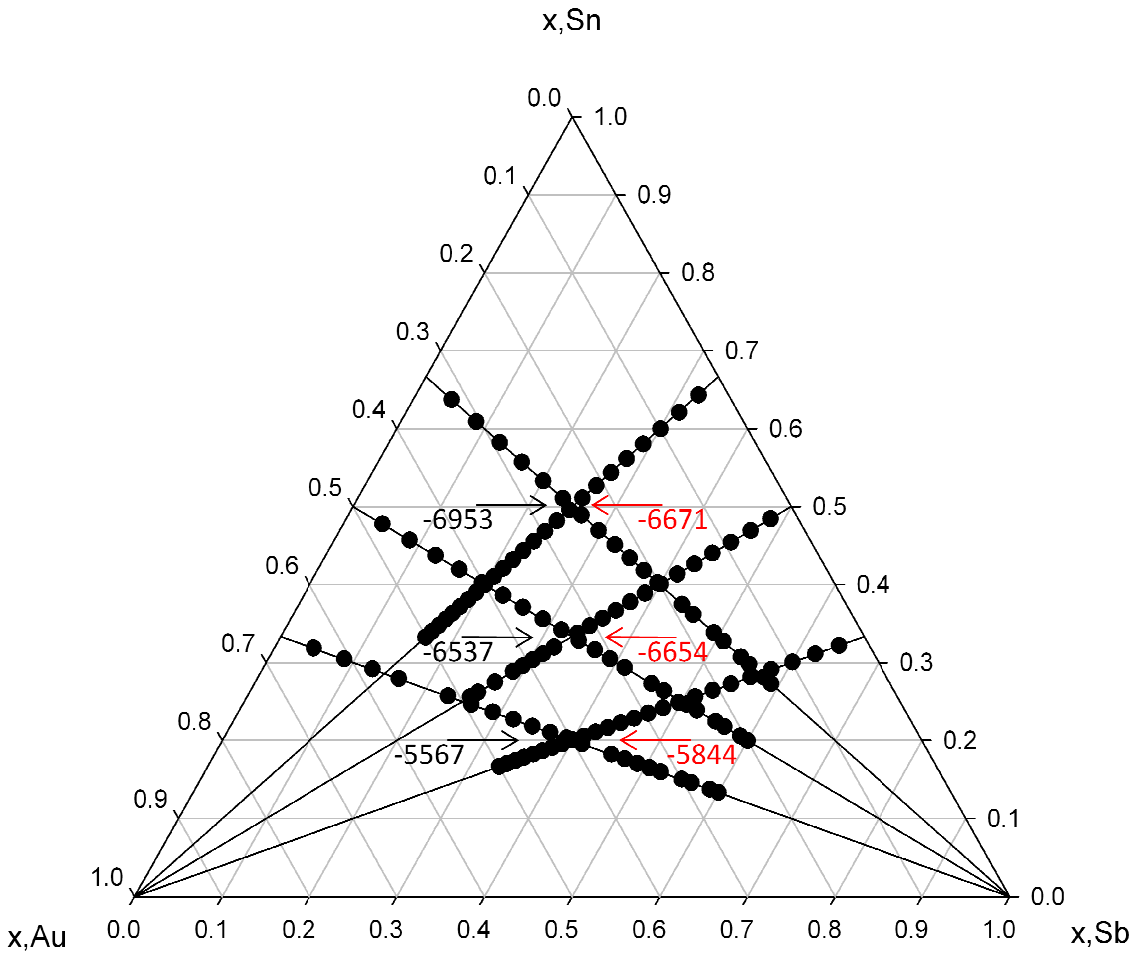

Fig. 6.7: Crossing points of the calorimetric investigations (values in J/mol) in the Au-Sb-Sn system at 873 K.

The values for the enthalpy of mixing (in J/mol) at the crossing points were checked for consistency:

The red numbers in Fig.6.7 indicate the values obtained by dropping Au at constant ratios of Sb:Sn, the black numbers are those for dropping Sb at constant ratios of Au:Sn. The values for all crossing points are listed in Table 6.3. Observed deviations are less than 400 J/mol which lies within the error of the instrument with ±250 J/mol. Another aspect which should not be forgotten is that deviations also depend on the starting values of the binary systems.

x, Au	x, Sb	x, Sn	ΔH (J/mol) (Au dropped)	ΔH (J/mol) (Sb dropped)
0.4	0.4	0.2	-5844	-5567
0.25	0.5	0.25	-4595	-4538
0.5	0.25	0.25	-7703	-7306
0.14	0.57	0.29	-3237	-3164
0.33	0.33	0.33	-6654	-6537
0.2	0.4	0.4	-5003	-4828
0.4	0.2	0.4	-8572	-8364
0.25	0.25	0.5	-6671	-6953

Table 6.3: Enthalpies of mixing for the crossing points of the calorimetric investigations in the Au-Sb-Sn system at 873 K.

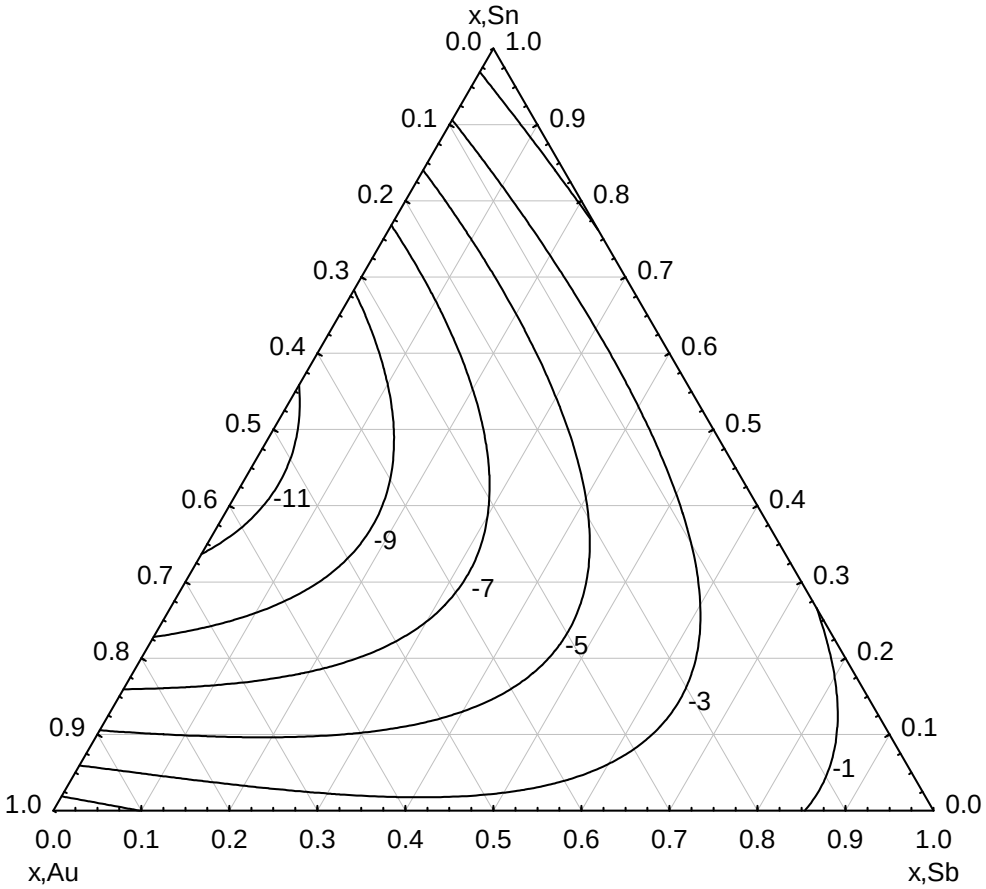

Fig. 6.8: Iso-enthalpy curves (kJ/mol) of the ternary Au-Sb-Sn system at 873 K determined by calorimetric measurements.

The iso-enthalpy curves are shown for the Au-Sb-Sn system at 873 K. The minimum can be found in the binary Au-Sn with about 55% of Au.

6.2.2 Comparison of EMF with calorimetric measurement

The substitutional solution model of Redlich–Kister–Muggianu was used for a least square fit of the experimental data in order to get an analytical expression for the integral enthalpy of mixing to compare values with the cross-sections that were measured with the EMF method (Fig.4.3.).

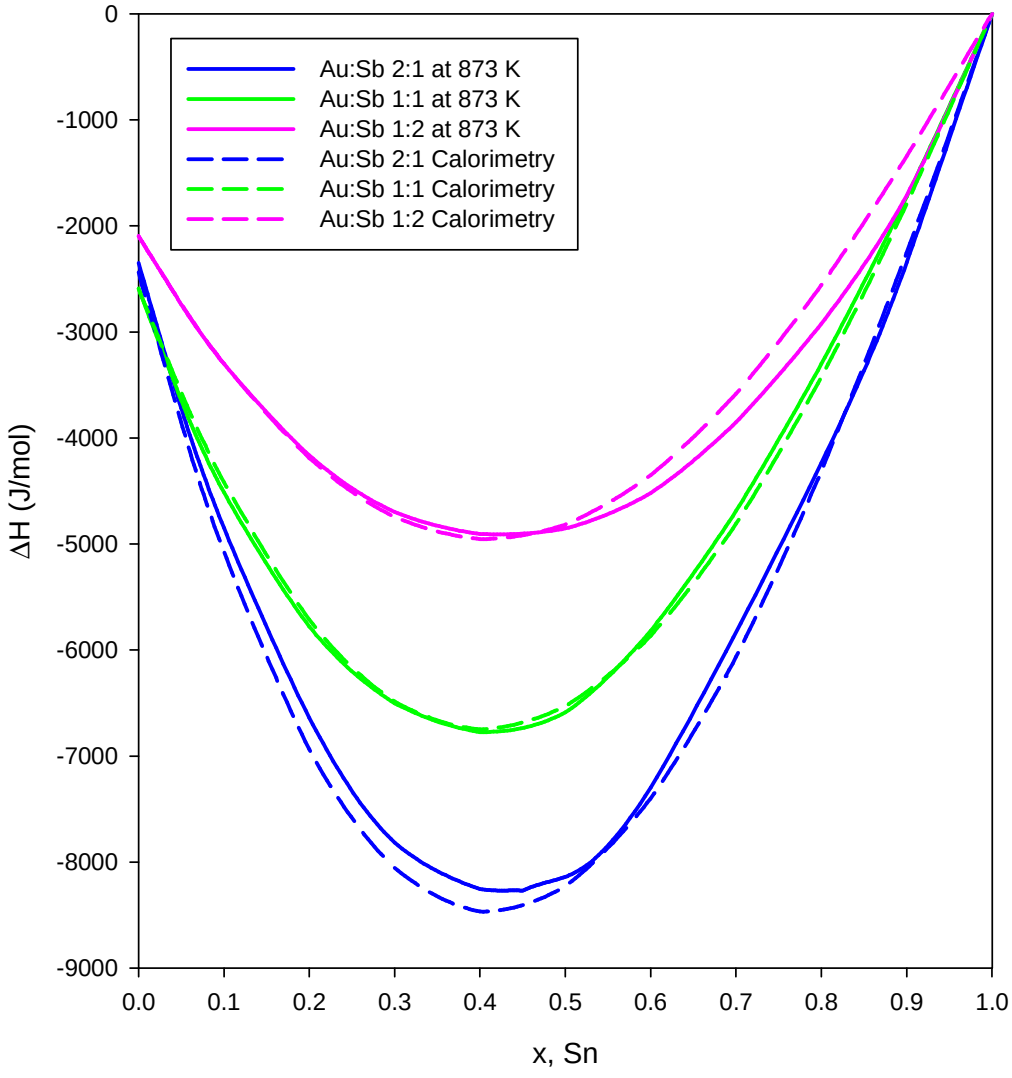

Fig. 6.9: Integral enthalpy of mixing for the Au:Sb = 2:1, 1:1, and 1:2 cross-sections at 873 K.

The comparison shows that the enthalpies of mixing obtained with the emf method are in excellent agreement with the data obtained by calorimetric measurements.

6.2.3. Conclusion

The partial and integral enthalpies of mixing in the liquid ternary Au-Sb-Sn system were investigated calorimetrically. The experimental data were optimized based on the Redlich-Kister-Muggianu model. The measurements at different temperatures show that the enthalpies of mixing of liquid ternary alloys are not temperature dependent. The comparison shows that the enthalpy of mixing determined by calorimetric measurements is in very good agreement with the data obtained by the emf method.

Chapter 7: Surface tension of Sn and the ternary Ag-Bi-Sn system

7.1 Literature review

7.1.1 Sn

Various surface tension measurements have been done on tin [1921 Hogness, 1926 Bircumshaw, 1927 Matuyama, 1934 Bircumshaw, 1948 Pelzel, 1957 Melford, 1961 Lauermann, 1971 White, 1976 Kasama, 1982 Goumiri, 1986 Nogi, 1988 Nogi, 1990 Passerone, 1992 Taimatsu] and many others with maximum drop pressure, maximum bubble pressure, drop weight, capillary rise, levitated drop and sessile drop method. The authors presented versatile values of surface tension. Some measurements are compared with this one in the results section.

7.1.2 Ag-Bi system

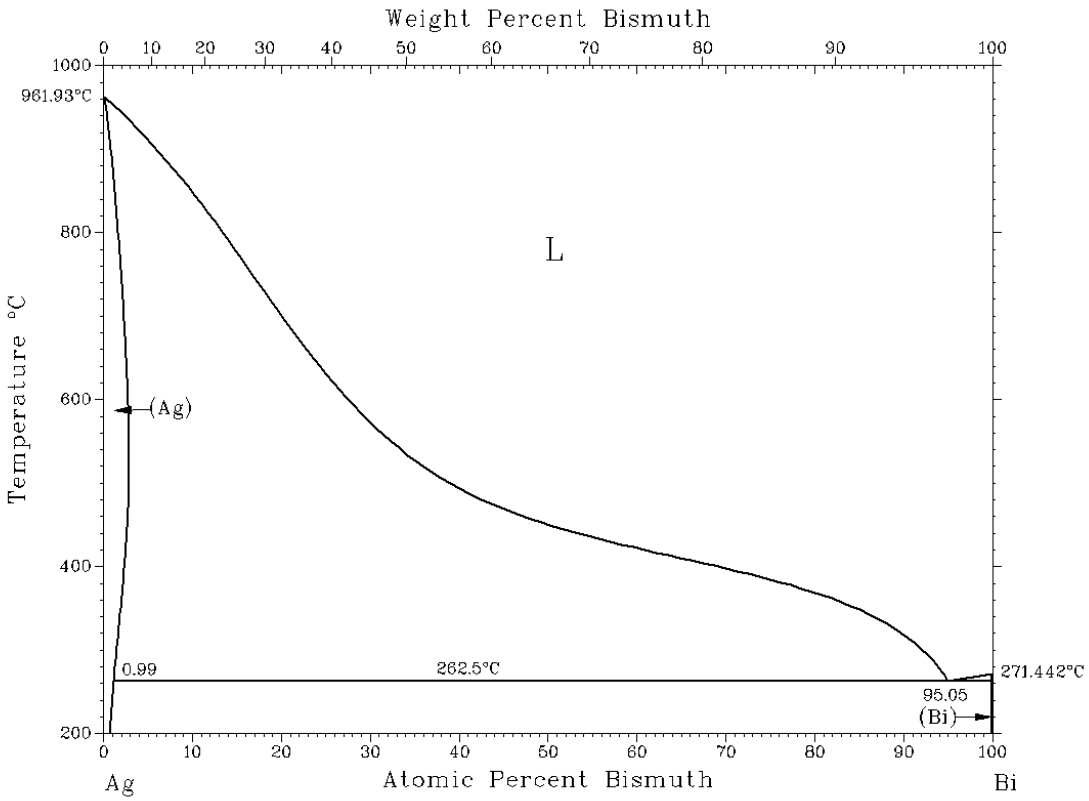

Fig. 7.1: Phase diagram of the Ag-Bi system [1990 Massalski].

Surface tension has been measured by Kucharski [2005 Kucharski].

7.1.3 Bi-Sn system

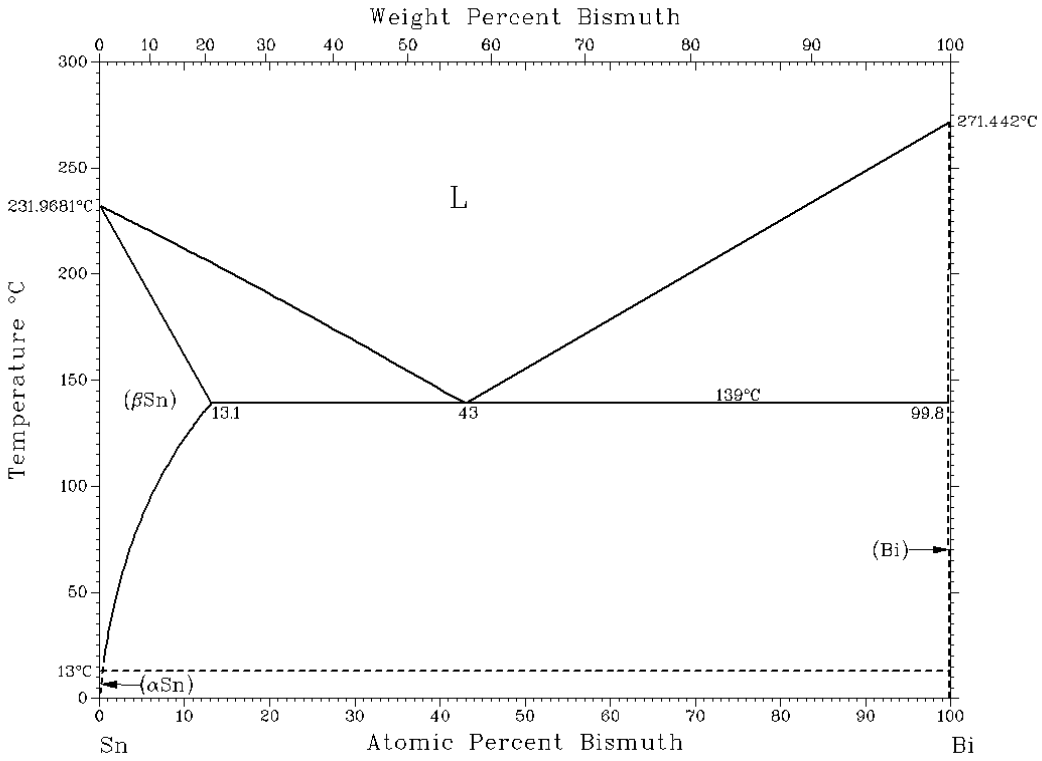

Fig. 7.2: Phase diagram of the Bi-Sn system [1990 Massalski].

Surface tension has been measured by Kucharski [2005 Kucharski].

7.1.4 Ag-Bi-Sn system

The surface tension values for the pure metals at their melting points are compiled by Iida [1988 Iida] and are shown in Table 7.1. Activity measurements with fused salts have been done by Katayama [2005 Katayama]. Emf measurements using a solid electrolyte were performed by Garzel [2006 Garzel]. Li [2008 Li] published activities from emf measurements using a liquid electrolyte. Surface tension and surface concentrations were calculated by Terzieff [2007 Terzieff]. The surface tension of Ag-Bi-Sn alloys in dependence from Ag was measured by Fima [2008 Fima].

Element	σ (mN/m)
Ag	966
Bi	378
Sn	560

Table 7.1: Surface tension values σ of the pure metals at their melting point.

7.2 Experimental procedure

For the measurements, samples with weights from 50-150 mg were used to minimize the influence of gravity. For pure tin the measurement has been done from 573-873 K. The measurements of the alloys in the Ag-Bi-Sn system were performed from 873-973 K. The lower temperature limit was chosen with 873 K as a result of the liquidus temperatures (Fig.7.2) determined by Li [2006 Li] to have the same starting temperature for all samples. The upper temperature limit was 973 K because at higher temperatures the sample holder started to shake. Before the measurements of the samples started, a rotationally symmetric standard consisting of sintered aluminium oxide with a diameter of 2.9 mm was used to determine the magnification factor. The measurements were executed under a reducing argon/hydrogen (5%) atmosphere with a flow of 150 ml/min. Small titan sheets were used as an oxygen getter. The Ag-Bi-Sn samples were heated up to 873 K and were kept there for 30 minutes to make sure that they were liquid. At the measuring temperature the samples were kept for 30 minutes, respectively. The measured samples are shown in Fig.7.3.

7.3 Results

7.3.1 Liquidus temperatures

Table 7.2: Liquidus temperatures for the Ag:Bi 2:1, 1:1 and 1:2 cross-section [Li 2006].

	Ag:Bi=2:1	Ag:Bi=1:1	Ag:Bi=1:2
x, Sn	Liquidus *T* (K)	Liquidus *T* (K)	Liquidus *T* (K)
0.1	817	793	762
0.2	812	786	749
0.3	787	762	724
0.4	758	732	706
0.5	730	706	680
0.6	708	689	667
0.7	684	664	603
0.8	637	613	552
0.9	499	492	488

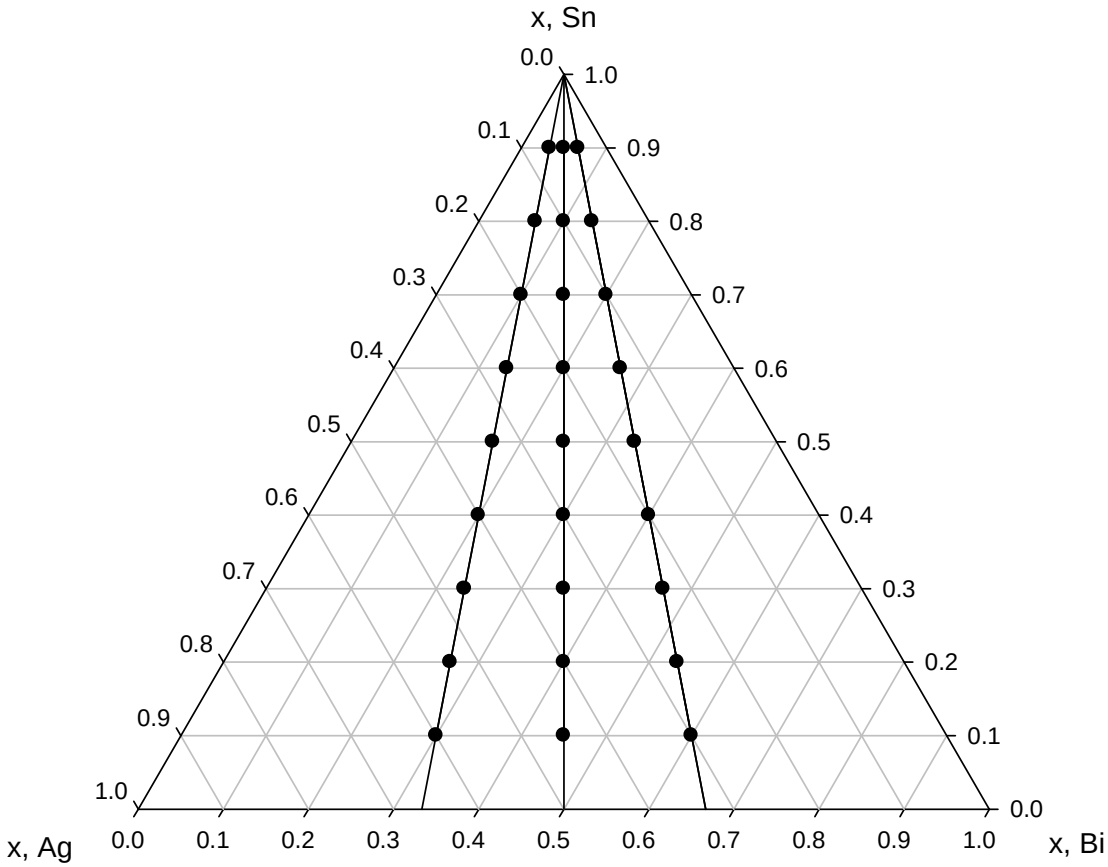

Fig. 7.3: Measured cross-sections and alloy compositions in the ternary Ag-Bi-Sn system.

7.3.2 Surface tension and density of Sn

T (K)	ρ (g/cm^3)	σ (mN/m)
573	7.03	525
623	6.96	522
673	6.92	519
723	6.89	516
773	6.87	513
823	6.83	510
873	6.80	508

Table 7.3: Densities and surface tension values of pure tin at different temperatures.

Like expected the density of pure Sn is falling with rising temperature. The same is true for the surface tension values.

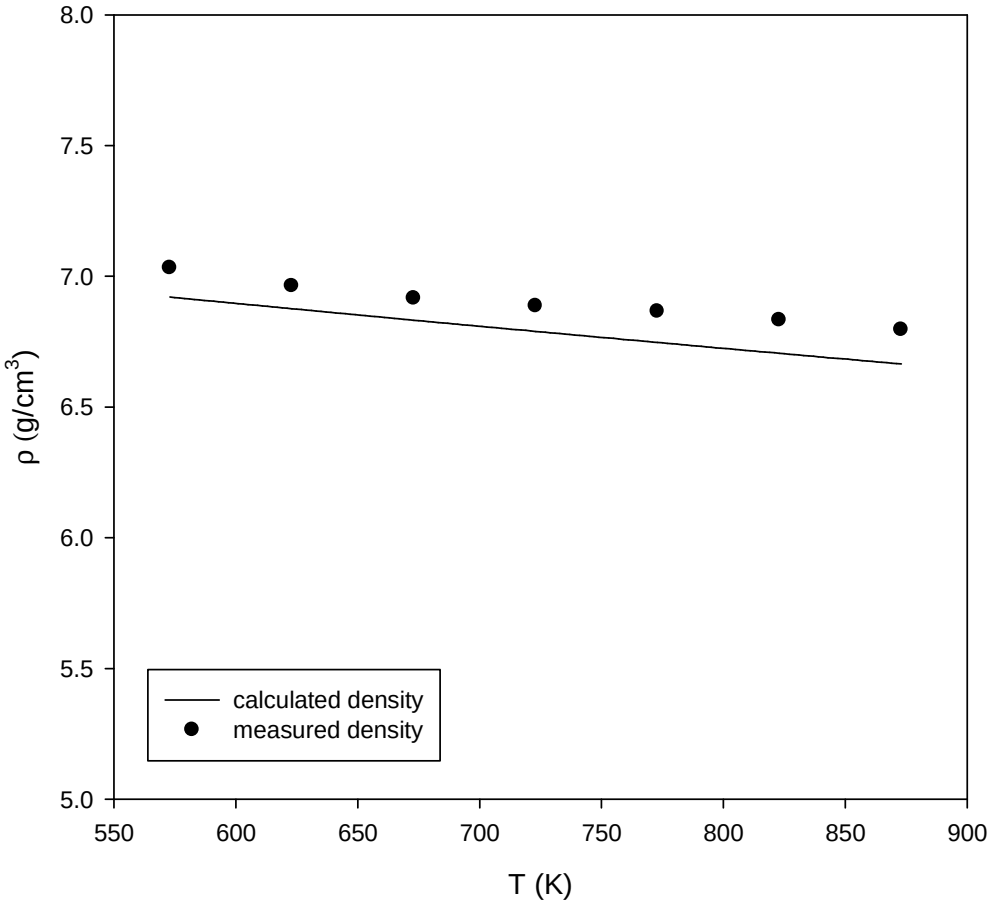

Fig. 7.4: Measured and calculated densities of pure tin at different temperatures.

The measured density values of Sn are compared with the values from Wang who measured densities of Sn by an Archimedean method and described the temperature dependence by a quadratic equation [2003 Wang]. The deviation between both techniques is less than 2%.

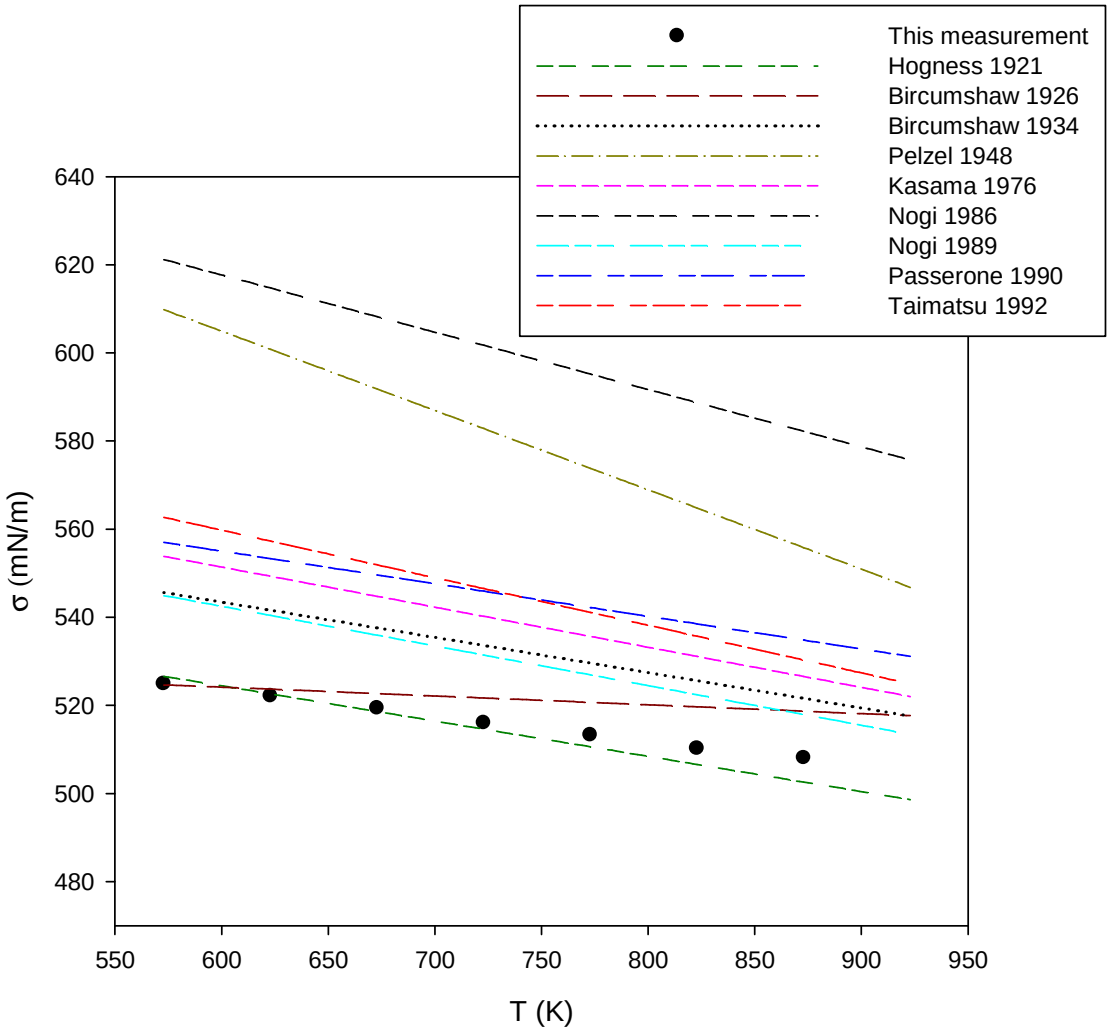

Fig. 7.5: Surface tension of tin reported between 1921 and 2010.

The result of the surface tension measurement of Sn is compared with various other works [1921 Hogness, 1926 Bircumshaw, 1934 Bircumshaw, 1948 Pelzel, 1976 Kasama, 1986 Nogi, 1988 Nogi, 1990 Passerone, 1992 Taimatsu]. The variety of about 100 mN/m between the different works for the surface tension of tin shows that it is complicated to get well-defined values for liquid metals.

7.3.3 Surface tension of liquid Ag-Bi-Sn alloys.

	Ag:Bi=2:1	Ag:Bi=1:1	Ag:Bi=1:2
x, Sn	σ (mN/m)	σ (mN/m)	σ (mN/m)
0.1	443	359	380
0.2	459	430	378
0.3	512	436	366
0.4	509	406	445
0.5	506	446	477
0.6	522	473	439
0.7	529	457	459
0.8	573	450	410
0.9	551	468	461

Table 7.4: Surface tension values of the Ag-Bi-Sn system for the Ag:Bi=2:1, 1:1 and 1:2 cross-sections.

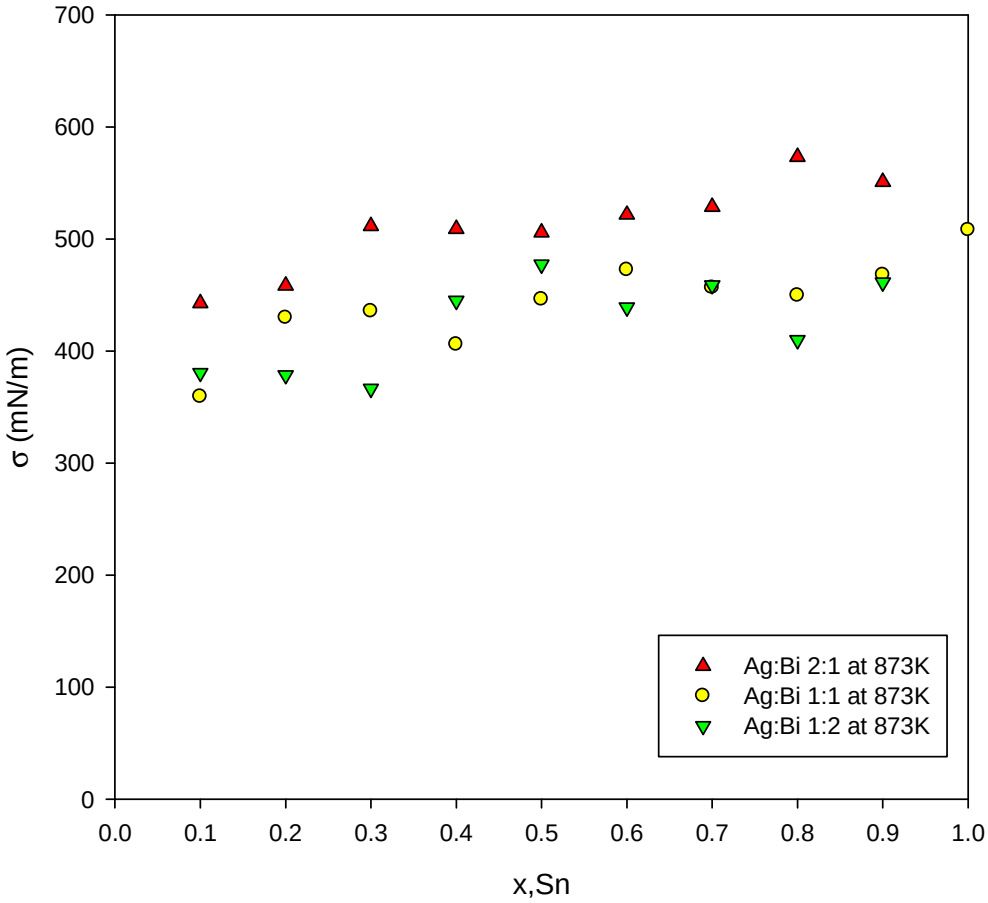

Fig. 7.6: Surface tension of liquid Ag-Bi-Sn alloys at 873 K.

The results show that with increasing amount of bismuth from the silver-rich to the bismuth-rich side the surface tension starts to drop slightly. The silver-rich cross-section shows that silver has no appreciable effect on increasing the surface tension in ternary Ag-Bi-Sn alloys compared to pure tin. The surface tension tends to be always near the value for pure tin.

7.3.4 Densities of liquid Ag-Bi-Sn alloys.

	Ag:Bi=2:1	Ag:Bi=1:1	Ag:Bi=1:2
x, Sn	ρ (g/cm^3)	ρ (g/cm^3)	ρ (g/cm^3)
0.1	9.0	9.62	9.92
0.2	9.71	9.79	9.22
0.3	9.29	9.23	8.92
0.4	8.53	8.78	8.87
0.5	8.26	8.48	8.56
0.6	7.9	8.14	8.16
0.7	7.72	7.71	7.74
0.8	7.5	7.34	7.7
0.9	6.96	7.14	7.35

Table 7.5: Densities of the Ag-Bi-Sn system for the Ag:Bi=2:1, 1:1 and 1:2 cross-sections.

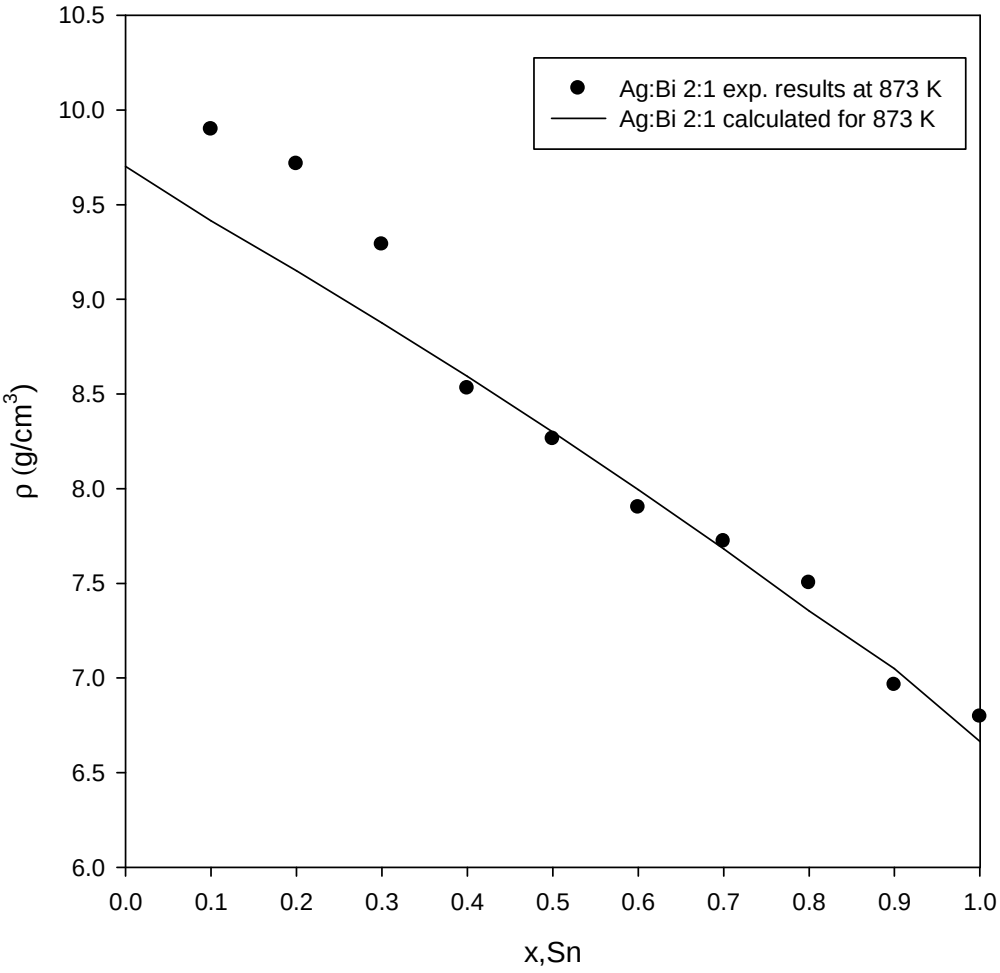

Fig. 7.7: Measured and calculated densities of the Ag:Bi=2:1 cross-section at different temperatures.

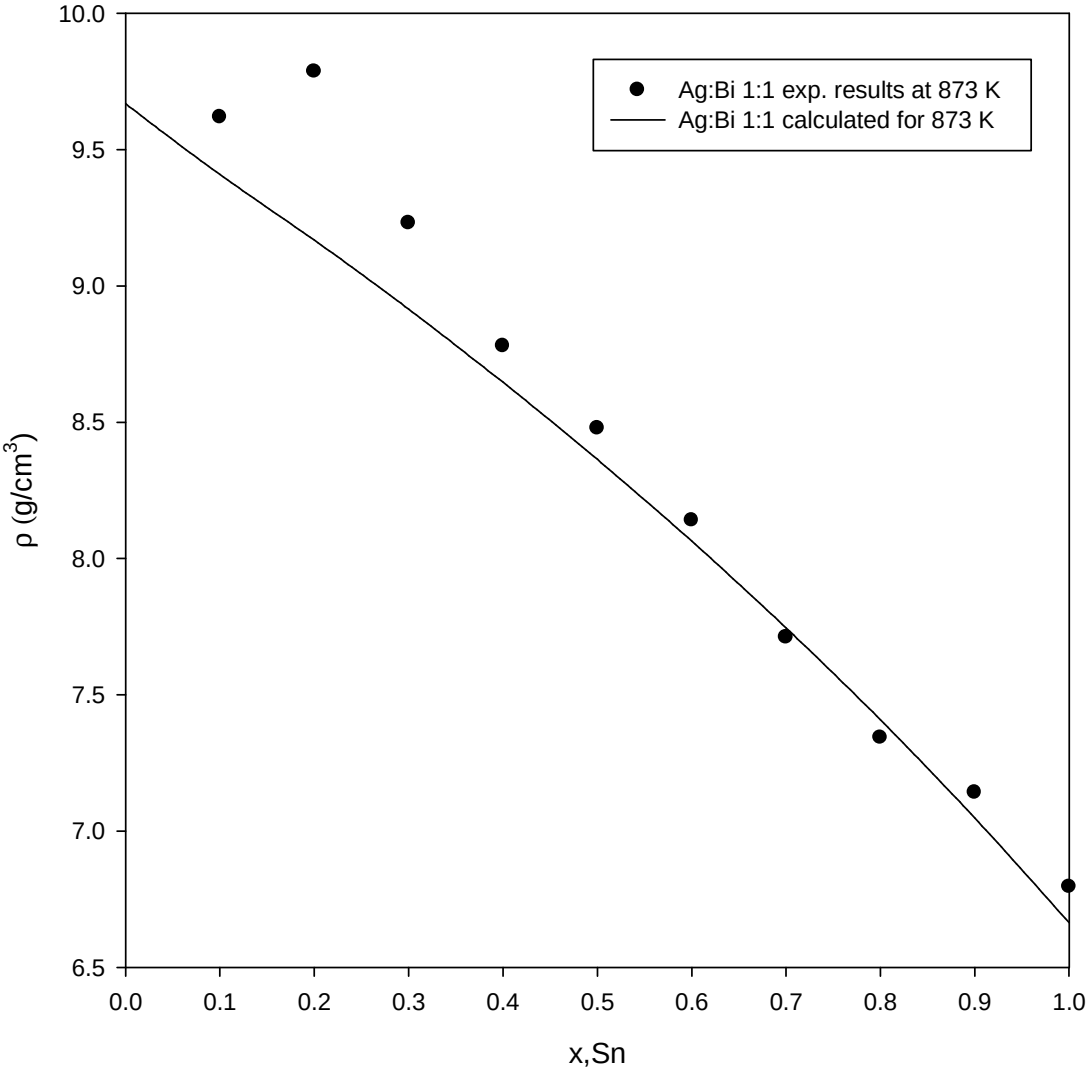

Fig. 7.8: Measured and calculated densities of the Ag:Bi=1:1 cross-section at different temperatures.

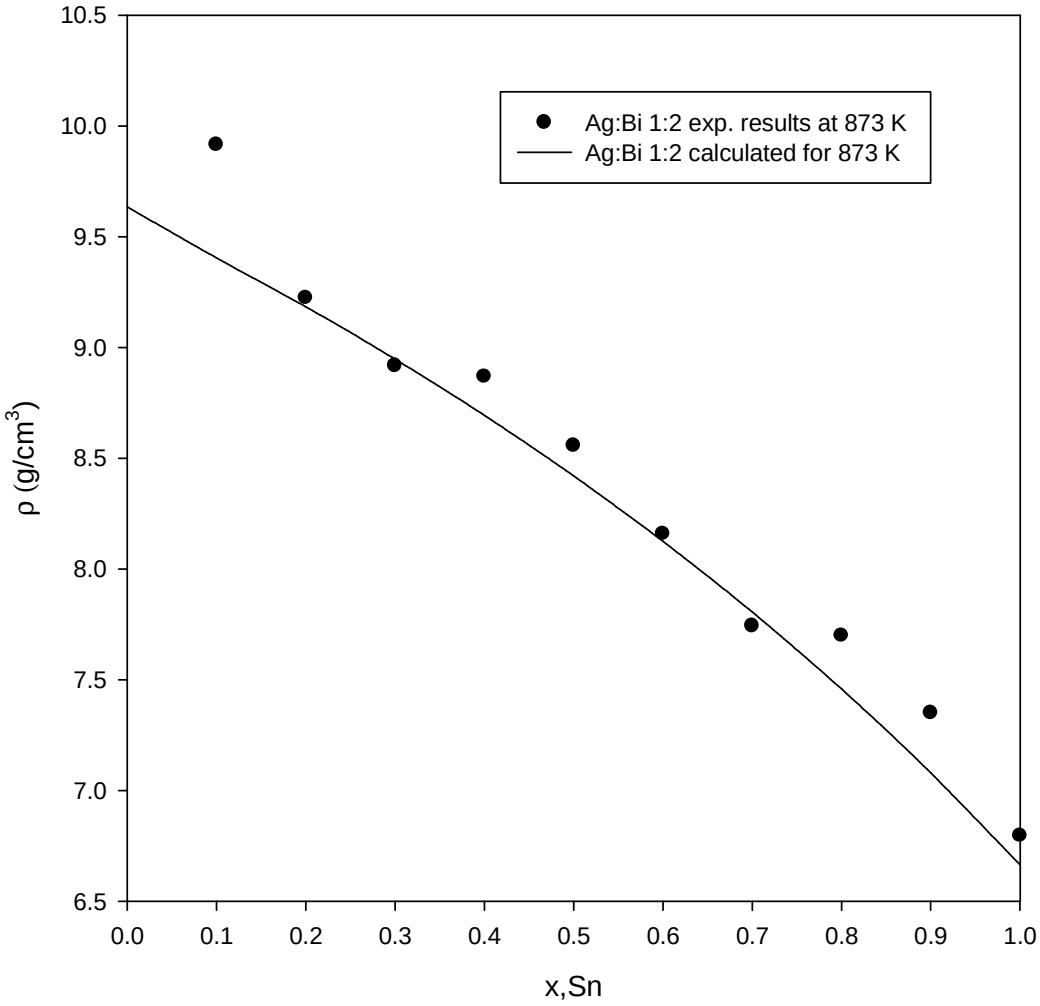

Fig. 7.9: Measured and calculated densities of the Ag:Bi=1:2 cross-section at different temperatures.

The measured density values of the Ag-Bi-Sn alloys are compared with densities calculated from equations for the pure elements at the given temperature and weighted by the mass percents of the elements. The equations for calculating the densities of Bi and Sn are taken from [2003 Wang]. The equation for Ag has been taken from [1929 Matsuyama]. Comparing the results shows that the measured values are getting closer to the calculated ones with higher contents of tin.

7.3.5 Conclusion

The surface tension of ternary Ag-Bi-Sn alloys was measured with the sessile drop method. The measured densities are compared with calculated densities weighted by mass and are in good agreement with each other. For the Ag-Bi = 2:1, 1:1 and 1:2 cross-sections, no influence of silver on the surface tension in the liquid alloys could be observed. With increasing amount of Bismuth the surface tension decreases slightly.

Chapter 8: Summary

8.1 Summary (Englisch version)

The aim of the present work is the investigation of thermodynamic properties and surface tension of new possible lead-free solder alloys. In this work investigations have been done on the Ag-Au-Sn, Au-Sb-Sn, Au-Sb and the Ag-Bi-Sn system.

For the Ag-Au-Sn system, the activities of Sn in liquid Ag-Au-Sn alloys were determined with the emf method as a function of concentration and temperature using the following cell arrangement:

$$W, Sn_{(l)}/KCl\text{-}LiCl\text{-}SnCl_2/Ag\text{-}Au\text{-}Sn_{(l)},W$$

Thermodynamic properties were determined for 24 alloys. The compositions were situated on three cross-sections with constant molar ratios of Ag:Au = 2:1, 1:1 and 1:2 with tin content from 20-90 at.%. The integral thermodynamic properties were calculated at 973 K by Gibbs-Duhem integration. Comparisons of the integrated enthalpy of mixing with literature results from calorimetric experiments show very good agreement.

For the Au-Sb-Sn system, the activities of Sn in liquid Au-Sb-Sn alloys were also determined with the emf method as a function of concentration and temperature using the following cell:

$$W, Sn_{(l)}/KCl\text{-}LiCl\text{-}SnCl_2/Au\text{-}Sb\text{-}Sn_{(l)},W$$

Thermodynamic properties were determined for 30 alloys at three cross-sections with constant molar ratios of Au:Sb = 2:1, 1:1 and 1:2 with tin content from 5-90 at.%. The integral thermodynamic properties were calculated at 873 K by Gibbs-Duhem integration. The Au-Sb-Sn system was

also investigated by calorimetric measurements at 873 K and 1073 K using a Calvet-type microcalorimeter. Comparisons show that the enthalpies of mixing obtained by the emf method are in excellent agreement with the results gained by calorimetric measurements.

The Au-Sb system was remeasured at 913 K by the emf method, as no reliable data were found in literature. Problems were instable emf values and evaporation of $SbCl_3$ out of the electrolyte during the measurements which could be solved by powdering, sealing in a quartz ampoule under vacuum and tempering the electrolyte at 383 K for several weeks after cleaning the electrolyte with chlorine gas. The obtained stable compounds did not vaporize during the heating process of the emf measurement.

For the Ag-Bi-Sn system, the surface tension and densities were determined between 873 K and 973 K for 27 liquid alloys with the sessile drop method. The compositions were situated on three cross-sections with constant molar ratios of Ag:Bi = 2:1, 1:1 and 1:2 with tin content from 10-90 at.%. The measured densities are compared with calculated densities and are in good agreement with each other. For the Ag-Bi = 2:1, 1:1 and 1:2 cross-sections, no appreciable influence of silver on the surface tension in the liquid alloys could be observed. With increasing amount of Bismuth the surface tension decreases slightly.

8.2 Summary (German version)

Das Ziel der vorliegenden Arbeit ist die Bestimmung thermodynamischer Eigenschaften und der Oberflächenspannung von möglichen neuen, bleifreien Lötmaterialien. Es wurden Untersuchungen an folgenden Systemen durchgeführt: Ag-Au-Sn, Au-Sb-Sn, Au-Sb und Ag-Bi-Sn.

Für das Ag-Au-Sn System wurden die Aktivitäten von Sn in flüssigen Ag-Au-Sn Legierungen durch Messung der elektromotorischen Kraft (EMK) in Abhängigkeit von Konzentration und Temperatur bestimmt. Der Aufbau der Messkette kann wie folgend beschrieben werden:

$$W, Sn_{(l)}/KCl\text{-}LiCl\text{-}SnCl_2/Ag\text{-}Au\text{-}Sn_{(l)},W$$

Thermodynamische Eigenschaften wurden für 24 Legierungen an den drei Schnitten Ag:Au = 2:1, 1:1 und 1:2 mit einem jeweiligen Zinngehalt von 20-90 Atomprozent bestimmt. Die integralen thermodynamischen Eigenschaften wurden für 973 K mittels Gibbs-Duhem Integration berechnet. Vergleiche der integralen Mischungsenthalpie mit Literaturwerten aus kalorimetrischen Messungen zeigen sehr gute Übereinstimmungen.

Für das Au-Sb-Sn system wurden die Aktivitäten von Sn in flüssigen Au-Sb-Sn Legierungen ebenfalls durch Messung der elektromotorischen Kraft bestimmt. Dafür wurde folgende Zellanordnung verwendet:

$$W, Sn_{(l)}/KCl\text{-}LiCl\text{-}SnCl_2/Au\text{-}Sb\text{-}Sn_{(l)},W$$

Thermodynamische Eigenschaften wurden für 30 Legierungen an den drei Schnitten Au:Sb = 2:1, 1:1 und 1:2 mit einem jeweiligen Zinngehalt von 5-90 Atomprozent bestimmt. Die integralen thermodynamischen Eigenschaften wurden für 873 K mittels Gibbs-Duhem Integration

berechnet. Es wurden zusätzlich kalorimetrische Messungen am Au-Sb-Sn system bei 873 K und 1073 K durchgeführt, um einen Vergleich für die Mischungsenthalpien der mittels EMK bestimmten Werte zu erhalten. Die Ergebnisse beider Techniken stimmen ausgezeichnet überein.

Das Au-Sb System wurde bei 913 K nachgemessen, da diese binären Startwerte für die Integration der partiellen thermodynamischen Größen im Au-Sb-Sn system mittels Gibbs-Duhem Integration benötigt werden und sich keine zuverlässige Literatur gefunden wurde. Probleme hierbei waren Schwankungen der gemessenen elektromotorischen Kraft und die Verdampfung des $SbCl_3$ aus dem Elektrolyten. Dieses Problem wurde gelöst, indem nach der Reinigung des Elektrolyten mit Chlorgas, dieser pulverisiert, unter Vacuum in einer Quartzampulle versiegelt und anschließend mehrere Wochen bei 383 K getempert. Die anschließende erhaltene, stabile Verbindung verhinderte ein Verdampfen des $SbCl_3$ aus dem Elektrolyten während der Aufheizphase der Messung.

Für das Ag-Bi-Sn system wurden die Oberflächenspannung und die Dichten zwischen 873 K und 973 K bestimmt. Zur Anwendung kam die Methode des liegenden Tropfen. Es wurden 27 flüssige Legierungen an den Schnitten Ag:Bi = 2:1, 1:1 und 1:2 mit einem jeweiligen Zinngehalt von 10-90 Atomprozent untersucht. Die gemessenen Dichten wurden mit berechneten Werten verglichen und sind in guter Übereinstimmung. Für die Schnitte Ag:Bi = 2:1, 1:1 und 1:2 konnte kein merklicher Einfluss von Silber auf die Oberflächenspannung von Bismut und Zinn festgestellt werden. Mit ansteigender Bismutmenge ist ein leichter Abfall der Oberflächenspannung zu beobachten.

List of tables

List of figures

References

[1892] F. Bashforth and J.C. Adams, *An Atempt to Test the Theory of Capillary Action*. 1892: Cambridge University Press and Deighton Bell & Co.

[1921] T.R. Hogness, *Surface tensions and densities of liquid mercury, cadmium, zinc, lead, tin and bismuth.* J. Am. Chem. Soc., 1921. **43**: p. 1621-8.

[1923] J. Kendall, E.D. Crittenden, and H.K. Miller, *A study of the factors influencing compound formation and solubility in fused salt mixtures.* J. Am. Chem. Soc., 1923. **45**: p. 963-96.

[1926] L.L. Bircumshaw, *The surface tension of liquid metals. I. Tin and lead.* Philos. Mag. (1798-1977), 1926. **2**: p. 341-50.

[1927] Y. Matuyama, *The surface tension of molten metals and alloys.* Sci. Rep. Tohoku Imp. Univ., Ser. 4, 1927. **16**: p. 555-62.

[1929] Y. Matsuyama, *A further measurement of the density of molten metals and alloys.* Sci. Rep. Tohoku Imp. Univ., Ser. 1, 1929. **18**(1st Ser.): p. 737-44.

[1934] L.L. Bircumshaw, *Surface tension of liquid metals. V. The surface tension of the lead-tin alloys.* Philos. Mag. (1798-1977), 1934. **17**: p. 181-91.

[1948] E. Pelzel, *The surface tension of liquid metals and alloys.* Berg- Huettenmaenn. Monatsh. Montan. Hochsch. Leoben, 1948. **93**: p. 248-54.

[1950] L.S. Darken, *Application of the Gibbs-Duhem equation to ternary and multicomponent systems.* J. Am. Chem. Soc., 1950. **72**: p. 2909-14.

[1950] O.J. Kleppa, *A thermodynamic study of liquid metallic solutions. II. The system tin-gold.* J. Am. Chem. Soc., 1950. **72**: p. 3346-52.

[1951] J.F. Elliott and J. Chipman, *The thermodynamic properties of liquid ternary cadmium solutions.* J. Am. Chem. Soc., 1951. **73**: p. 2682-93.

[1954] C. Wagner, *Thermodynamics of the liquidus and the solidus of binary alloys.* Acta Metall., 1954. **2**: p. 242-9.

[1957] D.A. Melford and T.P. Hoar, *Determination of the surface tensions of molten lead, tin, and indium by an improved capillary method.* J. Inst. Metals, 1957. **85**: p. 197-205;Paper No 1742.

[1959] J.L. White, *Thermodynamics of the liquidus-solidus gap in binary alloys: the silver-gold system.* Trans. Am. Inst. Min., Metall. Pet. Eng., 1959. **215**: p. 178-81.

[1961] I. Lauermann and G. Metzger, *Surface-tension measurements. VIII. Surface tension of liquid silver, tin, and silver-tin alloys.* Z. Phys. Chem. (Leipzig), 1961. **216**: p. 42-9.

[1966] A.K. Jena and J.S.L. Leach, *A calorimetric investigation of liquid gold-tin alloys.* Acta Metall., 1966. **14**(11): p. 1595-1605.

[1966] G.H. Laurie, A.W.H. Morris, and J.N. Pratt, *Electromotive-force and calorimetric studies of thermodynamic properties of solid and liquid silver-tin alloys.* Trans. Metall. Soc. AIME, 1966. **236**(10): p. 1390-5.

[1966] J. Lumsden, *Thermodynamics of Molten Salt Mixtures*. Academic Press, London, New York, 1966. 351 pp.

[1968] A.K. Jena and M.B. Bever, *Heat of formation of the compound AuSb2 and the partial enthalpies and enthalpy interaction coefficients of antimony and gold in liquid tin.* Trans. Met. Soc. AIME (Amer. Inst. Mining, Met., Petrol. Eng.), 1968. **242**(7): p. 1453-4.

[1968] A. Yazawa, T. Kawashima, and K. Itagaki, *Measurements of heats of mixing in molten antimony binary alloys.* Nippon Kinzoku Gakkaishi, 1968. **32**(12): p. 1288-93.

[1971] P.J. Roy-Chowdury and A. Gosh, *Thermodynamic Measurements in Liquid Sn-Ag Alloys.* Metallurgical Transactions, 1971. **2**.

[1971] D.W.G. White, *Surface tensions of lead, tin and lead-tin alloys.* Met. Trans., 1971. **2**(11): p. 3067-71.

[1972] P. Kubaschewski and C.B. Alcock, *Thermodynamic properties of silver + tin alloys.* J. Chem. Thermodyn., 1972. **4**(2): p. 259-66.

[1972] C. Petot, G. Petot-Ervas, and M. Rigaud, *Thermodynamic study of gold-tin liquid alloys.* Colloq. Int. Cent. Nat. Rech. Sci., 1972. **201**: p. 203-10.

[1972] C. Petot, G. Petot-Ervas, and M. Rigaud, *Thermodynamic study of liquid gold-tin alloys.* Phys. Chem. Liquids, 1972. **3**(1): p. 13-28.

[1973] R. Hultgren, P.D. Desai, D.T. Hawkins, M. Gleiser and K.K. Kelley, *Selected Values of the Thermodynamic Properties of Binary Alloys* 1973: ASM, Ohio.

[1974] D.S. Evans and A. Prince, *Thermal analysis of the silver-gold-tin ternary system in the region from 20 to 100% tin.* Met. Sci., 1974. **8**(9): p. 286-90.

[1974] R. Farhi, G. Petot-Ervas, C. Petot and J.P. Auffredic, *Thermodynamic study of liquid silver-tin alloys.* Phys. Chem. Liq., 1974. **4**(2-3): p. 171-82.

[1974] K. Kameda, T. Azakami, and M. Kameda, *Activities of indium and antimony in liquid gold base binary alloy systems.* Nippon Kinzoku Gakkaishi, 1974. **38**(5): p. 434-9.

[1974] D. Lapedes, *Dictionary of Scientific and Technical Terms*. 1974: McGraw-Hill.

[1975] M. Hino, T. Azakami, and M. Kameda, *Activity measurements of liquid antimony-silver and antimony-gold binary alloys.* Nippon Kinzoku Gakkaishi, 1975. **39**(11): p. 1175-81.

[1975] K. Itagaki and A. Yazawa, *Heats of mixing in liquid copper or gold binary alloys.* Trans. Jpn. Inst. Met., 1975. **16**(11): p. 679-86.

[1976] K. Itagak, *Measurements of heat of fusion and specific heat of gold binary compounds and derivation of excess free energy of mixing in liquid gold binary alloys.* Nippon Kinzoku Gakkaishi, 1976. **40**(10): p. 1038-46.

[1976] A. Kasama, T. Iida, and Z. Morita, *Temperature dependence of the surface tension of pure liquid metals.* Nippon Kinzoku Gakkaishi, 1976. **40**(10): p. 1030-8.

[1976] S. Seetharaman and L.I. Staffansson, *Activity of tin in liquid silver-tin alloys.* Chem. Scr., 1976. **10**(2): p. 61-6.

[1977] K. Kameda, S. Sakairi, and Y. Yoshida, *Activities of tin in the liquid gold base binary alloy system.* Nippon Kinzoku Gakkaishi, 1977. **41**(9): p. 950-5.

[1978] S.M. Howard and J.P. Hager, *Thermodynamic properties of the liquid tin-germanium and tin-gold systems by mass spectrometry.* Metall. Trans., B, 1978. **9B**(1): p. 51-9.

[1978] M. Iwase, M. Yasuda, S. Miki, and T. Mori, *A thermodynamic study of liquid tin-silver alloys by means of solid-oxide galvanic cell.* Trans. Jpn. Inst. Met., 1978. **19**(11): p. 654-60.

[1981] E. Hayer, K.L. Komarek, J.P. Bros, and M. Gaune-Escard, *Enthalpy of mixing of liquid gold-tin alloys.* Z. Metallkd., 1981. **72**(2): p. 109-15.

[1982] L. Goumiri and J.C. Joud, *Auger electron spectroscopy study of aluminum-tin liquid system.* Acta Metall., 1982. **30**(7): p. 1397-405.

[1983] Y. Rotenberg, L. Boruvka, and A.W. Neumann, *Determination of surface tension and contact angle from the shapes of axisymmetric fluid interfaces.* J. Colloid Interface Sci., 1983. **93**(1): p. 169-83.

[1983] F. Sommer, R. Lueck, N. Rupf-Bolz, and B. Predel, *Chemical short range order on liquid Sb-Sn alloys proved with the aid of the dependence of the mixing enthalpies on temperature.* Materials Research Bulletin, 1983. **18**.

[1984] H. Okamoto and T.B. Massalski, *The Au-Sb (gold-antimony) system.* Bull. Alloy Phase Diagrams, 1984. **5**(2): p. 166-71, 199-200.

[1984] J. Rakotomavo, M. Gaune-Escard, J.P. Bros, and P. Gaune, *Enthalpies of formation at 1373 K of the liquid alloys silver-gold, silver-tin, gold-tin, and silver-gold-tin.* Ber. Bunsen-Ges. Phys. Chem., 1984. **88**(7): p. 663-70.

[1984] L. Topor and O.J. Kleppa, *Thermochemistry of Binary Liquid Gold Alloys: The Systems Gold-Copper and Gold-Silver at 1379 K.* Metall. Trans A, 1984. **15A**.

[1986] K. Nogi, K. Ogino, A. McLean, and W.A. Miller, *The temperature coefficient of the surface tension of pure liquid metals.* Metall. Trans. B, 1986. **17B**(1): p. 163-70.

[1987] W.A. Badawi and A.E. Eid, *Behavior of the enthalpy of formation in the tin-antimony system.* Bull. Chem. Soc. Jpn., 1987. **60**(10): p. 3771-4.

[1987] Hayer, E., Gehringer, F., Gaune-Escard, M., Bros, J. P., *Complete automatization of a high-temperature calorimeter. Example of results: enthalpy of formation of a liquid alloy gold-gallium.* Calorim. Anal. Therm., 1987. **18**: p. 317-21

[1987] K. Kameda, *Thermodynamic properties of liquid silver-tin alloys.* Trans. Jpn. Inst. Met., 1987. **28**(7): p. 542-9.

[1988] P.Y. Chevalier, *A thermodynamic evaluation of the gold-tin system.* Thermochim. Acta, 1988. **130**: p. 1-13.

[1988] P.Y. Chevalier, *A thermodynamic evaluation of the silver-tin system.* Thermochim. Acta, 1988. **136**: p. 45-54.

[1988] S. Hassam, M. Gaune-Escard, J.P. Bros, and M. Hoch, *Enthalpies of formation of the silver-gold-silicon, silver-gold-germanium, and silver-gold-tin ternary liquid alloys: experimental determinations and application of the Hoch-Arpshofen model.* Metall. Trans. A, 1988. **19A**(8): p. 2075-89.

[1988] T. Iida and R. Guthrie, *The Physical Properties of Liquid Metals*. 1988: Oxford Science Publications.

[1988] K. Nogi, K. Oishi, and K. Ogino, *Wettability of solid oxides by liquid pure metals.* Nippon Kinzoku Gakkaishi, 1988. **52**(1): p. 72-8.

[1989] W.A. Badawi, *A calorimetric study on the beta ' phase in the system tin-antimony. Enthalpies of mixing and formation.* Bull. Chem. Soc. Jpn., 1989. **62**(1): p. 279-84.

[1989] P.Y. Chevalier, *A thermodynamic evaluation of the gold-antimony and gold-thallium systems.* Thermochim. Acta, 1989. **155**: p. 211-25.

[1989] S. Parker, P., *Encyclopedia of science and technology*. Second ed. 1989: McGraw-Hill.

[1990] T.B. Massalski, H. Okamoto, P.R. Subramanian, and L. Kacprzak, *Binary Alloy Phase Digrams*. Second Edition ed. 1990: ASM International, Ohio.

[1990] A. Passerone, E. Ricci, and R. Sangiorgi, *Influence of oxygen contamination on the surface tension of liquid tin.* J. Mater. Sci., 1990. **25**(10): p. 4266-72.

[1991] A.T. Dinsdale, *SGTE data for pure elements.* CALPHAD Comput. Coupling Phase Diagrams Thermochem., 1991. **15**(4): p. 317-425.

[1992] H. Taimatsu and R. Sangiorgi, *Surface tension and adsorption in liquid tin-oxygen system.* Surf. Sci., 1992. **261**(1-3): p. 375-81.

[1994] P. Anres, H. Bros, and R. Castanet, *Thermodynamic investigation of the solid and liquid Au-Sb alloys.* Intermetallics, 1994. **2**(4): p. 285-8.

[1995] E. Hayer and R. Castanet, *A thermodynamic investigation of liquid gold-antimony alloys.* Z. Metallkd., 1995. **86**(1): p. 8-14.

[1997] Y.A. Chang and F. Sommer, *Thermodynamics of Alloy Formation. (Proceedings of a Symposium held at the Annual Meeting in Orlando, Florida, 9-13 February 1997.)*. 1997. 313 pp.

[1997] V. Vassiliev M. Lelaurain, and J. Hertz, *A new proposal for the binary (Sn,Sb) phase diagram and its thermodynamic properties based on a new e.m.f. study.* J. Alloys Compd., 1997. **247**(1-2): p. 223-233.

[1998] D.G. Ivey, *Microstructural characterization of Au/Sn solder for packaging in optoelectronic applications.* Micron, 1998. **29**(4): p. 281-287.

[1999] K. Fitzner, Q. Guo, J. Wang, and O.J. Kleppa, *Enthalpies of liquid-liquid mixing in the systems Cu-Ag, Cu-Au and Ag-Au by using an in-situ mixing device in a high temperature single-unit differential calorimeter.* J. Alloys Compd., 1999. **291**(1-2): p. 190-200.

[2000] J. Hwang, *Solder Materials*, in *SMT*. 2000.

[2001] Z. Moser, W. Gasior, and J. Pstrus, *Surface tension measurements of the Bi-Sn and Sn-Bi-Ag liquid alloys.* J. Electron. Mater., 2001. **30**(9): p. 1104-1111.

[2001] Z. Moser, W. Gasior, and J. Pstrus, *Surface tension of liquid Ag-Sn alloys: experiment versus modeling.* J. Phase Equilib., 2001. **22**(3): p. 254-258.

[2002] H. Flandorfer, F. Gehringer, and E. Hayer, *Individual solutions for control and data acquisition with the PC.* Thermochim. Acta, 2002. **382**(1-2): p. 77-87.

[2002] J.H. Kim, S.W. Jeong, and H.M. Lee, *A thermodynamic study of phase equilibria in the Au-Sb-Sn solder system.* J. Electron. Mater., 2002. **31**(6): p. 557-563.

[2003] EU. *DIRECTIVE 2002/95/EC OF THE EUROPEAN PARLIAMENT AND OF THE COUNCIL of 27 January 2003*. Official Journal of the European Union 2003; Available from: http://eur-lex.europa.eu/LexUriServ/LexUriServ.do?uri=OJ:L:2003:037:0019:0023:EN:PDF.

[2003] H.A. Pearson and D.J. Schonfeld, *Lead*, in *Rudolph´s Pediatrics*, C.D. Rudolph, Editor. 2003, McGraw-Hill.

[2003] L. Wang, Q. Wang, A. Xian, and K. Lu, *Precise measurement of the densities of liquid Bi, Sn, Pb and Sb.* J. Phys. Condens. Matter, 2003. **15**(6): p. 777-783.

[2005] F. Barbosa, Jr., J. Tanus-Santos, R. Gerlach, and P. Parsons, *A critical review of biomarkers used for monitoring human exposure to lead: adavanteages, limitations, and future needs.* Environmental health perspectives, 2005. **113**(12).

[2005] I. Katayama, et al., *Activity measurement of liquid Sn-Ag-Bi alloys by fused salt EMF method.* Mater. Sci. Forum, 2005. **502**(New Frontiers of Processing and Engineering in Advanced Materials): p. 129-134.

[2005] M. Kucharski and P. Fima, *The surface tension and density of liquid Ag-Bi, Ag-Sn, and Bi-Sn alloys.* Monatsh. Chem., 2005. **136**(11): p. 1841-1846.

[2005] J. Lee, W. Shimoda, and T. Tanaka, *Temperature and oxygen partial pressure dependences of the surface tension of liquid Sn-Ag and Sn-Cu lead-free solder alloys.* Monatsh. Chem., 2005. **136**(11): p. 1829-1834.

[2005] J. Lee, W. Shimoda, and T. Tanaka, *Temperature dependence of surface tension of liquid Sn-Ag, In-Ag and In-Cu alloys.* Meas. Sci. Technol., 2005. **16**(2): p. 438-442.

[2005] M.T. Sheen, Y.H. Ho, C.L. Wang, K.C. Hsieh, and W.H. Cheng, *The joint strength and microstructure of fluxless Au/Sn solders in InP-based laser diode packages.* J. Electron. Mater., 2005. **34**(10): p. 1318-1323.

[2005] J.Y. Tsai, C.W. Chang, Y.C. Shieh, Y.C. Hu, and C.R. Kao, *Controlling the microstructures from the gold-tin reaction.* J. Electron. Mater., 2005. **34**(2): p. 182-187.

[2006] G. Garzel and L.A. Zabdyr, *Electromotive force study of the liquid silver-bismuth-tin alloys.* J. Phase Equilib. Diffus., 2006. **27**(2): p. 140-144.

[2006] Y.T. Lai and C.Y. Liu, *Study of wetting reaction between eutectic AuSn and Au foil.* J. Electron. Mater., 2006. **35**(2): p. 353-359.

[2006] Z. Li, *Thermodynamic and physicochemical investigations of lead-free solder alloys, PhD thesis*. 2006, University of Vienna.

[2007] P. Terzieff, Z. Li, S. Knott, and A. Mikula, *Physicochemical properties of liquid Ag-Bi-Sn.* Phys. B (Amsterdam, Neth.), 2007. **388**(1-2): p. 312-317.

[2007] A.J. Trevor, B.G. Katzung, and S.B. Masters, *Heavy metals*, in *Katzung & Trevor´s Pharmacology: Examination & Board Review*, B.G. Katzung and A.J. Trevor, Editors. 2007, McGraw-Hill.

[2007] J. Wang, H.S. Liu, L.B. Liu, and Z.P. Jin, *Thermodynamic description of the Sn-Ag-Au ternary system.* CALPHAD Comput. Coupling Phase Diagrams Thermochem., 2007. **31**(4): p. 545-552.

[2008] S.-W. Chen, C.-C. Chen, W. Gierlotka, A.-R. Zi, P.-Y. Chen, and H.-J. Wu, *Phase Equilibria of the Sn-Sb Binary System.* J. Electron. Mater., 2008. **37**(7): p. 992-1002.

[2008] P. Fima and M. Kucharski, *The surface tension and density of Ag-Bi-Sn alloys.* Int. J. Mater. Res., 2008. **99**(2): p. 159-161.

[2008] H. Flandorfer, C. Luef, and U. Saeed, *On the temperature dependence of the enthalpies of mixing in liquid binary (Ag, Cu, Ni)-Sn alloys.* J. Non-Cryst. Solids, 2008. **354**(26): p. 2953-2972.

[2008] Z. Li, Z. Cao, S. Knott, A. Mikula, Y. Du, and Z. Qiao, *Thermodynamic investigation of the Ag-Bi-Sn ternary system.* CALPHAD Comput. Coupling Phase Diagrams Thermochem., 2008. **32**(1): p. 152-163.

[2008] Z. Li, M. Dallegri, and S. Knott, *Calorimetric measurements of the ternary Ag-Au-Sn system.* J. Alloys Compd., 2008. **453**(1-2): p. 442-447.

[2008] J. Park and J. Lee, *Phase diagram reassessment of Ag-Au system including size effect.* CALPHAD Comput. Coupling Phase Diagrams Thermochem., 2008. **32**(1): p. 135-141.

[2008] E. Rossi, *Low Level Environmental Exposure - A Continuing Challenge.* The Clinical Biochemist Reviews/Australian Association of Clinical Biochemists, 2008. **29**(2).

[2009] F. Gao, C.P. Wang, Y.Y. Li, X.J. Liu, Y. Takaku, I. Ohnuma, and K. Ishida, *Experimental Investigation and Thermodynamic Assessment of Phase Equilibria in the Ag-Au-Sn System.* J. Electron. Mater., 2009. **38**(10): p. 2096-2105.

[2009] S. Gruner, M. Koehler, and W. Hoyer, *Surface tension and mass density of liquid Cu-Ge alloys.* J. Alloys Compd., 2009. **482**(1-2): p. 335-338.

[2009] P. Ragan and T. Turner, *Working to prevent lead poisoning in children: getting the lead out.* official journal of the American Academy of Physician Assistants, 2009. **22**(7).

[2010] IPC. *Materials Declaration*. 2010; Available from: http://www.ipc.org/ContentPage.aspx?PageID=Materials-Declaration.

[2010] H. Ipser, A. Mikula, and I. Katayama, *Overview: The emf method as a source of experimental thermodynamic data.* CALPHAD Comput. Coupling Phase Diagrams Thermochem., 2010. **34**(3): p. 271-278.

[2010] Y. Plevachuk, W. Hoyer, I. Kaban, M. Koehler, and R. Novakovic, *Experimental study of density, surface tension, and contact angle of Sn-Sb-based alloys for high temperature soldering.* J. Mater. Sci., 2010. **45**(8): p. 2051-2056.

Publications and conference contributions:

Publications list

M. Hindler, S. Knott, A. Mikula, Thermodynamic Properties of Liquid Ag-Au-Sn Alloys, Journal of Electronic Materials, 2010, 39(10): p.2051-2056

M. Hindler, A. Mikula, Calorimetric investigations on the ternary Au-Sb-Sn system, 2011, in preparation.

M. Hindler, Z. Guo, A. Mikula, Thermodynamic properties of liquid Au-Sb and Au-Sb-Sn alloys, 2011, in preparation.

M. Hindler, P. Terzieff, A. Mikula, Surface tension and densities of liquid Ag-Bi-Sn alloys, 2001, in preparation.

Conference contributions

5.WACÖ - Graz/St.Martin, Austria, March, 2008
M. Hindler, S. Knott, A. Mikula
Thermodynamische Untersuchungen von ternären Legierungen mittels EMK. (oral presentation)

TOFA 2008 – Krakow, Poland, June, 2008
M. Hindler, S. Knott, A. Mikula
Thermodynamic investigations on the ternary Ag-Au-Sn system. (oral presentation)

MS&T 2008 – Pittsburgh, United States of America, October, 2008
S. Knott, M. Hindler, Z. Li, C. Schmetterer, P. Terzieff, A. Mikula
Investigation of various properties of lead free solders. (oral presentation)

TMS 2009 – San Francisco, United States of America, February, 2009
M. Hindler, S. Knott, C. Schmetterer, A. Mikula
Investigation of various properties of lead free solders. (oral presentation)

18. Ulm-Freiberger Kalorimetrietage – Freiberg, Germany, March, 2009
M. Hindler, S. Knott, A. Mikula
Thermodynamic properties of the Ag-Au-Sn and the Au-Sb-Sn system. (poster presentation)

COST Action MP0602 Working Group Meeting – Genova, Italy, November, 2009
M. Hindler, S. Knott, A. Mikula
Thermodynamic properties of the Ag-Au-Sn and the Au-Sb-Sn system. (oral presentation)

13. Österreichische Chemietage – Vienna, Austria, August, 2009
M. Hindler, S. Knott, A. Mikula
Thermodynamic properties of the Ag-Au-Sn system. (poster presentation)

6.WACÖ – Linz, Austria, March, 2010
M. Hindler, Z. Guo
Thermodynamic investigations on the ternary Au-Sb-Sn system. (oral presentation)

14th Liquid and amorphous metals conference – Roma, Italy, July, 2010
Z. Guo, M. Hindler, A. Mikula
Thermodynamic properties and surface tension of some ternary lead-free solders. (poster presentation)

TOFA 2010 – Porto, Portugal, September, 2010
Z. Guo, M. Hindler, A. Mikula
The surface tension and density of Cu-In-Sn. (oral presentation)

TOFA 2010 – Porto, Portugal, September, 2010
M. Hindler, Z. Guo, A. Mikula
Thermodynamic properties of the Au-Sb-Sn system. (oral presentation)

Curriculum Vitae

Date of birth:	April 22, 1980
Place of birth:	Berlin, Germany
Nationality:	Austria
Family status:	unmarried
Languages:	German, English , France

Education:

1986 – 1988	Primary school, Berlin/BRD
1988 – 1990	Primary school, Düsseldorf
1990 – 1994	Secondary school, Düsseldorf
1995 – 1997	Secondary school, Frankfurt
1997 – 2000	Secondary school, Düsseldorf
since 2000	Studying chemistry at the University of Vienna, Austria
2004	Practical course at Baxter
2006	Tutor in analytical chemistry
April 2007	Mag. rer. nat. in chemistry Thesis: Trace analysis on antique bronzes

2007- present	PhD studies in Materials science Thesis: Lead free solders
2007- present	Teaching assistant in several lab courses and seminars
2010	Sample preparation for the faculty of physics (department of physics of nanostrucured materials)